A LYSOSOMAL CALCIUM CHANNEL REGULATES MEMBRANE TRAFFICKING DURING PHAGOCYTOSIS

By

Mohammad Ali Samie

A dissertation submitted in partial fulfillment
of the requirements for the degree of
Doctor of Philosophy
(Molecular, Cellular, and Developmental Biology)
In the University of Michigan
2014

Doctoral Committee

Associate Professor Haoxing Xu, Chair
Professor Richard I. Hume
Professor Joel A. Swanson
Associate Professor Yanzhuang Wang

Imagination is more important than knowledge. For knowledge is limited, whereas imagination embraces the entire world, stimulating progress, giving birth to evolution. It is, strictly speaking, a real factor in scientific research.

-Albert Einstein, 1931

DEDICATION

To my family

for their unconditional love and support

and because

they are my haven in this heartless world

ACKNOWLEDGEMENT

The work presented in this thesis would not have been possible without the help and support of many people. I would never have been able to finish this work without the guidance of my advisor and committee members, help from friends, and support from my family. I take this opportunity to extend my appreciation to all of those who made this work possible.

First and foremost, I would like to extend my sincere gratitude to my thesis advisor, Dr. Haoxing Xu, for his dedicated help, advice, inspiration, and encouragement throughout my thesis work. His passion for science, enthusiasm, integral view on research, and his mission for providing high-quality work have made a deep impression on me. During the course of our interactions and discussions I have learned extensively from him, including how to raise new possibilities, how to regard an old question from a new perspective, how to approach a problem by systematic thinking, and paying close attention to details. More importantly he has been continuously supportive and has given me the freedom to pursue various projects without objections. He has played an important role in my training as a critical and independent scientist and I owe him my deepest gratitude for this.

I would also like to thank the rest of my thesis committee members for their encouragement, insightful comments, and hard questions. Dr. Richard Hume has provided invaluable guidance and support throughout my thesis work and has been extremely helpful in

many aspects. I have never seen a scientist more knowledgeable and insightful than him and he has always been willing to help anytime I needed him. Dr. Yanzhuang Wang helped to move my project forward with his great understanding of cellular compartments and organelle trafficking, in addition to allowing me use of his facilities and reagents. The completion of this project was definitely not possible without the vital help of Dr. Joel Swanson. His expertise on macrophage physiology and phagocytosis has provided invaluable support and has been fundamental to the formulation of my hypothesis and deriving the project.

It's certainly impossible to get through graduate school and survive without the help and support of friends. In the past four and a half years I have been blessed to be associated with a friendly and cheerful group of fellow students and colleagues in Xu lab. I am deeply grateful to Xiping Cheng for her constant support, guidance, and cooperation. I owe a lot of gratitude to her for always being there for me. No matter how busy she was, she always tried to help anytime I needed her. I feel privileged to have been associated with such a kind and hardworking person like her during my graduate life and hopefully will be for many more years to come.

I have greatly benefited from the expertise of Xiang Wang and Xiaoli Zhang throughout my project. They are both great electrophysiologist that have provided invaluable technical help and support in order to complete my project. Additionally, I would like to thank Xiaoli for introducing me to some great traditional Chinese food, such as dumplings, and often making sure that I didn't starve during the long days in lab.

I have always enjoyed my scientific and insightful discussions with Xinran Li. He is an expert in molecular biology and cloning and I have benefited from his help and company. I also want to thank him for teaching me more about Chinese culture and traditions. In addition I want to thank him for giving me some professional training on how to play Ping Pong.

I would also like to thank Qiong Gao for her generous support and for always standing by my side and being willing to help. I will always cherish the warmth shown by her. I also want to thank Abigail Garrity for her help and company. Moreover, I would like to thank Wuyang Wang and Nirakar Sahoo for their help and support.

In the past several years I had the privilege to work and mentor a group of great undergraduate students. I owe a very important debt to Andrew Goschka, a very talented and smart student whose help was instrumental to complete my project. I truly enjoyed our philosophical discussions and appreciated the passion we shared for Russian and French literature. Also, I would like to thank Evan Gregg for his help. A great athlete and very bright student who, despite his busy schedule and his commitment to Michigan swimming team, managed to help me with various experiments and provided great support. I am deeply grateful to Marlene Azar for her help and support. In spite of her quiet nature, she has proven to be a vibrant and smart student who has truly impressed me with her willingness to learn. In addition, I would like to thank Megan Lemorie. It is not often that someone comes along who is a good person and Megan is certainly one of them. I have only known her for a short time, but she has become a good friend whom I cherish the company of every day. I would like to thank Brennan Schiller, whose friendly smile and graceful hello make my day every time I see her. Also, I want to thank Dmitry Davydov who has fascinated me with his ability to learn and navigate complicated projects. Also I would like to thank Crystal Collier, Adam Awerbuch, Sara Levey, and Cyrus Tsang for their help and support.

I would like to offer my special thanks to Kathy Dong. I have had the pleasure to know her for the past two years and she has truly inspired me in many ways. With her great personality and friendly nature she has always made me feel at ease. I could always look back to her for any

support. She has always been there for me whenever I needed it the most and I have become to respect and admire here in many ways. There has been no limit to her kindness and I am forever thankful to her for all that she has done for me.

I would also like to thank Katherine Lelito for always standing by my side and sharing a great relationship as compassionate friends. She was the first friend I made at Michigan and I certainly hope that our friendship will last for many more years to come.

I would also like to thank Marcelo de Oliveira for his friendship and support. I truly enjoyed our deep theological discussions and treasure our shared passion for Michigan football.

I owe my deepest gratitude to my family for always being there for me and for their unconditional love and support throughout my life. I am extremely grateful for my parents as their love and support has always been my strength. Their patience and sacrifice will remain my inspiration throughout the rest of my life. Without their help I would not have been able to complete much of what I have done or been able to become the person that I am. I am thankful to my father, Hossein, for his care and love. He has worked hard to support our family and spared no effort to provide the best possible environment for my brother and me in order to grow up and attend school. I am also thankful to my mother, Shahin, for her endless love and kindness. I have no suitable words to fully describe her everlasting love and care for my brother and me and we will always be grateful for that. I am also thankful to my brother, Hamid, for being there any time I needed him and for his endless support and friendship.

As always it is impossible to mention everybody who had an impact on this work, but I would like to thank everybody and say thanks for everything you have done.

PREFACE

About four and half years ago I started my journey to graduate school. These years have been a challenging trip with both ups and downs. Fortunately, I was not alone on this road, but instead accompanied by an extended team of great scientists who eventually became more than colleagues and became close friends. I cannot express the long days spent in the lab, the joy from obtaining good results (or any results), the hope for good outcomes, and the sadness/exhaustion felt with each failed attempt. But if you are reading these lines, that means I have survived all of these years and I am almost at the end of the road. This was certainly not possible without the support of my mentor, Dr. Haoxing Xu, and the help of the entire group of Xu lab members. For this, I would like to kindly thank them all.

Although I joined the graduate program for the Department of Molecular, Cellular, and Developmental Biology at the University of Michigan in the August of 2009, the main body of my work presented here in my PhD thesis started in the summer of 2011 and was published in the summer of 2013 in the journal of *Developmental Cell*. I was originally set to work on a different project and a different class of proteins, however, an observation in a non-related experiment in the spring of 2011, right before my preliminary examinations, led me to this current project and eventually publication.

The conceptual materials presented in the first Chapter are modified from my first two author review papers (*Samie et. al, 2010. Studying TRP Channels in Intracellular Membranes.*

CRC press, Book chapter, TRP Channels-Methods in Signal Transduction Series, Chapter 19 and *Samie et. al, 2013. Lysosomal Exocytosis and Lipid Storage Disorders. Journal of Lipid Research, manuscript under review*) in addition to another review paper I coauthored with Xiping Cheng and Dongbio Shen (*Cheng et. al, 2010. Mucolipins: Intracellular TRPML1-3 Channels. FEBS Letters*).

Materials presented in the second, third, and fourth chapters are adapted with modification from my first author article published in *Developmental Cell* (*Same et. al. 2013, A TRP channel in the lysosome regulates large particle phagocytosis via focal exocytosis. Dev Cell;26(5):511-24*). In the second chapter, the preparation of bone marrow macrophages (BMMs) from WT and TRPML1 knockout (KO) mice was performed in collaboration with Andrew Goschka. Lysosomal recording in TRPML1 KO BMMs and macrophage cells lines (Figures 2.1B and 2.4A) were performed in collaboration with Xiaoli Zhang. In the third chapter, the molecular characterization of TRPML1 specific inhibitor, ML-SI1, was performed in collaboration with Xiang Wang who performed the electrophysiology experiments (Figure 3.3A-C) and Abbie Garrity who performed the calcium imaging experiments (Figure 3.3D and E). Direct recording of newly formed phagosomes was performed in collaboration with Xiang Wang (Figure 3.5). Also, the whole-cell patch-clamp method used to detect the plasma membrane insertion of TRPML1 during particle uptake was developed in collaboration with Xiang Wang (Figure 3.7A). SytVII construct was developed in collaboration with Qiong Gao (Figure 3.7D). Particle uptake evaluation in SytVII and VAMP7 dominant negative transfected cells was performed in collaboration with Evan Gregg (Figure 3.7D and E). Spleen sections and tissue staining was perfumed in collaboration with Marlene Azar (Figure 3.8B and D). Live brain sectioning and staining was performed in collaboration with Kathy Dong (Figure 3.8I). In the

fourth chapter, the localization of $PI(3,5)P_2$ during particle uptake was studied using a $PI(3,5)P_2$ specific probe developed by Xinran Li (Figure 4.1A and B). HPLC experiments evaluating the dynamics of phosphoinositides during particle uptake was performed in collaboration with Sergey Zolov from the Lois Wesiman Lab at the Life Science Institute at the University of Michigan (Figure 4.1 C).

The data presented in the fifth chapter regarding the influence of TRPML1 on bacteria elimination are unpublished material and it is an ongoing project who I am handing over to a smart graduate student in our lab named Qiong Gao. Lysosomal isolation method was developed and optimized in collaboration with Andrew Goschka (Figure 5.3A-C) and it was published in 2012 in a paper I coauthored with Xiang Wang (*Wang et.al, 2012, TPC Proteins are Sodium-selective Ion Channels in the Endosomes and Lysosomes. Cell 151, 373-383, Oct. 12*)

Throughout all these projects, Megan Lemorie helped with genotyping and maintaining the mouse lines, while Brennan Schiller helped amplify different constructs necessary for the different experiments. Additionally, the invaluable help and support of Xiping Cheng was crucial to move the project forward. Also, none of these projects were possible without the help of my mentor Haoxing Xu who helped me to develop and formulate the key concepts and experiments necessary to complete all these projects.

At the end, I would like to give thanks to all of you who are reading this. If you are reading this line after the others, you at least read one page of my thesis and for that, I thank you!

TABLE OF CONTENTS

LIST OF FIGURES

CHAPTER I

CHAPTER II

CHAPTER III

CHAPTER IV

CHAPTER V

CHAPTER VI

LIST OF ABBREVIATIONS

AP	*Acid phosphatase*
ARF6	*ADP-ribosylation factor 6*
BAPTA	*1,2-bis(o-aminophenoxy)ethane-N,N,N',N'-tetraacetic acid*
BAPTA-AM	*BAPTA-acetoxymethyl ester*
BMM	*Bone marrow derived macrophages*
BMP	*Bis(monoacylglycero)phosphate*
BSA	*Bovine serum albumin*
CFU	*Colony factor unit*
CHO	*Chinese hamster ovary*
CLEAR	*Coordinated lysosomal expression and regulation*
CMT	*Charcot-Marie-Tooth*
EEA1	*Early endosome antigen 1*
EGTA	*Ethylene glycol-bis(2-aminoethylether)-N,N,N',N'-tetraacetic acid*
EGTA-AM	*EGTA-acetoxymethy*
ER	*Endoplasmic reticulum*
ERT	*Enzyme replacement therapy*
ESCRT	*Endosomal sorting complexes required for transport*
GFP	*Green fluorescent protein*
H&E	*Hematoxylin and eosin stain*
HEK293	*Human Embryonic Kidney 293*
HPLC	*High-performance liquid chromatography*
ICP-MS	*Inductively-coupled plasma mass spectrometry*
IgG	*Immunoglobulin G*

KD	*Knockdown*
KO	*Knockout*
LAMP	*Lysosomal-associated membrane protein 1*
LB	*Luria broth*
LDH	*Lactate de-hydrogenase*
LEL	*Late endosome-lysosome*
LSD	*Lysosomal storage disorder*
MHCII	*Major Histocompatibility Complex II*
ML1	*TRPML1*
MLIV	*Mucolipidosis type IV*
ML-SA1	*TRPML1 specific synthetic agonist-1*
ML-SI1	*TRPML1 specific synthetic inhibitor-1*
MOI	*Multiplicity of infection*
mTOR	*Mammalian target of rapamycin*
MVB	*multi-vesicular bodies*
Neu1	*Neuraminidase 1*
NPC	*Niemann–Pick type C*
NRK	*Normal rat kidney*
O/E	*Over expressed*
PBS	*Phosphate buffered saline*
PDGF-R	*Platelet-derived growth factor receptors*
PFA	*Paraformaldehyde*
PtdIns	*Phosphatidylinositols*
PI	*Phosphoinositides*
PI3P	*Phosphatidylinositol 3-phosphate*
PI4P	*Phosphatidylinositol 4-phosphate*
PI5P	*Phosphatidylinositol 5-phosphate*
$P1(4,5)P_2$	*Phosphatidylinositol 4,5-bisphosphate*
$PI(3,4)P_2$	*Phosphatidylinositol 3,4-bisphosphate*
$PI(3,5)P_2$	*Phosphatidylinositol 3,5-bisphosphate*
$PI(3,4,5)P_3$	*Phosphatidylinositol (3,4,5)-triphosphate*

PI3K	*Phosphoinositide 3-kinase*
RBC	*Red blood cell*
RNAi	*RNA interference*
RT-PCR	*Reverse transcription polymerase chain reaction*
SCV	*Salmonella-containing vacuoles*
SNAP23	*Synaptosome-associated protein of 23kDa*
SNARE	*Soluble N-ethylmaleimide-sensitive factor-attachment protein receptor*
SSM	*Sulphide-silver method*
SytI	*Synaptotagmin I*
SytV	*Synaptotagmin V*
SytVII	*Synaptotagmin VII*
TFEB	*Transcription factor EB*
TGN	*Trans-Golgi network*
TM	*Transmembrane*
TRP	*Transient receptor potential*
TRPML1	*Transient receptor potential-mucolipin 1*
TRPML2	*Transient receptor potential-mucolipin 2*
TRPML3	*Transient receptor potential-mucolipin 3*
TUNEL	*Terminal deoxynucleotidyl transferase mediated dUTP Nick End Labeling*
VAMP3	*Vesicle-associated membrane protein 3*
VAMP7	*Vesicle-associated membrane protein 7*
V-ATPase	*Vacuolar-type H+-ATPase*
WT	*Wild tyype*

ABSTRACT

Macrophages participate in two main biological functions; they actively participate in apoptotic body removal and are involved in pathogen elimination. Interestingly, lysosomal membrane trafficking events have been shown to be vital for both processes. Ingestion of large extracellular particles, such as apoptotic bodies, requires the fusion of lysosomal membranes with the plasma membrane (i.e. lysosomal exocytosis) in order to provide excess membrane for the formation of plasmalemmal pseudopod necessary for phagosome sealing and, consequently, particle ingestion. Conversely, pathogen elimination by macrophages involves the trafficking of the ingested pathogens to lysosomes for degradation. Here I identified Mucolipin TRP channel 1 (TRPML1) as the key lysosomal Ca^{2+} channel regulating both lysosomal trafficking events in macrophages. Both lysosomal exocytosis and particle ingestion are inhibited by synthetic TRPML1 blocker and are defective in macrophages isolated from TRPML1 knockout mice. Additionally, TRPML1 overexpression and TRPML1 agonists induce both lysosomal exocytosis and particle uptake. By using time-lapse confocal imaging I found that particle binding induces the production of lysosomal $PI(3,5)P_2$ in order to trigger TRPML1-mediated lysosomal Ca^{2+} release specifically at the site of particle uptake. This then promotes the fusion of TRPML1-containg lysosomal membranes with the plasma membrane at the site of particle uptake through lysosomal exocytosis. Thus, phagocytic ingestion of large particles activates a phosphoinositide- and Ca^{2+}- dependent exocytosis pathway in order to provide the membrane necessary for

pseudopod extension. In correlation with this, accumulation of apoptotic cells was observed in various tissues obtained from TRPML1 knockout mice, suggesting defective clearance of apoptotic cells *in vivo*. Moreover, I observed that bacteria elimination is inhibited by synthetic TRPML1 blocker and is defective in macrophages isolated from TRPML1 knockout mice. Time-lapse confocal imaging showed that the fusion of bacteria-containing phagosomes with the lysosomes is defective in macrophages lacking TRPML1 activity. Collectively, I have showed that TRPML1 regulates various lysosomal membrane trafficking events within macrophages by releasing lysosomal calcium into the cytoplasm and providing the calcium necessary for mediating the fusion machinery involved in membrane trafficking.

CHAPTER I

INTRODUCTION

1. Overview of lysosomal dynamics and function

1.1 Lysosomes as the degradation and nutrient-sensing center

Lysosomes are acidic compartments in mammalian cells that are primarily responsible for the breakdown of various biomaterials such as membranes, proteins, polysaccharides, and complex lipids into their respective building blocks: amino acids, monosaccharaides, fatty acids, or nucleotides (Kornfeld and Mellman 1989; Braulke and Bonifacino 2009). Hence, since their discovery by Christian Duve in 1955, lysosomes have been viewed as the cell's degradation center (Luzio, Pryor et al. 2007). Each mammalian cell has several hundred lysosomes, all heterogeneous in size (about 200-1000 nm) and morphology, which collectively constitute approximately 5% of the cell volume (Mellman 1989). As single membrane-bounded vesicles, lysosomes are filled with 50 different types of hydrolases, such as lipases, proteases, and glycosidases, which effectively convert proteins and complex lipids into their building block molecules (Schulze, Kolter et al. 2009; Kolter and Sandhoff 2010). The functions of most lysosomal hydrolytic enzymes require an acidic lumen, which is established and maintained by V-ATPase proton pumps located on the perimeter membrane (Mellman, Fuchs et al. 1986). To protect the perimeter membrane and its resident membrane proteins from degradation, the inner

leaflet of the lysosomal membrane is coated with a polysaccharide layer called the glycocalyx (Neiss 1984).

The biomaterials destined for degradation are delivered to lysosomes through endocytic/phagocytic and autophagic pathways (**Fig. 1.1**). Endocytosis or phagocytosis of extracellular particles and plasma membrane proteins begins with the invagination of the plasma membrane to form an endocytic vesicle, which then undergo a series of maturation process to first become early endosomes, then late endosomes, and eventually lysosomes (Huotari and Helenius 2011). In the late endosomes, cargo and substrates destined for degradation are sorted into intraluminal vesicles, called multi-vesicular bodies (MVBs), via the endosomal sorting complexes required for transport (ESCRT) system. Mature late endosomes containing MVBs then fuse with lysosomes to become endolysosome hybrids to mediate the degradation (**Fig. 1.1**). In parallel with endocytosis, dysfunctional intracellular organelles and misfolded proteins reach lysosomes through the autophagic pathway (**Fig. 1.1**). Double membrane-bound autophagosomes fuse directly with lysosomes to form autolysosomes in which autophagic substrates are broken down for reutilization (Mizushima, Levine et al. 2008; Mizushima 2011). The products of lysosomal degradation, or lysosomal catabolites, leave lysosomes through specific exporters on the perimeter membrane or through vesicular membrane trafficking (Sagne and Gasnier 2008; Ruivo, Anne et al. 2009) (**Fig. 1.1**). Once they reach the cytoplasm or Golgi apparatus, these catabolites are either further degraded to provide energy or re-utilized by the anabolic and biosynthetic pathways to produce complex molecules. Indeed, the synthesis of many complex lipids, such as the glycosphingolipids, mainly utilizes these lysosomal catabolites as their building blocks (Gillard, Clement et al. 1998). Therefore, lysosomal function is important not only for catabolism, but also for cellular recycling and anabolism.

Because the catabolic and anabolic pathways cross-talk with each other to regulate metabolic homeostasis, the endocytic and autophagic pathways that supply the catabolic cargo are highly regulated by cellular signaling and nutrient status (Settembre, Zoncu et al. 2012; Settembre, Fraldi et al. 2013). For example, autophagy is triggered by starvation but terminated upon completion of lysosomal degradation (Yu, McPhee et al. 2010). Indeed, lysosomes contain the amino acid and nutrient-sensing machinery that consists of V-ATPase, Rag GTPase, and mTOR (Settembre, Zoncu et al. 2012). Consistent with this, lysosomes have been shown to have a much broader role in cellular physiology than just degradation, including roles in secretion, plasma membrane repair, cellular metabolism, and signaling transduction (Luzio, Pryor et al. 2007; Settembre, Fraldi et al.). Hence, lysosomes should not be viewed as a dead-end degradative compartment, but rather as highly dynamic organelles that integrate multiple metabolic pathways to maintain cellular homeostasis.

1.2 Lysosomal storage disorders

Lipids, such as sphingolipids, glycolipids, phospholipids, and cholesterol, are the essential structural constitutes of plasma membranes and the membranes of intracellular compartments (Schulze and Sandhoff 2011). In addition, many of them, such as phospholipids, also serve as signaling molecules. While lipid synthesis is initiated in the endoplasmic reticulum (ER), lipid degradation occurs in lysosomes, which are filled with various acid lipases (Schulze and Sandhoff 2011). Unlike water soluble substrates, such as proteins that are directly accessible to lysosomal proteases and peptidases, the digestion of membrane-bound complexes takes place in intraluminal vesicles, and requires both lipid-binding activator proteins and anionic lipids such as bis(monoacylglycero)phosphate (BMP) (Kolter and Sandhoff 2010).

While lysosomal perimeter membrane is protected from degradation by the glycocalyx, it has been shown that intraluminal vesicles (the MVBs) are the main degradation sites for membrane lipids (**Fig. 1.1**) (Kolter and Sandhoff 2010). Within the MVBs, membrane stabilizing cholesterol is sorted and exported out via the cholesterol-binding NPC1 and NPC2 proteins (Cheruku, Xu et al. 2006; Infante, Wang et al. 2008). Auxiliary lipid binding proteins then solubilize and present the complex lipids to hydrolases for degradation (Schulze, Kolter et al. 2009; Kolter and Sandhoff 2010). Complex lipids such as sphingoglycolipids require both lipases and carbohydrases for degradation (Kolter and Sandhoff 2010). Because there are multiple steps involved in lipid degradation, impairment of any of these lipid or carbohydrate hydrolases would be expected to result in an accumulation of the various undigested lipids in the lysosome (Schulze and Sandhoff 2011).

Accumulation of undigested lipids or other biomaterials in the lysosome leads to a group of metabolic disorders collectively called lysosomal storage diseases (LSDs) (Parkinson-Lawrence, Shandala et al. 2010). LSDs are traditionally classified by the nature of undigested materials within the lysosomes; hence, lipidoses are the most common LSDs. However, undigested lipids may also accumulate due to secondary mechanisms, for example, secondary to carbohydrate accumulation or membrane trafficking (Neufeld 1991). Therefore, a more useful classification is based on the mutations specific for each LSD. Most LSDs are caused by mutations in lysosomal hydrolases (Schulze, Kolter et al. 2009; Schulze and Sandhoff 2011). However, defective membrane trafficking and catabolite export could cause a "traffic jam", resulting in secondary lipid storage in the lysosome (**Fig. 1.2**) (Parkinson-Lawrence, Shandala et al. 2010). Furthermore, primary accumulation of undigested, insoluble lipids may also cause a "traffic jam" to slow down membrane trafficking and sorting and ultimately affects the delivery

of lysosomal hydrolases to lysosomes and the inhibition of cargo degradation (Parkinson-Lawrence, Shandala et al. 2010). In addition, insoluble lipids may also precipitate in the lysosomes to reduce the activity of hydrolytic enzymes. Subsequently, secondary storage of ubiquitinated proteins, carbohydrates, or other lipids may occur. Hence, most LSDs manifest heterogeneity in storage lipids in the lysosome.

Progressive accumulation of undigested lipids and protein aggregates, primarily or secondarily, leads to build-up of enlarged (> 500 nm) but dysfunctional lysosomes. These enlarged "lysosomes" are presumably endolysosomes and autolysosomes, which under normal conditions are used to regenerate new lysosomes, via the process of lysosome reformation, upon completion of lysosomal degradation (Yu, McPhee et al. 2010). Hence, LSD is a state of endocytic and autophagic "block" or "arrest" (Lieberman, Puertollano et al. 2012). Subsequently, although total number of lysosomes is not reduced in LSDs, the overall lysosomal function within a cell is compromised, and this can lead to severe cellular consequences. First, accumulation of undigested materials in the lysosome causes the depletion of the building blocks that are necessary for the biosynthesis of complex molecules and anabolism. Hence, LSDs must bear the consequence of cellular starvation (Schulze and Sandhoff 2011) (**Fig. 1.2**). Second, accumulation of various membrane-bound lipids may affect the properties and integrity of the perimeter membrane (Walkley 2009; Walkley and Vanier 2009). Third, lipid storage may alter the functionality of lysosomal membrane proteins, such as V-ATPase, lysosomal ion channels, or catabolite exporters, eventually affecting the physiology and ionic composition of lysosomes. Altered heavy metal ion homeostasis may increase oxidative stress to cause lipid peroxidation, affecting membrane integrity (Dong, Cheng et al. 2008).

In an attempt to compensate for lysosomal dysfunction and reduced power in degradation, most LSD cells exhibit an increase in basal autophagy and expression levels of house-keeping lysosomal proteins such as Lamp-1 (Ballabio and Gieselmann 2009). These compensatory changes may allow LSD cells to survive under normal, non-stressed conditions. Under stressed conditions, however, altered luminal ion homeostasis and membrane integrity may cause lysosomal membrane permeabilization, leading to the leakage of lysosomal enzymes into the cytoplasm thereby triggering cell death (Boya and Kroemer 2008). An increase in cell death would result in permanent damage to tissues and organs with large amounts of post-mitotic cells, including the brain, liver, eye, muscle, and spleen (Neufeld 1991). Hence, the most common manifestations in LSDs are neurodegeneration, mental retardation, and motor disabilities (Parkinson-Lawrence, Shandala et al. 2010).

Several therapeutic approaches have been developed for LSDs, such as substrate reduction, bone-marrow transplantation, gene therapy, and enzyme replacement therapy (ERT) (Cox and Cachon-Gonzalez 2012). However, most of these approaches are limited to only one type of LSD, and often not very effective. More importantly, for most LSDs, an effective therapeutic approach is still lacking. To develop a common approach for most LSDs, it is necessary to understand how defective cellular pathways are interconnected to impact the cellular viability and physiology. Several recent studies revealed that lysosomal exocytosis, one of the two most important lysosomal trafficking pathways in the outward direction (**Fig. 1.1**), is defective in multiple LSDs (LaPlante, Sun et al. 2006; Medina, Fraldi et al. 2011). Most intriguingly, induction of lysosomal exocytosis was found to facilitate the clearance of stored materials regardless of the nature and cause of the storage (Medina, Fraldi et al. 2011; Settembre,

Fraldi et al. 2013). The importance of lysosomal exocytosis as a therapeutic target for LSDs is explored more in later chapters.

2. Dynamics of lysosomal exocytosis

2.1 Regulated secretion of lysosomes and its biological importance

Exocytosis of secretory lysosomes (lysosome-related organelles) has been long known to be present in specialized cell types such as hematopoietic cells (Stinchcombe and Griffiths 1999). However, the regulated exocytosis of conventional lysosomes was first observed in CHO and NRK fibroblasts, but is now known to be present in all cell types (Andrews 2000; Gerasimenko, Gerasimenko et al. 2001; Reddy, Caler et al. 2001). Upon stimulation, lysosomes translocate from the perinuclear region to the plasma membrane along the microtubules (Rodriguez, Webster et al. 1997; Andrews 2000; Reddy, Caler et al. 2001; Jaiswal, Andrews et al. 2002). After docking, lysosomes fuse directly with the plasma membrane and release the lysosomal contents into the extracellular space. Lysosomal exocytosis represents the major output pathway of the lysosome (**Fig. 1.1**) and is important for a variety of cellular processes. There are two primary purposes for lysosomal exocytosis depending on the tissue and cell type; membrane remodeling and secretion (**Fig. 1.3**). Lysosomal exocytosis induced membrane remodeling has been shown to contribute to neurite outgrowth in neurons (Arantes and Andrews 2006), membrane repair in muscle cells (Reddy, Caler et al. 2001), particle ingestion during phagocytosis in macrophages (Braun, Fraisier et al. 2004; Czibener, Sherer et al. 2006), and cancer cell metastasis and motility (Kirkegaard and Jaattela 2009). On the other hand, lysosomal exocytosis induced secretion contributes to antigen presentation by major histocompatibility complex class II (MHC II) (Cresswell 1994), bone absorption in osteoclasts (Mostov and Werb

1997), axonal myelination in Schwann cells (Chen, Zhang et al. 2012), and lytic granule content secretion by cytotoxic T lymphocytes (Blott and Griffiths 2002) (**Fig. 1.3**). Collectively, all of these indicate the importance of lysosomal exocytosis in a variety of biological functions and the importance of understanding its molecular machinery.

2.2 The molecular machinery and regulators of lysosomal exocytosis

Compared with synaptic vesicle exocytosis, a process sharing many similarities with lysosomal exocytosis (Sudhof 2013), the molecular mechanisms underlying lysosomal exocytosis are much less understood (Rodriguez, Webster et al. 1997; Sudhof 2013). Both processes involve several pre-fusion steps in tethering/docking and several post-docking steps in membrane fusion. However, distinct sets of exocytosis machinery are employed, including SNAREs that bring the two membranes closer to each other. More importantly, both fusion events are regulated by Ca^{2+} and the same family of Ca^{2+} sensors.

2.2.1 Microtubule and motor proteins.

Lysosomes undergo both short range actin-based and long-range microtubule-based movements (Luzio, Pryor et al. 2007; Huotari and Helenius 2011). Under resting conditions, lysosomes are mostly localized in the perinuclear microtubule-organizing center (Settembre, Fraldi et al. 2013). Upon stimulation, there is an increase in both lysosome mobility and the number of lysosomes localized under the plasma membrane (lysosomal docking) (Spampanato, Feeney et al. 2013). It has been shown that lysosome mobility is increased when the microtubule-dependent motor kinesin and dynein motor proteins are up-regulated (Mrakovic, Kay et al. 2012). Likewise, lysosomal docking is also dependent on microtubules (Medina,

Fraldi et al. 2011). Therefore, it is possible that the conditions needed to increase lysosome mobility may also increase lysosomal docking and exocytosis. It remains to be investigated whether lysosomal exocytosis is increased under these manipulations.

2.2.2 SNARE proteins

Similar to the exocytosis of synaptic vesicles as well as endosome-endosome fusion, the fusion of lysosomes with the plasma membrane is mediated by soluble N-ethylmaleimide-sensitive factor-attachment protein receptor (SNARE) complexes (Jahn and Scheller 2006). SNARE proteins are characterized by the existence of a coiled-coil homology domain (Jahn and Scheller 2006; Jahn and Fasshauer 2012). During lysosomal exocytosis vesicle-associated membrane protein 7 (VAMP7) localizes on the surface of the lysosomes, forms a trans-SNARE complex with syntaxin-4 and synaptosome-associated protein of 23kDa (SNAP23) on the plasma membrane (Rao, Huynh et al. 2004) (**Fig. 1.4**). The formation of the trans-SNARE complex pulls the lysosome and plasma membrane toward each other and docks the lysosome on the cytoplasmic side of the plasma membrane (**Fig. 1.4**). Lysosomal exocytosis is blocked by the expression of dominant-negative VAMP7 constructs in macrophages (Braun, Fraisier et al. 2004).

2.2.3 The role of Ca^{2+} in lysosomal exocytosis

After lysosomes are docked on the plasma membrane by the formation of the trans-SNARE complex, the final step of fusion requires a localized rise in intracellular Ca^{2+} levels (Rodriguez, Webster et al. 1997; Andrews 2000; Reddy, Caler et al. 2001). In response to a small increase in free Ca^{2+} levels in the cytoplasm, artificially induced by Ca^{2+} ionophores or

membrane disruptions, lysosomal exocytosis levels have been shown to increase (Chavez, Miller et al. 1996; Coorssen, Schmitt et al. 1996; Ninomiya, Kishimoto et al. 1996; Rodriguez, Webster et al. 1997; Rodriguez, Martinez et al. 1999). The cytosolic [Ca^{2+}] required for lysosomal exocytosis is predicted to be > 1 μM (Rodriguez, Webster et al. 1997), which is higher than the optimal 0.5 μM required for late endosome-lysosome fusion in cell-free vesicle mixing assays (Pryor, Mullock et al. 2000). During synaptic exocytosis, a very rapid increase in cytosolic Ca^{2+} is required to mediate the fast (< 1 ms) fusion of synaptic vesicles with the pre-synaptic membrane (Pang and Sudhof 2010). This increase in Ca^{2+} occurs locally near the site of exocytosis and is mediated by the flux of Ca^{2+} via the voltage-gated Ca^{2+} channels on the pre-synaptic membrane in response to depolarization (Xu, Mashimo et al. 2007). In contrast, the source of Ca^{2+} and the identity of the Ca^{2+} channel(s) for lysosomal exocytosis have remained elusive.

The Ca^{2+} required for the late endosome-lysosome and lysosome-plasma membrane fusion has been suggested to come from the lysosomal lumen (**Fig. 1.4**). Like the ER, which is the main intracellular Ca^{2+} store with an estimated $[Ca^{2+}]_{lumen}$ of 0.5-2 mM (Miyawaki, Llopis et al. 1997; Burdakov, Petersen et al. 2005), lysosomes are also Ca^{2+} stores with free $[Ca^{2+}]_{lumen}$ of 400-600 μM (Haller, Dietl et al. 1996; Haller, Volkl et al. 1996; Lloyd-Evans, Waller-Evans et al. 2010; Lloyd-Evans and Platt 2011). In cell-free vesicle fusion assays, late endosome-lysosome fusion is inhibited by the Ca^{2+} chelator BAPTA, but not EGTA (Luzio, Rous et al. 2000; Luzio, Bright et al. 2007). Although both BAPTA and EGTA have a high binding affinity for Ca^{2+}, BAPTA binds to Ca^{2+} approximately 100 times faster than EGTA does. Therefore, it is likely that the source of Ca^{2+} must be very close to the fusion spot. In other words, lysosomes themselves most likely provide the Ca^{2+} required for lysosomal fusion (Pryor, Mullock et al.

2000; Luzio, Bright et al. 2007). Therefore, lysosomes may provide Ca^{2+} for membrane fusion between lysosomes and plasma membrane during lysosomal exocytosis (**Fig. 1.4**). Collectively, these data suggest that the Ca^{2+} required for lysosomal exocytosis can potentially be provided from the lumen of the lysosomes undergoing lysosomal exocytosis. This possibility is explored in Chapter II and the results will be discussed later.

2.2.4 The lysosomal Ca^{2+} sensor Synaptotamin VII

The Synaptotagmin (Syt) family of Ca^{2+} sensor proteins has 16 members, each containing two Ca^{2+}-binding C2 domains on the cytosolic side (Chapman 2008). During synaptic vesicle fusion with the plasma membrane, the localized increase in cytoplasmic [Ca^{2+}] activates Syt-I on the surface of the synaptic vesicles triggering the final step of fusion (Sudhof 2013). Due to the following pieces of evidence, it is likely that SytVII is the Ca^{2+} sensor for lysosomal exocytosis (**Fig. 1.4**). First, Syt-VII is ubiquitously expressed and localized on the lysosomes (Rodriguez, Webster et al. 1997; Rodriguez, Martinez et al. 1999; Andrews 2000; Reddy, Caler et al. 2001; Rao, Huynh et al. 2004; Arantes and Andrews 2006). Second, cells isolated from SytVII KO mice exhibit reduced ionomycin-induced lysosomal exocytosis (Coorssen, Schmitt et al. 1996; Rodriguez, Webster et al. 1997; Rodriguez, Martinez et al. 1999; Andrews 2000; Gerasimenko, Gerasimenko et al. 2001; Reddy, Caler et al. 2001; Rao, Huynh et al. 2004; Arantes and Andrews 2006; Czibener, Sherer et al. 2006). Lastly, dominant-negative SytVII also inhibits lysosomal exocytosis (Reddy, Caler et al. 2001; Czibener, Sherer et al. 2006). All together, these data indicate that SytVII is the Ca^{2+} sensor for lysosomal exocytosis. Likewise, lysosome-mediated bacterial killing is defective in SytVII KO macrophages (Roy, Liston et al. 2004) suggesting that SytVII is also involved in phagosome-lysosome fusion. However, vacuole fusion

studies by cell free fusion assays have shown that 0.5µM Ca^{2+} is optimal for fusion of late endosomes with lysosomes (Pryor, Mullock et al. 2000), which is significantly less than the 1µM Ca^{2+} suggested to be required for the activation of SytVII and lysosomal exocytosis (Rodriguez, Webster et al. 1997). Therefore, the involvement of SytVII in late endosome-lysosome fusion events is not clear. But it should be noted that cell free experiments do not resemble the native intracellular environment and the experimental conditions used in these assays do not allow for the accurate measurement of Ca^{2+} concentrations, therefore, these data should be considered with caution. Because lysosomal exocytosis is not completely abolished in the SytVII KO, other Syt proteins may also participate in lysosomal exocytosis. In addition, other Ca^{2+} sensors may also be involved. For example, calmodulin, which is implicated in late endosome-lysosome fusion (Pryor, Mullock et al. 2000), and ALG-2, a lysosome-targeted EF hand Ca^{2+} binding protein, may play roles in lysosomal exocytosis (Vergarajauregui, Martina et al. 2009).

The mechanisms by which SytVII promote lysosomal exocytosis are not clear. Extrapolated from synaptic vesicle exocytosis (Chapman 2008; Sudhof 2013), the Ca^{2+}-bound C2 domain may increase phosphoinositide binding in order to bring the lysosomes within close proximity of the plasma membrane. The resulting force may increase membrane curvature, facilitating lipid bilayer mixing (Chapman 2008).

2.2.5 TFEB the transcription factor regulating lysosomal exocytosis

bHLH-leucine zipper transcription factor EB (TFEB) is a master regulator of both lysosomal biogenesis and autophagy (Sardiello and Ballabio 2009; Sardiello, Palmieri et al. 2009; Settembre, Di Malta et al. 2011; Settembre, Fraldi et al. 2013). When autophagy is triggered or when lysosomes are under stressed conditions, such as lysosomal storage, TFEB

proteins translocate from the cytoplasm to the nucleus, inducing the expression of its target genes. Bioinformatics analysis suggested that TFEB regulates the expression of lysosomal related genes by binding to the coordinated lysosomal expression and regulation (CLEAR) motif (Sardiello and Ballabio 2009; Settembre, Di Malta et al. 2011). Indeed overexpression of TFEB in HeLa cells causes an increase in the expression of 291 genes, mostly involved in lysosomal biogenesis through the CLEAR network, supporting the hypothesis that lysosomal related genes are regulated under a similar master network (Sardiello and Ballabio 2009; Settembre, Di Malta et al. 2011).

TFEB has been shown to regulate both docking and fusion of lysosomes with plasma membrane through the expression of a specific set of genes (**Fig. 1.4**) (Medina, Fraldi et al. 2011). TFEB most likely regulates lysosomal fusion with the plasma membrane through the expression of TRPML1, the lysosomal Ca^{2+} channel on the surface of lysosomes, as TFEB overexpression has been shown to induce a TRPML1 mediated Ca^{2+} increase in the cytoplasm (Medina, Fraldi et al. 2011) (a detailed overview of TRPML1 function is discussed in the next section) . However, it is not clear how TFEB regulates lysosomal docking on the plasma membrane. TFEB can potentially increase the expression and activity of kinesin and dynein motor proteins along the microtubules responsible for the trafficking of lysosomes to the plasma membrane (Matteoni and Kreis 1987), therefore increasing the docking of sub-plasma membrane lysosomes.

2.2.5 Neuraminidase 1 as the negative regulator of lysosomal exocytosis

Neuraminidase 1 (Neu1) is a lysosomal enzyme responsible for the cleavage of the terminal sialic acid residues from a variety of substrates in the lysosomes such as glycoproteins

and glycolipids.(Bonten, van der Spoel et al. 1996). Mutations in this gene can lead to a type of LSD called sialidosis (Pshezhetsky, Richard et al. 1997). Interestingly, in addition to its degradation role inside lysosomes, Neu1 has been shown to negatively regulate lysosomal exocytosis by controlling lysosomal membrane integrity through the mediation of sialic acid in the lysosomal membrane protein Lamp-1 (Yogalingam, Bonten et al. 2008). Neu1 function has been shown to be essential for the docking of lysosomes on the plasma membrane as cells isolated from Neu1 KO mice exhibit a significant increase in docked lysosomes on the plasma membrane (Yogalingam, Bonten et al. 2008). Consequently, lysosomal exocytosis is up-regulated in Neu1 KO cells leading to increased lysosomal secretion into the extracellular space and abnormal remodeling of the plasma membrane.

3. TRPML1 as the principal lysosomal Ca^{2+} channel

3.1 TRPML family of cation channels

Transient Receptor Potentials (TRPs) are a family of non-selective Ca^{2+} channels that were initially believed to operate solely at the plasma membrane. TRPs were primarily shown to be involved in regulating intracellular Ca^{2+} levels (Montell 2005). TRPs include six subfamilies that have been shown to be expressed in most tissues and cell types. TRPML (TRP-Mucolipin) is one of the recently characterized subfamilies of the TRP channels. The TRPML subfamily includes three members, TRPML1, TRPML2, and TRPML3, with TRPML1 being the best characterized protein of the three (Cheng, Shen et al. 2010).

3.2 TRPML channel structure

Based on bioinformatic and biochemical studies, it is well accepted that all TRPML family members have six transmembrane domains (TM1-6) with the amino and carboxy termini facing the cytosol. In contrast to other TRP channels, TRPML channels contain a large loop expanding between TM1 and TM2 (**Fig. 1.5**) (Puertollano and Kiselyov 2009; Cheng, Shen et al. 2010). TRPML family proteins share high amino acid sequence similarity (about 75%), with the highest similarity being in the pore region between TM5 and TM6 (more than 90% sequence similarity) (Puertollano and Kiselyov 2009; Cheng, Shen et al. 2010). The large loop between TM1 and TM2 contains several N-glycosylation sites. This loop has been reported to get cleaved between the second and third glycosylation sites late in the biosynthetic pathway, which could potentially regulate TRPMLs localization and/or functions (Miedel, Weixel et al. 2006).

3.3 Subcellular localization and tissue expression pattern of TRPMLs

Studies using overexpressed TRPML proteins fused with various reporter genes have revealed that TRPMLs primarily localize to a population of membrane-bound vesicles along the endosomal/lysosomal pathways in a variety of host cells. GFP-fused TRPML (TRPML1-GFP) is mainly colocalized with Lamp-1, a late endosome and lysosome marker (Dong, Cheng et al. 2008). Thus, TRPML1 is considered to be a TRP channel specifically localized on the lysosomes (Cheng, Shen et al. 2010). Using a similar approach, TRPML2 and TRPML3 were also found in Lamp-1 labeled compartments. However, they were shown to have more diverse localization. TRPML3 was shown to be localized in compartments that are positive for Rab5, an early endosome-specific small GTPase (Kim, Li et al. 2007; Cuajungco and Samie 2008; Kim, Soyombo et al. 2009). TRPML2 is also present in Arf6-positive recycling endosomes

(Karacsonyi, Miguel et al. 2007). In addition to overexpression studies, the cellular localization of TRPML1 and TRPML3 has also been investigated using cellular fractionation (Kim, Soyombo et al. 2009). These studies confirmed that TRPML1 mainly localizes with Lamp-1, while TRPML3 was shown to localize with both markers of early and late endosomes (Karacsonyi, Miguel et al. 2007). The lysosomal localization of the TRPML1 is mediated by two individual di-leucine motifs existing near the N- and C- terminals of the protein. The acidic di-leucine motif at the N-terminal (E11TERLL) regulates the direct localization of the newly synthesized protein from the Golgi to the late endosomes-lysosomes. The di-leucine motif at the C- terminal tail (E573EHSLL) arbitrates an indirect localization of TRPML1 from the Golgi to the cell membrane where it is internalized and delivered to the late endosomal-lysosomal pathways. Mutations in both di-leucine motifs block the transport of TRPML1 from Golgi to late endosome-lysosomes (LELs) and trap the channel on the plasma membrane (Vergarajauregui and Puertollano 2006).

The tissue distribution of TRPMLs has mainly been investigated by measuring mRNA expression levels using nucleotide-based techniques such as real-time polymerase chain reaction (RT-PCR), northern blot, and in situ hybridization. By using such techniques, TRPML1 was shown to be expressed in most of the tissues across the body with the highest levels of expression in the brain, kidney, spleen, liver, and heart (Falardeau, Kennedy et al. 2002). In contrast to TRPML1, the expression of TRPML2 and TRPML3 was shown to be more restricted. Mouse TRPML2 mRNA was shown to be expressed mainly in lymphoid organs, such as thymus and spleen, suggesting an important and very selective physiological role for TRPML2 in the immune system (Samie, Grimm et al. 2009). TRPML3 mRNA was shown to be detectable in the thymus, lung, kidney, spleen, and eye (Samie, Grimm et al. 2009). In addition, in situ

hybridization revealed the expression of TRPML3 in epithelial cells of the inner ear, including strial and hair cells (Di Palma, Belyantseva et al. 2002).

3.4 The permeation properties of TRPML channels

The biophysical properties, including channel permeation, of TRPML channels were extremely difficult to study due to their localization on the lysosomal compartments. However, the development of a new patch-clamp technique allowed for direct patching of the lysosomes (whole-lysosomal recording) (Dong, Cheng et al. 2008; Dong, Shen et al. 2010), which allowed for the direct study of TRPMLs in their native environment. By using the whole-lysosome recording technique, it was shown that TRPML exhibits an inward rectifying current indicating the movement of cations out of the lysosomal lumen and into the cytoplasm (**Fig. 1.5**). TRPMLs exhibit high permeability to Ca^{2+}, serving as a potential lysosomal Ca^{2+} channel. In addition, TRPMLs are also permeable to divalent heavy trace metals such as iron and zinc (Dong, Cheng et al. 2008) which may have important implications in lysosomal functions.

3.5 The activation mechanism of TRPML proteins

Phosphoinositides have been shown to regulate the activation of TRPMLs depending on the cellular localization of the channel. The late endosome/lysosome specific phosphoinositide, $PI(3,5)P_2$, has been shown to strongly activate all three TRPML channels on the surface of lysosomes (Dong, Shen et al. 2010). $PI(3,5)P_2$ most likely activates TRPMLs by directly binding to a cluster of positively charged amino acid residues on the N-terminus of the channel which faces the cytoplasm (**Fig. 1.5**) (Dong, Shen et al. 2010). In contrast to the role of $PI(3,5)P_2$ as the endogenous activator for TRPMLs, the plasma membrane-specific phosphoinositide, $PI(4,5)P_2$, has been shown to inhibit the function of TRPML1 on the surface of cells (Zhang, Li et al.

2012). Interestingly, $PI(4,5)P_2$ mediated inhibition also depends on the positively charged amino acid residues on the N-terminus suggesting that the N-terminus of TRPML1 is involved in the compartment specific regulation of TRPML1 channel activity.

3.6 The channel function of TRPML1 proteins

Considering the permeability characteristics of TRPMLs, it has been suggested that the channel function of TRPMLs is to release divalent cations, such as Ca^{2+}, Fe^{2+}, or Zn^{2+}, from the lysosome lumen into the cytoplasm in response to various cellular cues (Cheng, Jin et al. 2010). Lysosomal Ca^{2+} release has been shown to be important for various biological functions such as signal transduction, organelle homeostasis, and lysosomal acidification (Luzio, Bright et al. 2007; Luzio, Pryor et al. 2007). As mentioned before, TRPML1 is the best characterized protein among the TRPML family and its role in lysosomal Ca^{2+} release has been heavily studied (Cheng, Jin et al. 2010). Collectively, all of these data established the importance of TRPML1 as the main lysosomal channel responsible for lysosomal Ca^{2+} release (Cheng, Jin et al. 2010).

TRPMLs are also permeable to Fe^{2+} and Zn^{2+}, suggesting that they may also participate in the regulation of cellular homeostasis for these heavy metals (Dong, Cheng et al. 2008). In correlation with this, cells lacking TRPML1 exhibit an overload of lysosomal Fe^{2+} (Dong, Cheng et al. 2008) and Zn^{2+} (Eichelsdoerfer, Evans et al. 2010), suggesting that TRPML1 contributes to the transport of cations out of the lysosomes.

3.7 The physiological importance of TRPML1

TRPML1 was first identified by positional cloning approach aiming to characterize the gene underlying the human Mucolipidosis type IV disease (Bassi, Manzoni et al. 2000; Bargal,

Avidan et al. 2001). Mucolipidosis type IV (MLIV) is a neurodegenerative LSD characterized by mental and psychomotor retardation, hypotonia, iron deficiency anemia, achlorhydria, retinal degeneration, and visual problems including corneal clouding and retinal degeneration (Amir, Zlotogora et al. 1987; Altarescu, Sun et al. 2002; Puertollano and Kiselyov 2009). On the cellular level, similar to other LSDs, MLIV is characterized by the formation of large vacuoles along the endo-lysosomal pathway. Consistent with the ubiquitous expression pattern of TRPML1 in most tissues, the enlarged vacuole phenotype is observed in all cell types of MLIV patients and TRPML1 knockout mice (Bargal, Avidan et al. 2000; Bassi, Manzoni et al. 2000; Bargal, Avidan et al. 2001).

Electron microscopy and HPLC analysis have illustrated that the enlarged vacuoles observed in TRPML1 deficient cells are filled with an abnormal amount of undigested lipids such as sphingolipids, phospholipids, and cholesterol (Micsenyi, Dobrenis et al. 2009). Based on these observations it was originally suggested that TRPML1 could potentially regulate lysosomal pH and therefore affect the function of lysosomal hydrolases involved in lipid metabolism. This hypothesis was supported by studies showing that lysosomes in TRPML1 deficient cells are over acidified (Soyombo, Tjon-Kon-Sang et al. 2006; Miedel, Rbaibi et al. 2008). However, later it was revealed by biochemical studies that the hydrolase activities of lysosomal enzymes are normal in TRPML1 deficient cells (Puertollano and Kiselyov 2009). Studies done in the past several years have suggested that TRPML1 is involved in membrane fusion process by acting as a lysosomal Ca^{2+} release channel, thereby regulating membrane trafficking along the endo-lysosomal pathway by providing the Ca^{2+} necessary for the final step of fusion (Cheng, Shen et al. 2010; Dong, Shen et al. 2010). Considering this, it was suggested that the accumulation of lipids in the lysosomes of MLIV patients is possibly due to defective lysosomal trafficking

pathways as a result of a lack of lysosomal Ca^{2+} release and defective fusion machinery (Miedel, Rbaibi et al. 2008).

In correlation with this idea, cells lacking TRPML1 have been shown to be defective in several lysosomal membrane trafficking pathways (**Fig. 1.6**). The knockdown of TRPML1 in macrophage cell lines and fibroblasts isolated from MLIV patients demonstrated a delay in the lysosomal delivery and subsequent degradation of endocytosed proteins, such as BSA and platelet-derived growth factor receptors (PDGF-R) (Thompson, Schaheen et al. 2007; Vergarajauregui, Oberdick et al. 2008) (**Fig. 1.6**). However, such a delay was not observed in HeLa cells with transient knockdown of TRPML1 (Miedel, Rbaibi et al. 2008), suggesting that the regulatory role of TRPML1 along the endosomal pathway is potentially cell type-specific.

Additionally, fibroblasts and neurons obtained from MLIV patients and TRPML1 KO mice showed an increase in autophagosome formation and delayed autophagosome degradation, which suggests that TRPML1 is possibly involved in the fusion of autophagosomes with lysosomes during autophagy (**Fig. 1.6**) (Vergarajauregui, Connelly et al. 2008). Consequently, autophagosomes undergo inefficient digestion and accumulate in TRPML-deficient cells. Interestingly, loss of TRPML1 function significantly enhances constitutive autophagy but not starvation-induced autophagy (Curcio-Morelli, Charles et al. 2010).

Several lines of evidence suggest that TRPML1 plays a role in mediating lysosomal exocytosis. First, overexpression of TRPML1*Va* (a gain-of-function mutation) results in the appearance of Lamp-1 lysosomal protein on the plasma membrane indicating an increase in lysosomal exocytosis (Dong, Wang et al. 2009). Second, TFEB induced lysosomal exocytosis has been shown to be dependent on the Ca^{2+} released through TRPML1 (Medina, Fraldi et al.

2011). Third, ML-IV patients exhibit impaired ionomycin-induced lysosomal exocytosis (LaPlante, Sun et al. 2006). Lastly, the shRNA knockdown of TRPML1 in macrophage cell lines delayed the transport of the major Histocompatibility Complex II (MHCII) from LEL compartments in response to immune stimulation, a process that has been shown to be dependent on lysosomal exocytosis (Thompson, Schaheen et al. 2007). Collectively, these data suggest that TRPML1 is possibly involved in regulating lysosomal exocytosis.

Even though several studies illustrated the importance of TRPML1 in membrane trafficking, the direct involvement of TRPML1 in these processes is not clear. Almost all these studies have been performed using genetic manipulations such as the use of TRPML1 KO cells. However, genetic defects could potentially lead to secondary chronic lysosomal disorders or other primary defects associated with TRPML1 (Miedel, Rbaibi et al. 2008). One way to separate the primary and secondary effects and to investigate the direct effect of TRPML1 in membrane trafficking is to evaluate such processes after acutely activating/inhibiting TRPML1 in different cells. Indeed, the activation of TRPML1 by its newly developed specific activator was sufficient to induce and rescue the retrograde trafficking defects seen in Niemann–Pick type C (NPC) disease (Shen, Wang et al. 2012) indicating the importance and the direct effect TRPML1 has on membrane trafficking. In Chapter II I will explore the direct role of TRPML1 in lysosomal exocytosis by using its specific activator. Additionally, in order to further evaluate the role of TRPML1 in membrane trafficking, we have developed a TRPML1 specific inhibitor which will be discussed in detail in Chapter III.

4. The dynamics of macrophages in different immunological functions

4.1 Macrophage function in health and disease

Almost all eukaryotic cells are able to internalize a variety of particles during their lifetime. Most cells are able to internalize small particles through receptor mediated endocytosis (Huotari and Helenius 2011; McMahon and Boucrot 2011). However, during evolution phagocytes, such as macrophages, have gained the ability to uptake large extracellular particles (1-10μm in diameter) through a very specialized process called phagocytosis (Aderem and Underhill 1999). Macrophages are produced during the differentiation of bone marrow derived monocytes and are found in most of the tissues across the body (Aderem and Underhill 1999).

Macrophages are large (30-50 μm in diameter) and irregularly shaped cells. However, their shape is largely mediated by their location and degree of activation (Chawla 2010). The surface of macrophages is ruffled, which allows them to form large membrane extensions during phagocytosis (Huynh, Kay et al. 2007). Macrophages are one of the most plastic cell types in the body and they are able to change their function depending on the tissue they reside in (Chawla 2010). In general, macrophages participate in two main biological functions; they actively participate in pathogen elimination in addition to being involved in tissue remodeling and apoptotic cell elimination (Aderem and Underhill 1999).

Macrophages participate in maintaining tissue homeostasis, development, and cellular turnover by eliminating apoptotic or damaged cells (Wynn, Chawla et al. 2013). This function of macrophages is usually mediated by resident macrophages of each tissue such as liver, brain, bone, and spleen. Depending on the tissue, defects or any alteration in macrophage mediated cellular turnover or particle elimination can lead to severe consequences such as autoimmune

disease, neurodegeneration, osteoporosis, obesity, and iron deficient anemia (Chawla 2010; Wynn, Chawla et al. 2013). On the other hand, macrophages also play a crucial role in immune responses by eliminating the invading pathogen. Macrophages circulating in the blood are recruited to the infection site upon pathogen invasion where they serve as the first line of defense against pathogen infection. They ingest and eliminate the foreign pathogen which leads to subsequent activation of adaptive immune responses. Defects in pathogen elimination will lead to a high susceptibility to infectious agents such as tuberculosis and salmonella (Murray and Wynn 2011).

4.2. Receptor mediated Phagocytosis

Macrophages participate in tissue remodeling and pathogen clearance by engulfing extracellular particles through a highly regulated process called phagocytosis (Flannagan, Jaumouille et al. 2012). Phagocytosis is a receptor mediated event and can be divided into two separate sections. First, particle uptake/ingestion is initiated by particle binding to specific phagocytic receptors on the surface of the macrophages. Receptor activation triggers a cascade of signaling events to rapidly extend the plasma membrane around the particle(s). Plasma membrane extensions, called plasmalemmal pseudopods, form the phagocytic cups that ingest particles into vacuole-like structures, called phagosomes, within several minutes after particle binding (Niedergang and Chavrier 2004). The second phase is the phagosome maturation phase. After phagosome formation, the newly formed phagosome content resembles the extracellular space, which is not suitable for particle degradation. Therefore, the newly formed phagosomes undergo a series of membrane fusion and fission events that closely resembles the endocytosis pathway. These events are collectively referred to as phagosomal maturation (Vieira, Botelho et al. 2002). Once the phagosome formation is complete, the nascent phagosomes will fuse with the

early endosomal compartments and acquire early endosomal proteins such as EEA1 and RAB5-GTPase. The association of phagosomes with early endosomes is transient and they will eventually fuse with lysosomes to create a new hybrid organelle called phagolysosomes. Phagolysosomes acquire lysosomal properties, such as lysosomal proteins (Lamp-1 and RAB7-GTPase), hydrolase enzymes, and acidic pH, which allow particle degradation (Vieira, Botelho et al. 2002) (**Fig. 1.7**). Depending on particle size and the nature of the particle, phagosome maturation can take up to 30-45 minutes.

4.3. Membrane requirement for phagosome formation during phagocytosis

As mentioned in the previous section, phagocytosis is initiated by the binding of macrophage surface receptors to ligands on the surface of the particles (Aderem and Underhill 1999). Particles with different nature and origins can be taken up by macrophages; therefore it is not surprising that macrophages express a variety of phagocytosis specific receptors on their surface. But no matter what kind of particle is being ingested or what kind of receptor is being activated, particle binding induces the formation of pseudopod extensions around the particle (Aderem and Underhill 1999; Flannagan, Jaumouille et al. 2012), that leads to the internalization and the formation of phagosomes (Niedergang and Chavrier 2004). An extensive amount of plasma membrane is used during pseudopod extension. Therefore, a large amount of plasma membrane is internalized during receptor mediated phagtocytosis, especially when multiple and/or large particles are ingested (Braun and Niedergang 2006; Huynh, Kay et al. 2007). So, it is reasonable to assume that the overall cell surface area decreases during the ingestion of large or multiple particles. Although, a large amount of plasma membrane is internalized during phagocytosis, paradoxically, the overall surface area of the phagocytosing cells does not

decrease, and indeed increases significantly before the closing of the phagocytic cups (Holevinsky and Nelson 1998; Huynh, Kay et al. 2007).

How do macrophages compensate for the loss of plasma membrane during phagosome formation? It was originally suggested that because the macrophage's surface is ruffled, during particle ingestion the macrophage surface could potentially get stretched and the opening of the ruffled regions could compensate for the portion of plasma membrane used during phagosome formation. However, biological membranes lose their structural stability after they get stretched by about 4% of their original size (Hamill and Martinac 2001). Nonetheless, macrophages overall surface area was shown to increase by about 20% of its original size during the uptake of large particles (Hackam, Rotstein et al. 1998; Holevinsky and Nelson 1998). So the small amount of stretch available in plasma membrane is certainly not enough to compensate for the uptake of large particles. Interestingly, the increase in cell surface area was prevented by inhibitors of phosphatidylinositol 3-kinase, an enzyme critical for intracellular membrane trafficking, suggesting the involvement of intracellular membrane in pseudopod formation and cell expansion during phagocytosis (Cox, Tseng et al. 1999).

4.4 The role of Endo-lysosomal membrane in phagosome formation

In the past decade a new hypothesis has emerged suggesting that a pool of intracellular membranes fuse with the plasma membrane and provides the excess membrane necessary for pseudopod extension during particle uptake in phagocytosis (Braun, Fraisier et al. 2004; Braun and Niedergang 2006; Czibener, Sherer et al. 2006; Huynh, Kay et al. 2007) (**Fig. 1.8**). In agreement with this hypothesis, disruption of the membrane fusion machinery, such as the disruption of SNARE complexes, resulted in defective phagocytosis (Allen, Yang et al. 2002; Braun, Fraisier et al. 2004; Vinet, Fukuda et al. 2008).

Several different cellular compartments have been suggested to be the source of the excess membrane during phagocytosis; however, recent studies have demonstrated that endosomal/lysosomal compartments are one of the main sources to provide the excess membrane required for pseudopod formation (**Fig. 1.8**). Most evidence to support this notion is based on the appearance of organelle-specific markers at the site of particle uptake before or at the time of phagosome formation. By performing such experiments, it was first established that fusion of recycling endosomes with plasma membrane is necessary for phagosome formation. Several recycling endosome specific proteins, such as VAMP3 (Allen, Yang et al. 2002), ARF6 (D'Souza-Schorey, Li et al. 1995), Rab11 (Cox, Lee et al. 2000), and SytV (Vinet, Fukuda et al. 2008), have been identified to be involved in this process, where the absence of any of these proteins leads to defective phagosome formation and particle uptake.

In recent years several studies have demonstrated that, in addition to recycling endosomes, lysosomal fusion with the plasma membrane (lysosomal exocytosis) plays a role in phagosome formation (**Fig. 1.8**) (Braun, Fraisier et al. 2004; Czibener, Sherer et al. 2006; Huynh, Kay et al. 2007). Under such conditions, lysosomes are involved in the early steps of phagosome biogenesis/formation prior to the closing of the phagocytic cups. Fusion of lysosomes with the plasma membrane and the delivery of lysosomal membranes/proteins to the surface of the newly formed phagosomes are observed at the site of particle ingestion. Manipulations blocking lysosomal exocytosis significantly reduce particle uptake in macrophages (Braun, Fraisier et al. 2004; Czibener, Sherer et al. 2006; Huynh, Kay et al. 2007). VAMP7 is a specific late endosome/lysosome SNARE protein that was shown to be present at the site of particle uptake during particle ingestion. Also, cells deficient in VAMP7 have been shown to be defective in lysosomal exocytosis, pseudopod extension, and consequently particle

uptake (Braun, Fraisier et al. 2004). Recent studies have revealed that the lysosomal specific Ca^{2+} sensor SytVII regulates the fusion of VAMP7 containing vesicles with the plasma membrane. Macrophages isolated from SytVII KO mice have been shown to be defective in particle uptake. Interestingly, the defective uptake phenotype seen in SytVII KO macrophages is more severe and more apparent when macrophages are exposed to large number of particles or large sized particles (Czibener, Sherer et al. 2006), which is consistent with the requirement of lysosomal membrane delivery to the site of particle uptake when large particles are being ingested.

Although it is not clear what distinguishes between the recruitment of recycling endosomes and lysosomes to the site of uptake, present data collectively suggest that the fusion of lysosomes with the plasma membrane is on demand and happens when macrophages are exposed to large particle (> 3 μm) or numerous amount of particles at once. In contrast, recycling endosomes fuse with the plasma membrane only when small particles are being ingested (Huynh, Kay et al. 2007). This difference between lysosome and recycling endosome may be related to the amount of plasma membrane that is required to enclose the particle and form the phagosome (**Fig. 1.8**).

5. Phosphoinositides in cell regulation and membrane dynamics

Phosphatidylinositols (PtdIns) are a group of membrane phospholipids existing on the cytosolic side of cellular compartments. PtdIns are synthesized mainly in the endoplasmic reticulum (ER) and then delivered to other cellular compartments. Once the PtdIns are delivered to their final cellular compartments they get reversibly phosphorylated on their inositol ring at the positions 3, 4, and 5, resulting in the generation of seven phosphoinositides (PI) molecules

(P13P, PI4P, PI5P, PI(3,4)P_2, PI(3,5)P_2, P1(4,5)P_2, and PI(3,4,5)P_3) (Di Paolo and De Camilli 2006). PIs are low-abundance membrane lipids, each having a unique subcellular localization largely localized on the compartments within the endo-lysosomal pathway. PI4P and PI(4,5)P_2 are the most abundant PIs. They are primarily localized on the plasma membrane and participate in a variety of plasma membrane specific functions. In addition to the plasma membrane, PI4P is also localized on the Golgi membrane (Falkenburger, Jensen et al. 2010). PI3P is found on the cytoplasmic side of early and late endosomes and newly formed phagosomes and autophagosomes (Poccia and Larijani 2009). PI(3,5)P_2 is produced on late endosomes and lysosomes using PI3P as the substrate (Zhang, Zolov et al. 2007; Zolov, Bridges et al. 2012). PI(3,4)P_2 and PI(3,4,5)P_3 are generated transiently upon activation of plasma membrane receptors (Falkenburger, Jensen et al. 2010).

PIs can regulate membrane trafficking through at least two mechanisms. First, they recruit a variety of cytoplasmic effector proteins to specific organelles that facilitate membrane trafficking (Falkenburger, Jensen et al. 2010). These proteins must be recruited to each organelle at a very precise time in order to mediate membrane trafficking events. Rapid production and elimination of specific phosphoinositides by their regulatory enzymes provides an effective mechanism for this purpose. For example, PI3P on the surface of the early endosomes have been shown to be responsible for the recruitment of EEA1 to the surface of the early endosomal compartments (Zhang, Zolov et al. 2007; Zolov, Bridges et al. 2012). EEA1 is a tethering molecule that couples vesicle docking with SNAREs in order to facilitate the transition from early to late endosomes (Mills, Jones et al. 1999). Second, PIs can directly bind and regulate the activity of different membrane proteins, such as ion channels, on the surface of the organelles potentially inducing membrane trafficking (Falkenburger, Jensen et al. 2010) For example, many

plasma membrane ion channels have been shown to be activated by $PI(4,5)P_2$ (Di Paolo and De Camilli 2006). In addition, as mentioned before, the lysosomal Ca^{2+} channel TRPML1 has been shown to be activated by $PI(3,5)P_2$ on the surface of the lysosomes and inactivated by $PI(4,5)P_2$ on the plasma membrane (Zhang, Li et al. 2012). Therefore, PIs have the ability to regulate organelle specific membrane trafficking events by recruiting trafficking specific proteins at the right time or directly activate molecules involved in trafficking.

6. The central goal of this study

New emerging data suggest that TRPML1 induced lysosomal Ca^{2+} release is involved in regulating lysosomal membrane trafficking events in various cell types, however, direct evidence to support this notion is still lacking. The overall goal of this work is to investigate the involvement of TRPML1 and lysosomal Ca^{2+} release in lysosomal membrane trafficking in macrophages. Here I first sought to investigate the direct involvement of TRPML1 in lysosomal exocytosis after acutely activating TRPML1 by its specific activator (Chapter II). Then, I investigating the role of TRPML1 in particle ingestion in macrophages, which is known to be dependent on Ca^{2+} dependent lysosomal exocytosis, by using mouse knockouts and synthetic agonists/antagonists of TRPML1 (Chapter III). Furthermore, I examined the activation mechanism of TRPML1 during lysosomal exocytosis and particle uptake (Chapter IV). In addition to the role of TRPML1 in lysosomal exocytosis, I also inspected the role of TRPML1 in late endocytic trafficking events in macrophages (Chapter VI).

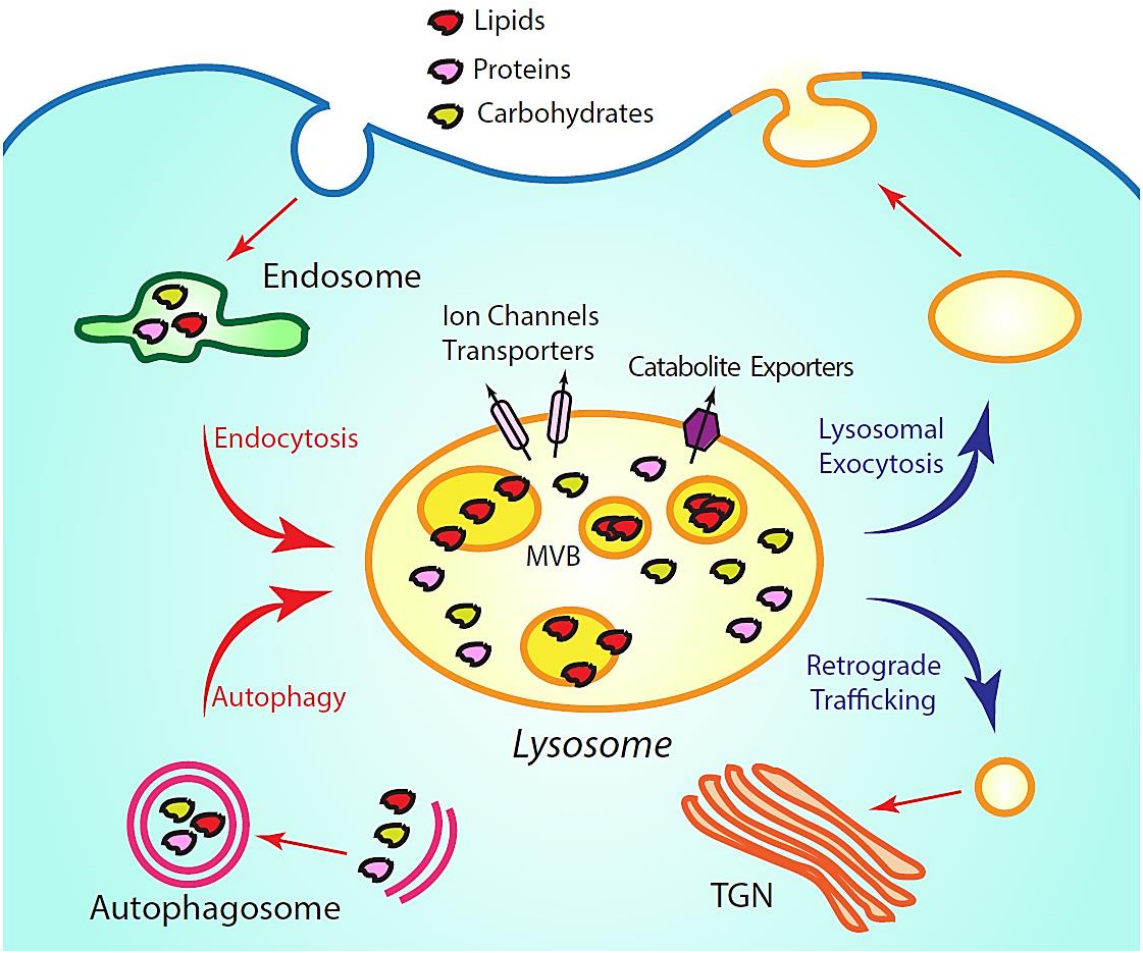

Figure 1.1 Major trafficking routes in and out of the lysosomes.

Lysosomes receive inputs from both endocytic and autophagic pathways. Endocytosed cargo including membranes, complex lipids, membrane proteins, and polysaccharides enter the endocytic pathway first to early endosomes and then intraluminal vesicle-containing late endosomes (MVBs). Late endosomes then fuse with lysosomes to form endolysosome hybrids. Damaged intracellular organelles enter the autophagic pathway in autophagosomes, which then fuse with lysosomes to form autolysosomes. Endocytosed and autophagocytosed cargo are degraded in endolysosomes and autolysosomes through lysosomal hydrolases. The resulting products are building-block precursor molecules for complex macromolecules. These catabolites are transported out of the lysosomes via specific exporters. Insoluble catabolites, such as lipids, can be transported to the Golgi apparatus for reutilization via the retrograde trafficking pathway. Alternatively, degradation products can also be released into the extracellular medium via lysosomal exocytosis. Lysosomal ion homeostasis and membrane trafficking are regulated by lysosomal ion channels and transporters on the perimeter membrane.

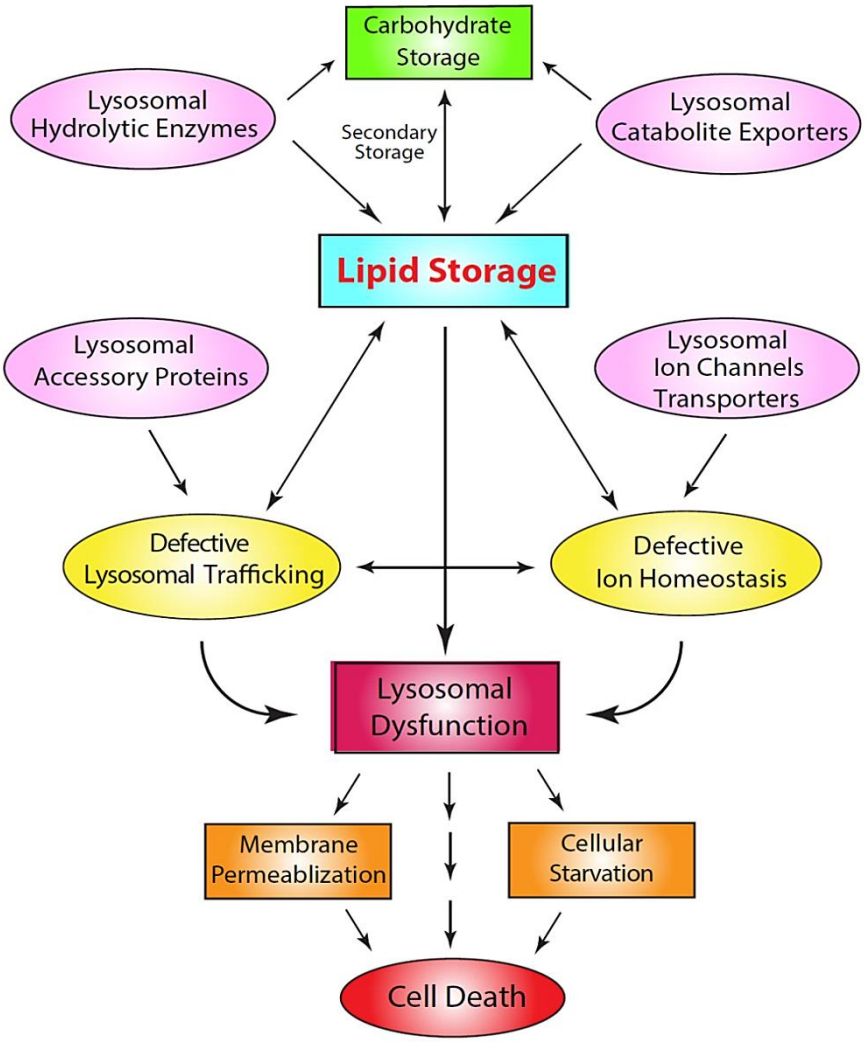

Figure 1.2 Mechanisms leading to lysosomal storage disorders and their cellular consequences.

Lysosome Storage Diseases (LSDs) are characterized by the progressive build-up of undigested materials, such as lipids or carbohydrates, within the lysosomes. Mutations in lipases, lipid phosphatases, and carbohydrases lead to the accumulation of undigested lipids and carbohydrates in the lysosome. Likewise, mutations in the catabolite exporters also lead to the accumulation of lipids and carbohydrates in the lysosome. Mutations in lysosomal accessory proteins lead to lysosomal trafficking defects. Mutations in lysosomal ion channels and transporters lead to defective ion homeostasis, which in turn affects membrane trafficking to cause lipid accumulation. Lipid storage causes "traffic jam" and secondary accumulation, resulting in lysosomal dysfunction, membrane permeabilization, and cellular starvation. Lysosomal membrane permeabilization may cause leakage of lysosomal enzymes into the cytoplasm to cause cell dearth

.

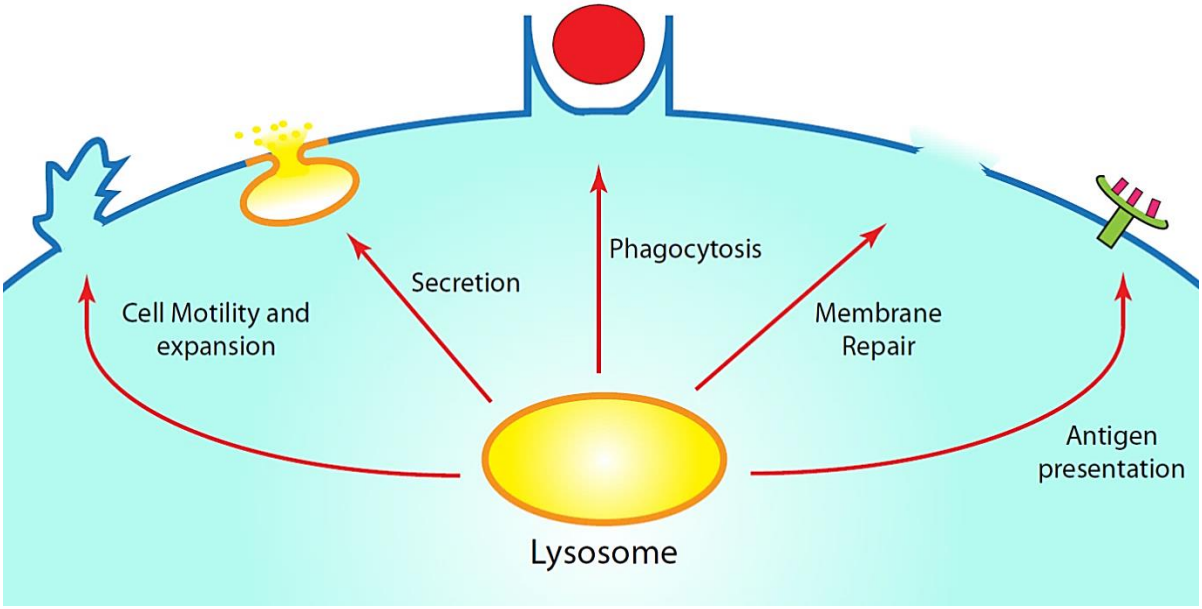

Figure 1.3 Processes known to be regulated by lysosomal exocytosis.

Lysosomal exocytosis has been shown to mediate several different biological functions in different cell types. Lysosomal exocytosis has been shown to be implicated in cell motility and expansion in cancer cells. In immunological cells, lysosomal exocytosis has been shown to be critical for several processes such as content secretion, antigen presentation and large particle ingestion through phagocytosis. Also, lysosomal exocytosis has been shown to be crucial for membrane repair in muscle cells.

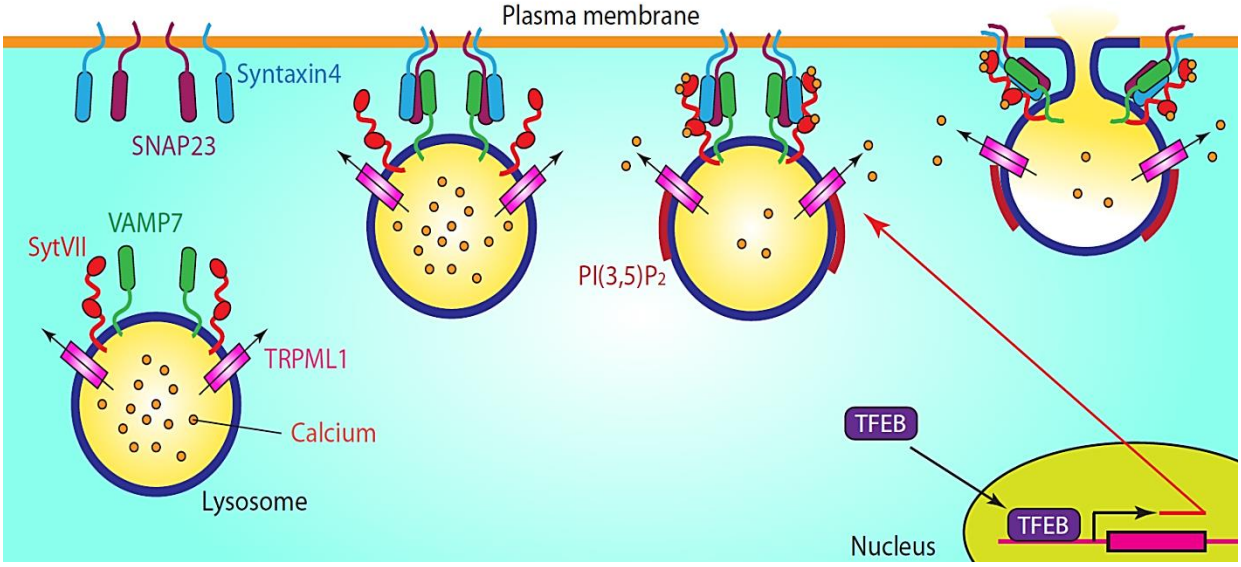

Figure 1.4 The core molecular machinery involved in lysosomal exocytosis.

Upon stimulation, VAMP7 on the surface of lysosomes interact with Syntaxin 4 and SNAP23 on the inner side of the plasma membrane to form the trans-SNARE complex. The formation of the trans-SNARE complex pulls lysosomes close to the plasma membrane and docks lysosomes on the inner side of the plasma membrane. The activity of Ca^{2+} sensor SytVII is required to initiate the final fusion step. The production of $PI(3,5)P_2$ on the fusing lysosomes induces the activation of the lysosomal Ca^{2+} channel TRPML1 and the release of lysosomal Ca^{2+} into the close vicinity of the fusion site. Ca^{2+} release mediates the activation of SytVII and the induction of lysosomal fusion with the plasma membrane. The transcription factor TFEB has been shown to regulate lysosomal exocytosis by mediating the docking and fusion steps through regulation of the expression of several proteins involved in lysosomal exocytosis machinery such as TRPML1.

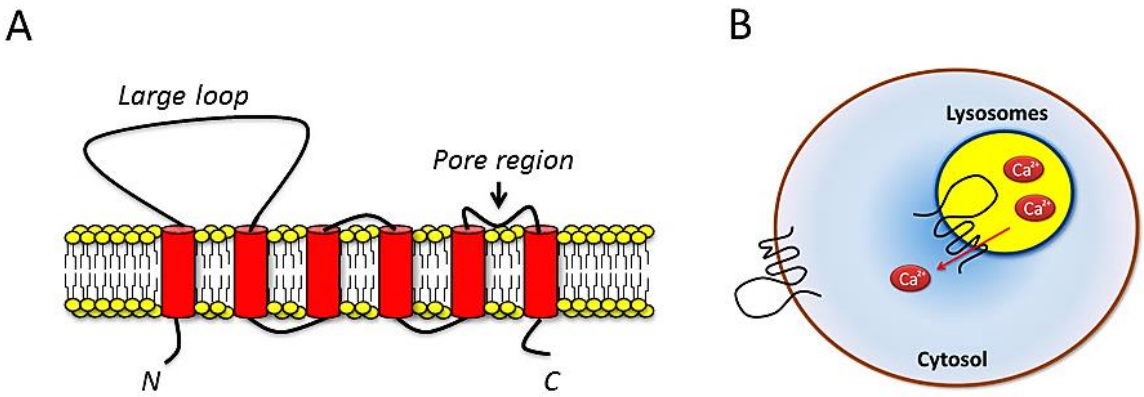

Figure 1.5 Schematic diagram of TRPML protein structure and molecular orientation.

(A) The putative membrane topology of TRPML1 proteins. TRPML1 is made of six transmembrane (TM) domains. There is large extra cellular loop between TM1 and TM2 and the predicted pore region between TM5 and TM6. (B) The proposed localization of TRPML at the plasma membrane and the membrane of lysosomes. Both N and C terminals face the intracellular region when the channel is located either at the cell membrane or at the lysosomes. TRPML activation leads to the release of cations, such as Ca^{2+} from the lumen of the lysosomes into the cytoplasm.

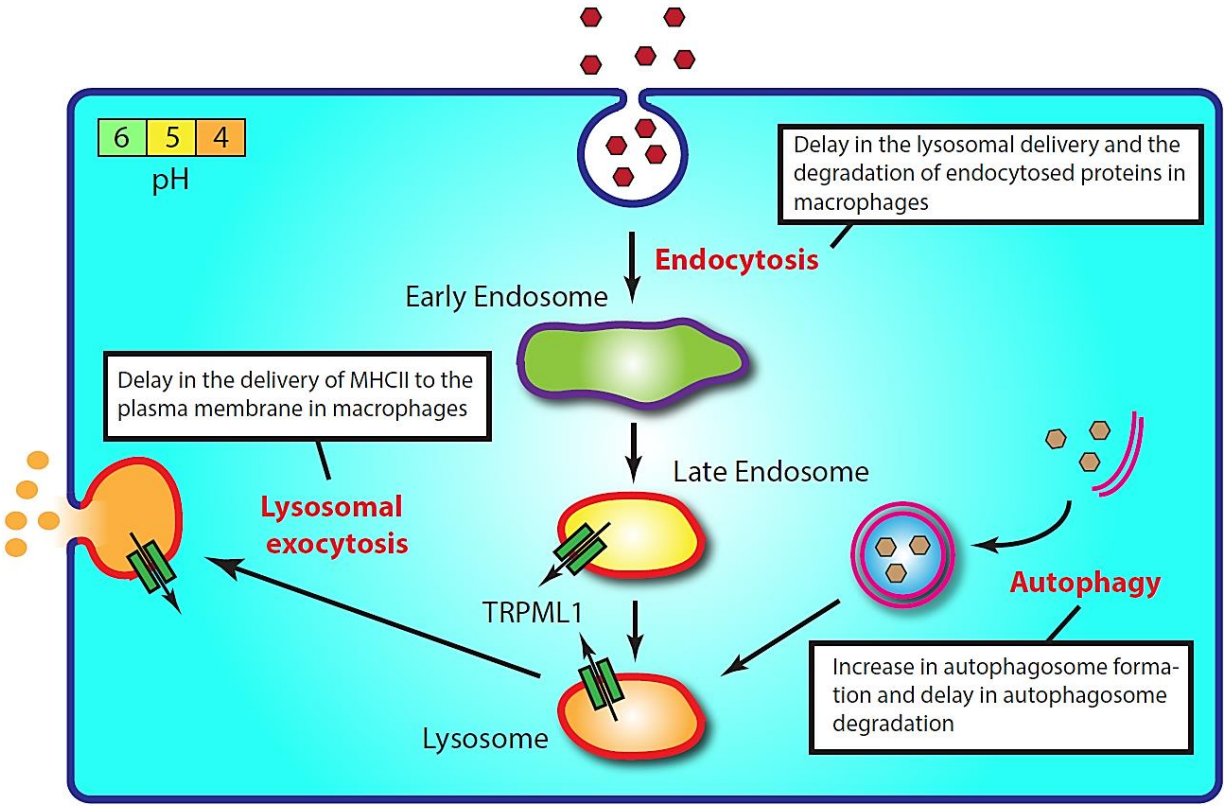

Figure 1.6 Lysosomal trafficking defects observed in TRPML1 KO cells

Cells lacking TRPML1 have been shown to be defective in several different lysosomal membrane trafficking pathways. The delivery of ingested materials through receptor mediated endocytosis has shown to be defective in TRPML1 KO cells late in the lysosomal pathway. Additionally, autophagosome fusion with lysosomes and subsequent degradation of autophagic materials has been shown to be defective in cells isolated from MLIV patients, leading to the accumulation of cellular waste in the cells. Also, Ca^{2+} dependent lysosomal exocytosis shown to be inhibited in TRPML1 KD immune cells resulted in decreased lysosomal dependent antigen presentation and secretion.

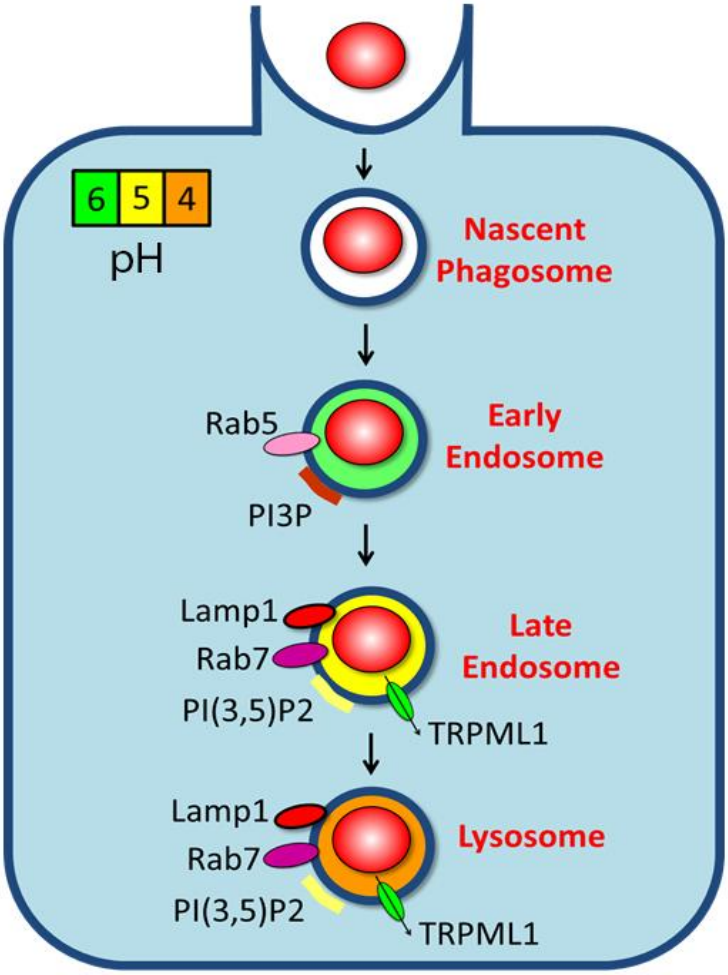

Figure 1.7 Schematic diagram of Receptor mediated phagocytosis

Diagram illustrating some of the known molecular events that dictate phagosomal maturation process. After the formation of the nascent phagosome they first acquire Rab5, which recruits VPS34 (not shown) to generate PI3P on the surface of the phagosomes. Subsequently, phagosomes acquire late endosome/lysosomal markers such as Rab7, Lamp-1, and TRPML1. The pH of the phagosomal lumen is gradually decreased which allows for the degradation of ingested particle. On the surface of the lysosomes the kinase PIKfyve (not shown) is recruited, which generates $PI(3,5)P_2$ from PI3P on the surface of the lysosomes.

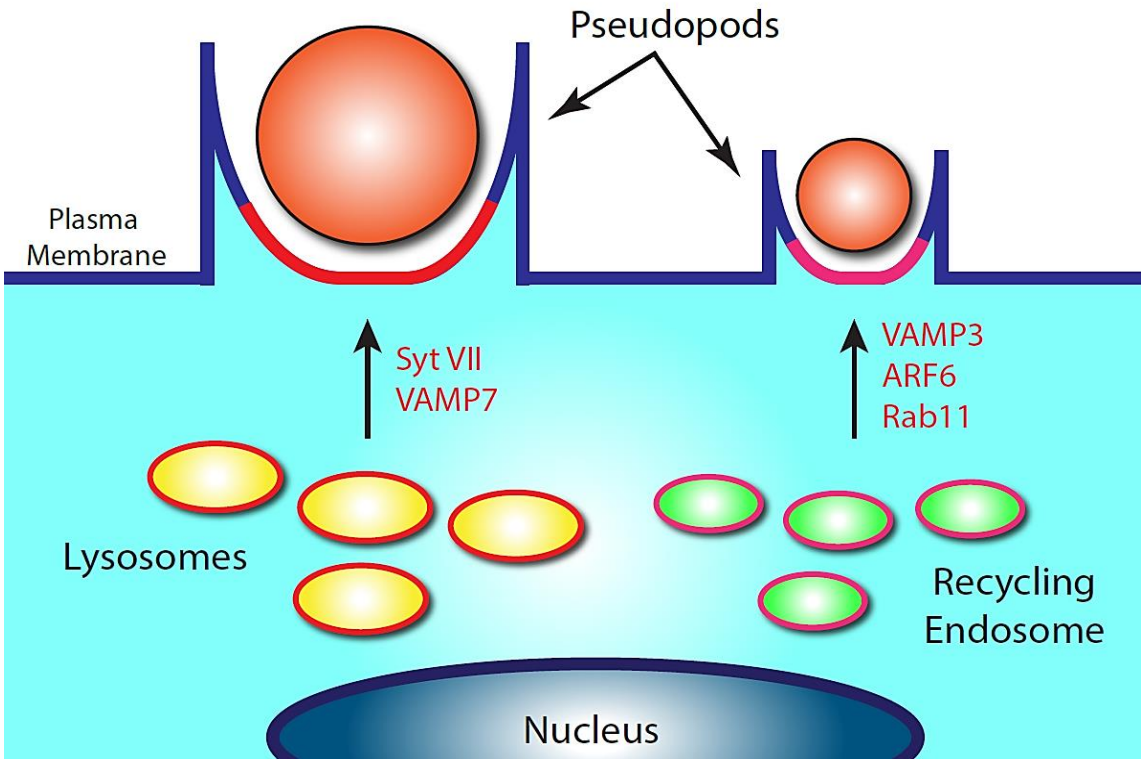

Figure 1.8 Sources of membrane delivered to the phagocytic cup

During particle uptake recycling endosomes are recruited to the site of small particle ingestion and they have been shown to be the primary source of membrane for the enlargement of the phagocytic cup and pseudopods formation. The translocation of recycling endosomes has shown to be regulated by several proteins such as VAMP3, Rab11, and ARF6. In contrast to the uptake of small particles, lysosomes have been shown to be drafted to the site of large particle uptake through lysosomal exocytosis. Lysosomes fuse with the plasma membrane and as a result lysosomal membrane and membrane integral proteins get translocated to the phagocytic cup. This has been shown to be facilitated by the function of VAMP7 and the lysosomal Ca^{2+} sensor SytVII.

CHAPTER II

TRPML1 ACTIVATION IS REQUIRED FOR LYSOSOMAL EXOCYTOSIS IN MACROPHAGES

Abstract

Fusion of lysosomes with the plasma membrane, i.e, lysosomal exocytosis, has been shown to play a critical role in several physiological processes such as plasma membrane repair, particle uptake, and cytokine secretion. Lysosomal exocytosis is known to be induced by the rise of intracellular Ca^{2+} concentrations, but the source of Ca^{2+} and the underlying Ca^{2+} channel(s) involved in this process remain elusive. Mucolipin TRP channel 1 (TRPML1) is a member of the TRP ion channel super-family known to be localized on the surface of the lysosomes. Here I found that the activation of TRPML1 by a potent TRPML1-specific membrane-permeable small-molecule agonist is sufficient to induce lysosomal Ca^{2+} release and thus lysosomal exocytosis in wild type cells. Furthermore, lysosomal exocytosis was defective in TRPML1 KO cells. Additionally, TRPML1 induced lysosomal exocytosis was shown to depend on the presence of the lysosomal specific phosphoinositide $PI(3,5)P_2$, suggesting that the production of $PI(3,5)P_2$ could potentially trigger lysosomal exocytosis.

Introduction

Lysosomes, the cell's recycling centers, are required for cells to eliminate waste materials and cellular debris (Kornfeld and Mellman 1989). Recent evidence, however, suggest that lysosomes are also involved in mediating membrane trafficking events and cellular signaling (Luzio, Pryor et al. 2007; Ballabio and Gieselmann 2009). Accumulated evidence has shown that lysosomes undergo exocytosis in response to an increase in intracellular Ca^{2+} levels in most cell types across the body (Coorssen, Schmitt et al. 1996; Andrews 2000; Reddy, Caler et al. 2001). Lysosomal exocytosis has been shown to play an important role in numerous physiological processes, such bone resorption in osteoclasts (Mostov and Werb 1997), plasma membrane repair in muscle fibers (Reddy, Caler et al. 2001), neurite outgrowth (Arantes and Andrews 2006), axonal remyelination in Schwann cells (Chen, Zhang et al. 2012), particle uptake (Czibener, Sherer et al. 2006) and antigen presentation (Cresswell 1994) in macrophages. Although, the Ca^{2+} dependence of lysosomal exocytosis has been known for years (Rodriguez, Webster et al. 1997) the source of Ca^{2+} responsible for providing the Ca^{2+} necessary for lysosomal exocytosis is elusive. Because the lysosomal lumen is believed to be the main source of Ca^{2+} for Ca^{2+}-dependent vesicular trafficking along the late endocytic pathways (Luzio, Rous et al. 2000; Luzio, Bright et al. 2007; Luzio, Pryor et al. 2007), it is possible that lysosomes themselves provide the Ca^{2+} required for lysosomal exocytosis. However, definitive evidence to support this hypothesis is still lacking, and more importantly, the ion channel(s) responsible for Ca^{2+} release remain unknown.

TRPML1 is Ca^{2+} channel on the surface of the lysosomes responsible for the release of Ca^{2+} from the luminal side of the lysosomes into the cytoplasm (Cheng, Shen et al. 2010; Dong, Shen et al. 2010). Human mutations of TRPML1 cause mucolipidosis type IV (MLIV), a

childhood neurodegenerative disorder with lysosomal trafficking defects at the cellular level (Bach 2001; Bargal, Avidan et al. 2001; Altarescu, Sun et al. 2002). Several lines of evidence suggest that TRPML1 plays a role in mediating lysosomal exocytosis (LaPlante, Sun et al. 2006; Dong, Wang et al. 2009). However, they all fail to establish a direct connection between TRPML1 activity and lysosomal exocytosis. By using TRPML1-specific activator, with TRPML1 KO as controls, I have shown that the acute activation of TRPML1 channel increases lysosomal exocytosis. Thus for the first time, my study provides direct evidence to show the importance of TRPML1 in lysosomal exocytosis

Methods

Macrophage cell culture. Murine bone marrow derived macrophages (BMMs) were prepared and cultured as described previously (Link, Park et al. 2010). Briefly, bone marrow cells from mouse femurs and tibias were harvested and cultured in macrophage differentiation medium (RPMI-1640 medium with 10% fetal bovine serum) and 100 unit/ml recombinant colony stimulating factor (PeproTech, Rocky Hill, NJ). After 7 days in culture at 37 °C with 5% CO_2, the adherent cells (> 95% are expected to be macrophages) were harvested for assays. RAW 264.7, RAW cells stably-expressing TRPML1 (ML1 overexpression or O/E), and RAW cells stably-expressing TRPML1-specific RNAi (ML1 knockdown or KD) (Thompson, Schaheen et al. 2007) were kindly provided by Dr. Hanna Fares (University of Arizona). Cells were cultured in DMEM/F12 media supplemented with 10% FBS at 37°C and 5% CO_2. BMM and RAW macrophages were transfected using electroporation (Invitrogen Neon Transfection System) according to the manufacture procedures. Briefly, cells were harvested and washed with PBS (Ca^{2+} and Mg^{2+}-free) once to remove DMEM. Cells were then centrifuged and the pellets were re-suspended in the R buffer. 2 μg of DNA per well was added to the cells, then gently mixed

and placed in the Neon System pipette. The electroporation was performed using program # 6 for RAW cells and program # 18 for BMMs, respectively. Transfected cells were then recovered with 500 µl of culture media in each plate.

Whole-endolysosome electrophysiology. Endolysosomal electrophysiology was performed in isolated endolysosomes using a modified patch-clamp method as described previously (Dong, Cheng et al. 2008; Dong, Shen et al. 2010). Briefly, cells were treated with 1 µM vacuolin-1 for 2-5h to increase the size of endosomes and lysosomes. Whole-endolysosome recordings were performed on isolated enlarged endolysosomes. The bath (internal/cytoplasmic) solution contained 140 mM K-gluconate, 4 mM NaCl, 1 mM EGTA, 2 mM Na2-ATP, 2 mM MgCl2, 0.39 mM CaCl2, 0.2 mM GTP, and 10 mM HEPES (pH adjusted with KOH to 7.2; free [Ca2+]i was estimated to be ~ 100 nM using the Maxchelator software (http://maxchelator.stanford.edu/)). The pipette (luminal) solution consisted of a 'Low pH Tyrode's solution' with 145 mM NaCl, 5 mM KCl, 2 mM CaCl2, 1 mM MgCl2, 10 mM HEPES,10 mM MES, and 10 mM glucose (pH 4.6). All bath solutions were applied through a perfusion system to achieve a complete solution exchange within a few seconds. Data were collected using an Axopatch 2A patch clamp amplifier, Digidata 1440, and pClamp 10.0 software (Axon Instruments). Currents were digitized at 10 kHz and filtered at 2 kHz. All experiments were conducted at room temperature (21-23 ºC) and all recordings were analyzed with pClamp 10.0, and Origin 8.0 (OriginLab, Northampton, MA).

Flow cytometry. BMMs were trypsinized and washed with PBS before incubation with ML-SA1(10 µM) at 37°C for 30 min. Cells were then washed and re-suspended in 1% BSA with anti-mouseLamp1 (1D4B) antibody on ice for 45 min. After this cells were fixed in 2% PFA for 30 min and then incubated with Alexa-546 conjugated anti–mouse secondary antibody at room temperature for 1h. Macrophages were then re-suspended in 0.5 ml PBS and analyzed on a FACS Flow

Cytometer. At least 10,000 cells per experiment were analyzed for the forward angle scatter, the right angle scatter, and the fluorescence intensity.

Lysosomal enzyme release/activity. After incubation with ML-SA1 or IgG-RBCs, the culture medium was collected for acid phosphatase (AP) activity measurement. AP activity was measured using an AP colorimetric assay kit, which uses p-nitrophenyl phosphate (pNPP) as a phosphatase substrate that turns yellow at a wavelength of 405 nm when dephosphorylated by AP. Lactate dehydrogenase (LDH) activity was measured using a LDH-Cytotoxicity Assay Kit.

Fluorescent microscopy and surface staining. Lamp-1 surface expression was detected in non-permeabilized WT and TRPML1 KO macrophages. After each treatment, cells were washed with ice cold PBS and live cells were stained with 1D4B anti–mouse Lamp1 monoclonal antibody (Iowa Hybridoma Bank), which recognizes the luminal epitope of mouse Lamp1. In order to detect surface Lamp-1, non-permeablized live cells were first exposed to Lamp-1 primary antibody for 3 hours, followed by anti-rat secondary antibody for another 2 hours (all at 4°C). Then cells were fixed with 4% PFA and stained again with the same antibody overnight to detect the total amount of lamp-1 (intracellular + surface).

Real-Time Semi-quantitative PCR. Total RNA was extracted from bone marrow-derived macrophages (BMMs) and dissolved in TRIzol (Invitrogen). First strand cDNA, synthesized using Superscript III RT (Invitrogen), was used for Semi-quantitative PCR (Bio-Rad iQ iCycler) analysis of ML1 expression based on the following intron-spanning primer pair: Forward: AAACACCCCAGTGTCTCCAG; Reverse: GAATGACACCGACCCAGACT

Results

Isolation and characterization of TRPML1 KO bone marrow macrophages

To study the role of TRPML1 in lysosomal exocytosis, I isolated monocytes from the bone marrow of wild-type (WT) and TRPML1 knockout (KO) mice (Venugopal, Browning et al. 2007). Monocytes were incubated with macrophage specific growth factors for 5 days at 37°C to allow the maturation of monocytes to bone marrow derived macrophages (BMMs) (Chow, Downey et al. 2004). TRPML1 KO BMMs contained no detectable level of full-length TRPML1 transcript, as shown by RT-PCR analysis (**Fig. 2.1A**). Consistent with this, direct patch-clamping of the endolysosomal membranes showed that ML-SA1, a membrane-permeable TRPML1 specific synthetic agonist (Shen, Wang et al. 2012), and $PI(3,5)P_2$, an endogenous activator of TRPML1 (Dong, Shen et al. 2010), activated whole-endolysosome TRPML1-like currents (I_{ML1}) in WT, but not TRPML1 KO BMMs (**Fig. 2.1B**) indicating the absence of a functional TRPML1 protein in TRPML1 KO BMMs. In contrast, no significant differences were noted in cell morphology, cell size, and CD11b (macrophage-specific surface receptor) immunoreactivity between WT and TRPML1 KO BMMs (**Fig. 2.1C**).

Activation of TRPML1 leads to Ca^{2+}-dependent lysosomal exocytosis in macrophages

To directly investigate the role of TRPML1 in lysosomal exocytosis, I acutely activated TRPML1 using ML-SA1 and evaluated lysosomal exocytosis by using Lamp1 surface immunostaining with the TRPML1 KO as a negative control. After lysosomal exocytosis, luminal lysosomal membrane proteins can be detected on the extracellular side of the plasma membrane. The surface expression of Lamp1 can be detected using a monoclonal antibody (1D4B) against a luminal epitope of Lamp1 on non-permeabilized cells (Reddy, Caler et al.

2001). To obtain a direct comparison with total (surface + intracellular) Lamp1 proteins, the same cells were then permeabilized and stained with the same primary antibody but a distinct secondary antibody. After incubation with the agonist, ML-SA1, for 30 min, WT, but not TRPML1 KO BMMs, exhibited a marked increase in Lamp1 staining (**Fig. 2.2A**) at the cell surface, which was shown using the plasma membrane marker DiI-C18(3) (**Fig. 2.2B**). Interestingly, although Lamp1-positive compartments were compensatory up-regulated in TRPML1 KO BMMs, much less ML-SA1-induced Lamp1 surface staining was seen in the same cells (**Fig. 2.2A**). Consistently, flow cytometry-based quantitative analysis demonstrated a ML-SA1-induced increase in Lamp1 surface staining in WT but not TRPML1 KO BMMs (**Fig. 2.2C&D**). ML-SA1-induced Lamp1 surface staining in WT BMMs was completely abolished after pre-treatment with the fast Ca^{2+} chelator BAPTA-AM (**Fig. 2.2C**). Collectively, these results suggest that the channel activity of TRPML1 is required for lysosomal exocytosis in macrophages in a Ca^{2+}-dependent manner.

Upon lysosomal exocytosis, lysosomal hydrolytic enzymes, such as acid phosphatases (APs), are released into the extracellular medium (Reddy, Caler et al. 2001). Thus, measuring the AP activity of the supernatant can provide a specific readout for lysosomal exocytosis. Incubation with ML-SA1 (1 or 10 μM for 15 and 30 min) caused a significant increase in the AP release/activity in WT but not TRPML1 KO BMMs (**Fig. 2.3A&B)**. In contrast, no release (activity) was detected for the cytosolic enzyme lactate dehydrogenase (LDH) indicating that the release of lysosomal enzymes was not due to cell damage (**Fig. 2.3C)**. Treating cells with Ca^{2+} ionophore ionomycin induced a large AP release in TRPML1 KO BMMs suggesting that the exocytosis machinery was operative (**Fig. 2.3D)**. BAPTA-AM treatment largely abolished ML-SA1-induced AP release in WT BMMs (**Fig. 2.3E)**, whereas removing extracellular Ca^{2+} only

had a minor effect on agonist-induced lysosomal AP release (**Fig. 2.3E)**. This suggests that lysosomal exocytosis is triggered by intracellular (lysosomal) TRPML1 mediated Ca^{2+} release under physiological conditions.

$PI(3,5)P_2$ is required for TRPML1 induced lysosomal exocytosis

The lysosomal specific phosphoinositied $PI(3,5)P_2$ has been shown to be the endogenous activator for TRPML1 on the surface of the lysosomes (Dong, Shen et al. 2010). $PI(3,5)P_2$ is produced by the kinase PIKfyve in association with the phosphatase FIG4 and the scaffolding protein Vac14 (Duex, Nau et al. 2006; Duex, Tang et al. 2006). Genetic or chemical disruption of any of these components results in decreased $PI(3,5)P_2$ levels within the cells and consequently defective lysosomal related trafficking events (Zolov, Bridges et al. 2012). In correlation with the role of TRPML1 in lysosomal exocytosis, macrophages isolated from FIG4 KO mice were also defective in ML-SA1 induced lysosomal exocytosis (**Fig. 2.3F**) indicating the crucial role of TRPML1 in lysosomal exocytosis.

Lysosomal exocytosis levels correlates with TRPML1 expression/activity

I also examined lysosomal exocytosis in the RAW 264.7 macrophage cell line as well as RAW cell lines stably expressing TRPML1 (ML1 overexpression or O/E) or TRPML1-specfic RNAi (ML1 knockdown or KD) (Thompson, Schaheen et al. 2007). TRPML1 expression levels in these three cell lines were confirmed using whole endolysosome recordings (**Fig. 2.4A**) and RT-PCR analysis (**Fig. 2.4B**). Interestingly, stably-expressing TRPML1 in RAW 264.7 cells (ML1 O/E cells) resulted in a higher level of ML-SA1-induced AP release compared with cells expressing only endogenous TRPML1 or stably-expressing TRPML1-specific RNAi (TRPML1

KD cells) (**Fig. 2.4C**). These findings established a correlation between the expression level and channel activity of TRPML1 and lysosomal exocytosis in macrophages.

Discussion

By using a TRPML1 specific activator and TRPML1 KO cells, for the first time, I showed the direct involvement of TRPML1 in lysosomal exocytosis. Several lines of evidence suggested TRPML1 plays a role in mediating lysosomal exocytosis. Fibroblast cells obtained from MLIV patients were shown to be defective in ionomycin-induced lysosomal exocytosis (LaPlante, Sun et al. 2006). However, ionomycin induces Ca^{2+} flux non-physiologically independent of any specific ion channels. Therefore, the effect of ionomycin on lysosomal exocytosis could be a secondary observation, since ionomycin presumably provides the Ca^{2+} for the activation of SytVII non-physiologically (Rodriguez, Webster et al. 1997; Rodriguez, Martinez et al. 1999; Reddy, Caler et al. 2001), thereby bypassing upstream TRPML1 activation. Later experiments demonstrated that the heterologous expression of the gain-of-function mutant TRPML1 enhanced lysosomal exocytosis in HEK293 cell. These experiments were performed using a Ca^{2+}-free extracellular solution, hence, the gain-of-function mutant TRPML1 construct most likely induced Ca^{2+} release from internal sources (Dong, Wang et al. 2009). In addition, the shRNA knockdown of TRPML1 in macrophage cell lines delayed the transport of the Major Histocompatibility Complex II (MHCII) from LEL compartments to the plasma membrane in response to immune stimulations, a process that has been known to be dependent on lysosomal exocytosis (Thompson, Schaheen et al. 2007). Collectively, these data suggest that TRPML1 is involved in regulating lysosomal exocytosis; however, all these studies failed to illustrate the direct and acute involvement of TRPML1 in lysosomal exocytosis.

By using the TRPML1 small molecule specific activator (ML-SA1) (Shen, Wang et al. 2012), I was able to directly induce lysosomal exocytosis in macrophages by activating the endogenous TRPML1. ML-SA1 was also able to induce Lamp-1 whole cell surface staining while it had no effect on TRPML1 KO macrophages, illustrating the specificity of ML-SA1. Moreover, ML-SA1 induced lysosomal exocytosis was abolished by BAPTA-AM while the extracellular EGTA had a minor effect. Collectively, these data indicate that the direct activation of TRPML1 on the surface of lysosomes is able to induce lysosomal exocytosis and provides definitive evidence that lysosomal Ca^{2+} is responsible for the induction of lysosomal exocytosis. TRPML1 activation most likely is one of the last steps in the overall lysosomal exocytosis machinery since Ca^{2+} is required post SNARE complex formation and is required for the activation of SytVII in order to facilitate fusion (Chapter I).

Although it is clear that lysosomes can undergo Ca^{2+} dependent exocytosis, it is not clear what percentage of the total lysosome population can be docked and undergo exocytosis upon stimulation in different cell types (Andrews 2000; Jaiswal, Andrews et al. 2002). It remains to be investigated whether all lysosomes respond equally to different stimuli or if there is a subpopulation of lysosomes specifically designated for lysosomal exocytosis in different cell types. Lysosomes are generally generated through two main processes within cells; endocytosis and autophagy (**Fig. 2.5**). It is not clear what percentage of a cell's total lysosomal population is generated from each pathway, nor is not known if lysosomes generated from one pathway are more responsive to lysosomal exocytosis stimulation (**Fig. 2.5**). Moreover, lysosomal mobility may be a key determinant of lysosomal docking and hence the size of the releasable lysosome pool. On the other hand, the nature of the stimulus may determine the size of the releasable pool. While activation of TRPML1 promotes post-docking fusion, TFEB regulates both lysosomal

docking and fusion (Medina, Fraldi et al. 2011). In NRK and MEF cells, under normal conditions, only about 10-15% of total lysosomal β-hexosaminidase can be released by ionomycin within minutes (Rodriguez, Webster et al. 1997). In macrophages, however, up to 40-50% of total lysosomal acid phosphatases were releasable by ionomycin (**Fig. 2.3 D**). As lysosomal enzyme release is an accumulative assay, a high level of lysosome mobility known to be associated with macrophages (Mrakovic, Kay et al. 2012) may account for the observed differences in the releasable pool. An outstanding question is whether an increase in the fusion of lysosomes with the plasma membrane has any feedback effects that could potentially facilitate lysosomal mobility and docking. Even more generally, how do cells determine the size, location, and number of lysosomes? It appears that the nutrient-sensing machinery in the lysosome, including mTOR and TFEB, plays a critical role in regulating these basic parameters for lysosomes (Settembre, Fraldi et al. 2013).

Emerging data in the past decade has changed the traditional view of lysosomes dramatically. Lysosomes were originally thought to be the dead-end of degradation pathways, however, recent data has illustrated that they play an active role in several cellular processes. The discovery of lysosomal exocytosis demonstrated that, unlike other cellular organelles, lysosomes are extremely dynamic compartments in the cell. They are constantly derived through endocytosis and/or autophagic pathways via the maturation of the late endosome or autophagosomes. Meanwhile they are consumed through lysosomal exocytosis where they fuse with the plasma membrane. It is critical for cells to maintain a balance between these two processes, endocytosis and exocytosis, as defects in either of them has been shown to result in an accumulation of lysosomal substances materials and dysfunctional lysosomes.

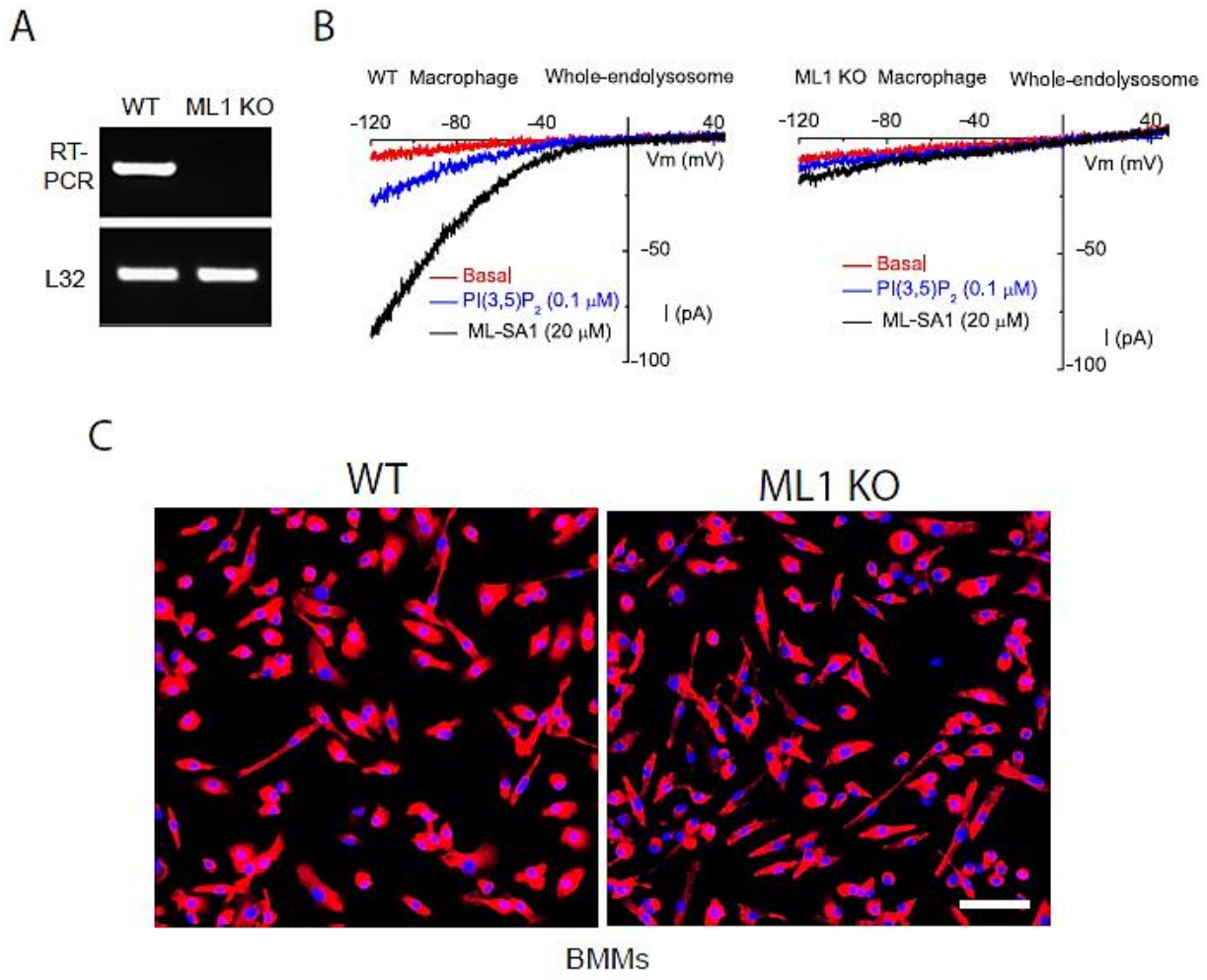

Figure 2.1 Isolation of TRPML1 KO macrophages.

(A) RT-PCR analysis of wild-type (WT) and TRPML1 KO (ML1 KO) bone marrow-derived macrophages (BMMs) using a primer pair targeting the deleted region (exons 3, 4, and 5) of the TRPML1 gene. The housekeeping gene L32 served as a loading control. (B) ML-SA1 and $PI(3,5)P_2$ robustly activated endogenous whole endolysosome ML1-like currents in WT but not ML1 KO BMMs. (C) Mature monocytes isolated from WT and ML1 KO mouse bone marrow had similar morphological characteristics, as revealed by CD11b (mature macrophage-specific surface receptor) staining. Scale bar = 30 μm. Isolated monocytes were cultured in DMEM/F12 and recombinant colony stimulating factor for 5-7 days and then fixed and stained with anti-CD11b antibody and DAPI to show cell's nucleus (blue). Electrophysiology experiments in section B were performed in collaboration with Xiaoli Zhang.

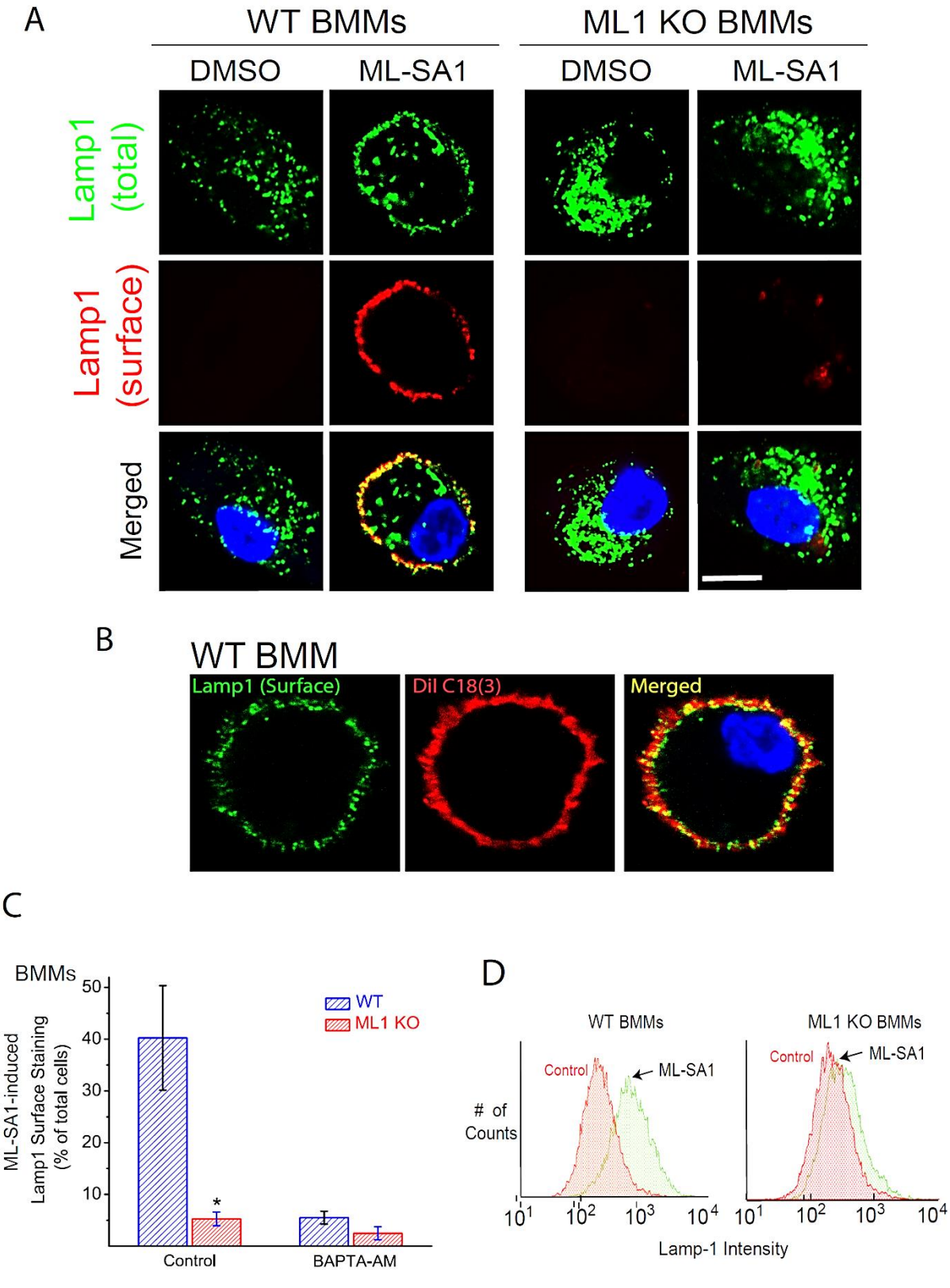
A
WT BMMs
ML1 KO BMMs
DMSO
ML-SA1
DMSO
ML-SA1
Lamp1 (total)
Lamp1 (surface)
Merged
B
WT BMM
Lamp1 (Surface)
DiI C18(3)
Merged
C
BMMs
ML-SA1-induced Lamp1 Surface Staining (% of total cells)
50
40
30
20
10
WT
ML1 KO
*
Control
BAPTA-AM
D
WT BMMs
ML1 KO BMMs
Control
ML-SA1
Control
ML-SA1
# of Counts
10^1
10^2
10^3
10^4
10^1
10^2
10^3
10^4
Lamp-1 Intensity

Figure 2.2 TRPML1 activation induces Lamp-1 translocation to the plasma membrane

(A) ML-SA1 (10 mM for 30 min) treatment resulted in localization of Lamp1 (red) on the plasma membrane in non-permeabilized WT but not ML1 KO BMMs. Lamp1 surface expression was detected using an antibody recognizing a luminal epitope (1D4B). After the cells were permeabilized, total (cell surface + intracellular; green) Lamp1 proteins were detected using the same antibody. Scale bar represents 5 µm. (B) Lamp1 surface staining was co-localized with the plasma membrane marker DiI-C18(3). Scale bar = 5 µm. (C) Flow cytometric analysis of ML-SA1-induced Lamp1 surface expression in WT and ML1 KO BMMs. Pre-treatment with BAPTA-AM (1 µM for 30 min) completely abolished Lamp1 surface staining in WT BMMs. (D) Histograms showing the flow cytometric analysis of Lamp1 surface staining.

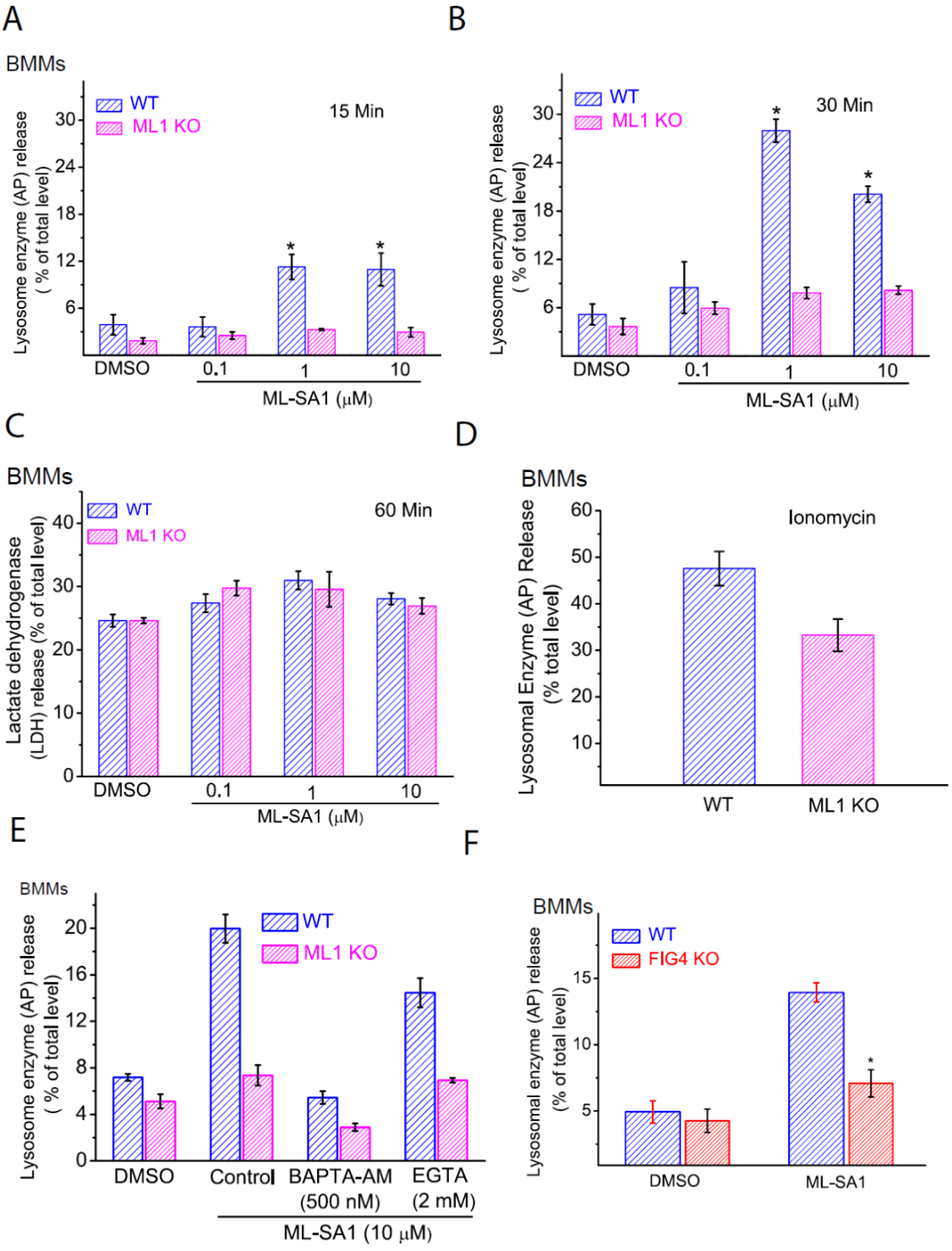
A
BMMs
WT
ML1 KO
15 Min
Lysosome enzyme (AP) release
(% of total level)
DMSO
0.1
1
10
ML-SA1 (μM)
B
WT
ML1 KO
30 Min
Lysosome enzyme (AP) release
(% of total level)
DMSO
0.1
1
10
ML-SA1 (μM)
C
BMMs
WT
ML1 KO
60 Min
Lactate dehydrogenase
(LDH) release (% of total level)
DMSO
0.1
1
10
ML-SA1 (μM)
D
BMMs
Ionomycin
Lysosomal Enzyme (AP) Release
(% total level)
WT
ML1 KO
E
BMMs
WT
ML1 KO
Lysosome enzyme (AP) release
(% of total level)
DMSO
Control
BAPTA-AM
(500 nM)
EGTA
(2 mM)
ML-SA1 (10 μM)
F
BMMs
WT
FIG4 KO
Lysosomal enzyme (AP) release
(% of total level)
DMSO
ML-SA1

Figure 2.3 TRPML1 activation mediated Ca^{2+} induced lysosomal exocytosis and the release of lysosomal content into the extracellular space.

(A & B) ML-SA1 (0.1-10 μM for 15 or 30 min) treatment increased the release of lysosomal enzymes into the culture medium in BMMs. The activity of lysosomal enzyme acid phosphatase (AP) was determined using an AP activity colorimetric assay kit. The data are presented as the percentage of the activity of the released vs. total (released + cell-associated) enzymes. (C) Lack of an effect of ML-SA1 on the release of cytosolic enzyme LDH. (D) Ionomycin-induced lysosomal enzyme acid phosphatase (AP) release/activity was comparable, but slightly reduced in ML1 KO BMMs. The data are presented as the percentage of the activity of the released enzymes versus total (released + cell-associated) enzymes. (E) The effects of intracellular and extracellular Ca^{2+} on ML-SA1 (10 μM for 30 min) -induced lysosomal AP release. BAPTA-AM (500 nM) and EGTA (2 mM with no added extracellular Ca^{2+}) were used to chelate intracellular and extracellular Ca^{2+}, respectively. (F) ML-SA1 induced lysosomal AP release was reduced in BMMs from FIG4 KO mice.

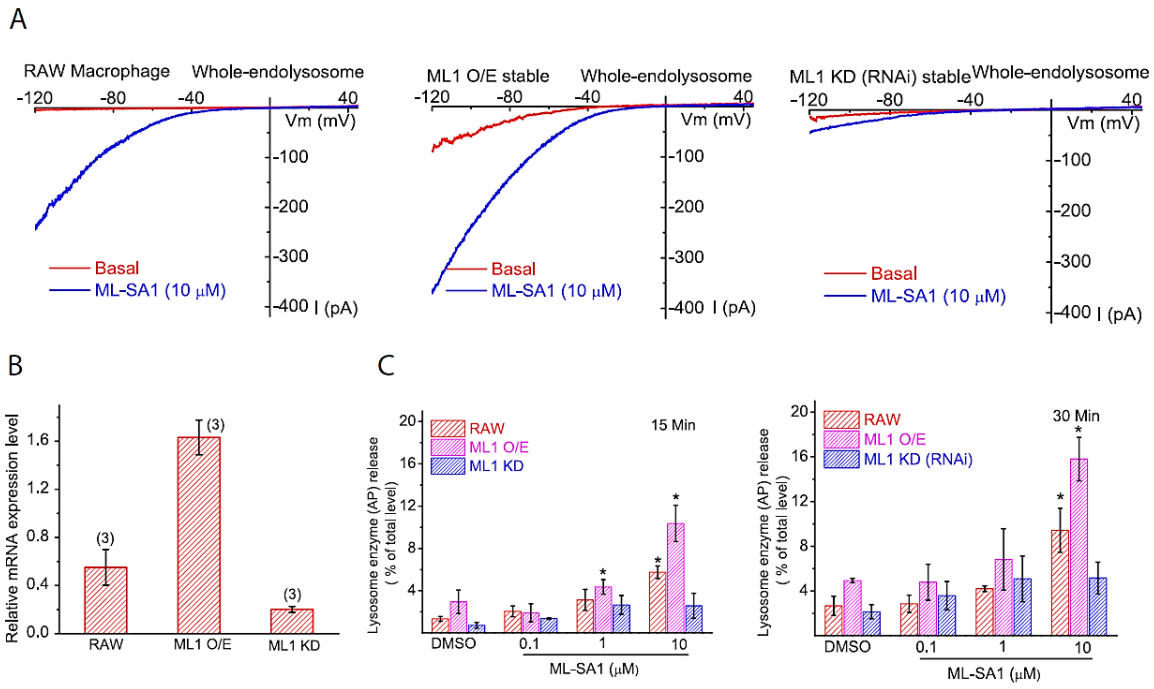

Figure 2.4 Lysosomal exocytosis correlates with TRPML1 activity/expression.

(A) ML-SA1-activated whole-endolysosome TRPML-like currents in RAW 264.7 macrophage cell lines, RAW cells stably expressing ML1-GFP (ML1 overexpression or O/E), and RAWcells stably expressing ML1-specific RNAi (ML1 knockdown or KD). (B) Real-time RT-PCR analysis of ML1 RNA expression level (relative to L32) in RAW macrophages (n = 3 batches of independent experiments for each cell type). (C) Lysosomal AP release in RAW 264.7, ML1 O/E, and ML1 KD RAW macrophages. The amount of AP release correlates with the expression/activity of TRPML1 in macrophages. Electrophysiology experiments in section A were performed in collaboration with Xiaoli Zhang.

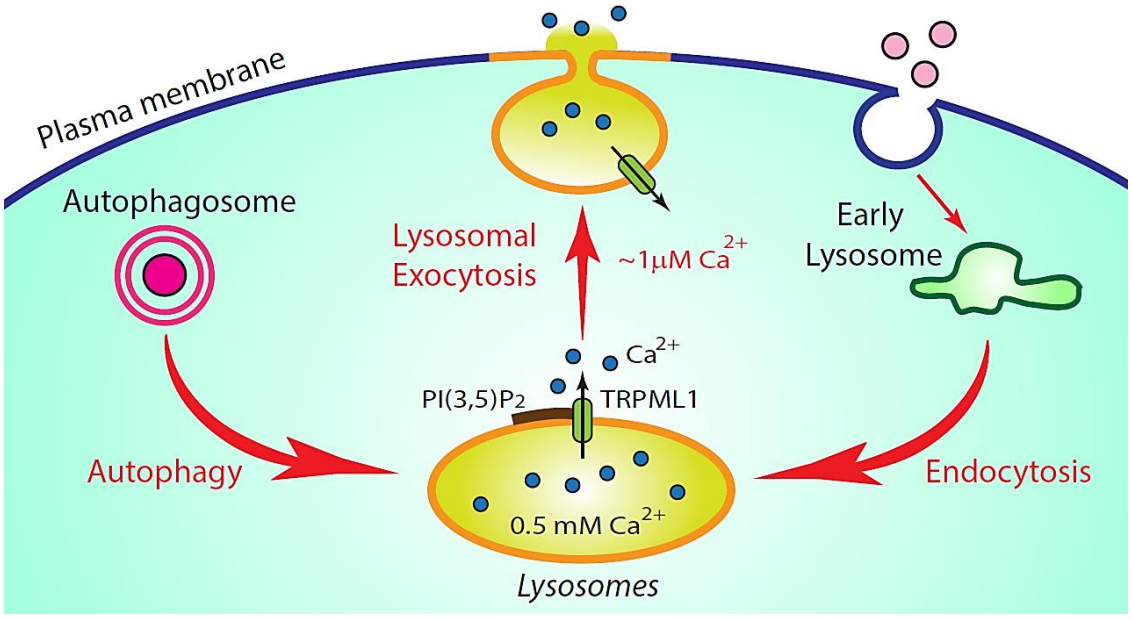

Figure 2.5 The role of TRPML1 in Ca^{2+} mediated lysosomal exocytosis

Lysosomal exocytosis is a Ca^{2+}-dependent process. Early endosomes are generated from nascent endocytic vesicles via endocytosis. Autophagosomes are generated via autophagy. Autophagosomes and endosomes then fuse with lysosomes, which contain high Ca^{2+} concentration (~ 0.5 mM). Therefore, both autophagy and endocytosis contribute to maintaining cellular lysosome populations. The generation of $PI(3,5)P_2$ and the activation of TRPML1 mediates lysosomal Ca^{2+} release, leading the induction of lysosomal exocytosis in response to different cellular stimuli. The induction of lysosomal exocytosis consumes cellular lysosomes, thus, keeping a balance between pathways leading to lysosome generation and lysosome consumption. All these processes have been shown to be crucial for cell health and functionality.

CHAPTER III

TRPML1 REGULATES LARGE PARTICLE UPTAKE IN MACROPHAGES VIA LYSOSOMAL EXOCYTOSIS

Abstract

Particle ingestion during phagocytosis depends on the extension of plasma membrane and the formation of filopodia-like structures around the particle to be ingested. Recent evidence indicates that membrane extension depends on the delivery of lysosomal membrane, through Ca^{2+} dependent lysosomal exocytosis, to the site of particle uptake to compensate for the plasma membrane that is lost during phagosome formation. However, the source of Ca^{2+} and the Ca^{2+}-channel(s) responsible for Ca^{2+} release during particle uptake are not fully characterized. Here I identified TRPML1 as the key lysosomal Ca^{2+} channel regulating particle uptake in macrophages. Particle ingestion is inhibited by a synthetic TRPML1 blocker and is defective in macrophages isolated from TRPML1 knockout mice. Furthermore, TRPML1 overexpression and TRPML1 agonists facilitate particle uptake. Using time-lapse confocal imaging, we found that particle binding triggered TRPML1-mediated lysosomal Ca^{2+} release specifically at the site of uptake, rapidly delivering TRPML1-resident lysosomal membranes to nascent phagosomes; thus, providing membranes necessary for pseudopod extension, leading to clearance of senescent cells in the tissues.

Introduction

Macrophages participate in tissue remodeling and cellular clearance by engulfing large extracellular particles, such as apoptotic cells or senescent red blood cells (RBCs) (Wynn, Chawla et al. 2013), through a highly regulated process called phagocytosis (Aderem and Underhill 1999). Particle binding to specific cell surface receptors, such as IgG Fc receptors, triggers a cascade of signaling events resulting in a rapid extension of plasma membrane around the particle(s) (Niedergang and Chavrier 2004). Plasma membrane extensions, called plasmalemmal pseudopod, form phagocytic cups to ingest particles into vacuole-like structures called phagosomes within several minutes after particle binding (Flannagan, Jaumouille et al. 2012). Nascent phagosomes then undergo membrane fusion and fission events, collectively called phagosomal maturation, in a time course of tens of minutes to become phagolysosomes to mediate particle digestion (Vieira, Botelho et al. 2002). Although a large amount of plasma membrane is internalized during phagocytosis, paradoxically, the overall surface area of the phagocytosing cells does not decrease (Huynh, Kay et al. 2007), and indeed increases significantly before the closing of the phagocytic cups (Holevinsky and Nelson 1998). Consistently, membrane fusion machinery is shown to be required for phagosome formation/biogenesis and efficient phagocytosis (Hackam, Rotstein et al. 1998). A substantial amount of membrane from intracellular compartments is added to the cell surface at the sites of particle uptake (so called "focal" exocytosis) (Braun, Fraisier et al. 2004; Czibener, Sherer et al. 2006).

Recycling endosomes have been shown to be a supply of intracellular membrane for phagosome formation and particle uptake in a Vesicle-Associated Membrane Protein 3 (VAMP3)-dependent manner (Allen, Yang et al. 2002). More recently, lysosomes have been

identified as another major source of intracellular membrane required for particle uptake, particularly under high load conditions, i.e., when large (> 5 μm) and/or multiple small particles are ingested by a single phagocyte (Braun, Fraisier et al. 2004; Czibener, Sherer et al. 2006). Under such conditions, lysosomes are involved in the very early steps of phagosome biogenesis/formation, prior to the closing of the phagocytic cups. Fusion of lysosomes with the plasma membrane (lysosomal exocytosis) and the delivery of lysosomal membranes/proteins to the surface of the newly formed phagosomes are observed at the site of particle ingestion. Manipulations blocking lysosomal exocytosis significantly reduces particle uptake in macrophages (Braun, Fraisier et al. 2004; Czibener, Sherer et al. 2006). Ca^{2+} is the only known trigger that has been identified for lysosomal exocytosis (Andrews 2000). However the source of Ca^{2+} involved in this process and the ion channel(s) responsible for Ca^{2+} release are not fully characterized.

Transient Receptor Potential Mucolipin-1 (TRPML1) is a member of the TRP cation channel superfamily, and is primarily localized on the lysosome membrane (Cheng, Shen et al. 2010). Human mutations of TRPML1 cause mucolipidosis type IV (MLIV), a childhood neurodegenerative disorder with lysosomal trafficking defects at the cellular level (Amir, Zlotogora et al. 1987; Bach 2001; Altarescu, Sun et al. 2002; Bargal, Goebel et al. 2002; Cheng, Shen et al. 2010). In a *Drosophila* model of MLIV, it has been proposed that the defective clearance of late apoptotic neurons by phagocytes contributes significantly to the neurodegeneration (Venkatachalam, Long et al. 2008). TRPML1 has been shown to be a Ca^{2+}-permeable channel on the lysosomal membrane conducting the flow of Ca^{2+} from the lysosome lumen into the cytosol {Cheng, 2010 #121; Dong, 2012 #122}. In the previous chapter, I demonstrated that TRPML1 plays a crucial role in regulating lysosomal exocytosis in

macrophages (Chapter II). Therefore, I hypothesized that TRPML1 could potentially regulate particle ingestion and cellular clearance by promoting lysosomal Ca^{2+} release and thus, trigger lysosomal exocytosis.

Methods

Mouse lines. The generation and characterization of ML1 (Venugopal, Browning et al. 2007) and FIG4 KO mice (Chow, Zhang et al. 2007) have been described previously. Animals were used under approved animal protocols and Institutional Animal Care Guidelines at the University of Michigan.

Macrophage cell culture. Murine BMMs were prepared and cultured as described previously (Link, Park et al. 2010). Briefly, bone marrow cells from mouse femurs and tibias were harvested and cultured in macrophage differentiation medium (RPMI-1640 medium with 10% fetal bovine serum (FBS) and 100 unit/ml recombinant colony stimulating factor (PeproTech, Rocky Hill, NJ). After 7 days in culture at 37 °C with 5% CO_2, the adherent cells (> 95% are expected to be macrophages) were harvested for assays. RAW 264.7, RAW cells stably-expressing ML1 (ML1 overexpression or O/E), and RAW cells stably-expressing ML1-specific RNAi (ML1 knockdown or KD) (Thompson, Schaheen et al. 2007) were kindly provided by Dr. Hanna Fares (University of Arizona) and cultured in DMEM/F12 media supplemented with 10% FBS at 37°C and 5% CO_2.

BMM and RAW macrophages were transfected using electroporation (Invitrogen Neon Transfection System) according to the manufacturer procedures. Briefly, cells were harvested and washed with PBS (Ca^{2+} and Mg^{2+}-free) once to remove DMEM. Cells were then centrifuged and the pellets were re-suspended in the R buffer. 2 µg of DNA per well was added to the cells, which were gently mixed and placed in the Neon System pipette. The electroporation was performed

using program # 6 for RAW cells and program # 18 for BMMs, respectively. Transfected cells were then recovered with 500 µl of culture media in each plate.

Phagocytosis assay. Sheep RBCs (Lampire Biological Laboratories) were washed twice with PBS and then fixed with 4% paraformaldehyde (PFA) overnight at 4°C in an end-over-end rotator. Free aldehyde groups were quenched by re-suspension in PBS containing 100 mM glycine for 30 minutes at 4°C. RBCs were opsonized with rabbit IgG antibody (Equitech-Bio, Inc) at 37°C for 1h. Phagocytosis was initiated by adding IgG-RBCs onto adherent BMMs at a ratio of 50:1 (RBC: BMM). To synchronize binding and internalization, IgG-RBCs were centrifuged at 300 rpm for 3 minutes together with adherent BMMs. BMMs were placed at 37°C with 5% CO_2 for various time points (15-90 minutes). Non-ingested IgG-RBCs were lysed by incubating the cells with water (1 ml) for 2-3 min at 4°C (Chow, Downey et al. 2004). RBC-containing BMMs were fixed in 2% PFA and stained with goat-anti rabbit IgG AlexaFluor488 (1:500 dilution, Invitrogen). Approximately 150-200 BMMs were typically analyzed for each experiment. Ingested RBCs were counted by experimenters who were blinded to the genotype and treatment.

Fluorescence and time-lapse imaging. Live imaging of RBC uptake by BMMs was performed on a heated stage using a Spinning Disk confocal imaging system consisting of an Olympus IX81 inverted microscope, a 100X Oil objective NA 1.49 (Olympus, UAPON100XOTIRF), a CSUX1 scanner (Yokogawa), an iXon EM-CCD camera (Andor), and MetaMorph Advanced Imaging acquisition software v.7.7.8.0 (Molecular Devices). For Lamp1 detection, BMMs were fixed with 4% PFA, and permeabilized with 0.03% Triton X-100, then stained with 1D4B anti–mouse Lamp1 monoclonal antibody (Iowa Hybridoma Bank). For phalloidin staining of phagosomes, BMMs were incubated for 10 minutes with IgG-RBCs, fixed with 4% PFA, permeabilized with 0.03% Triton X-

100 for 5 min, and labeled with phalloidin- Alexa-Fluor633 (Invitrogen) for 30 minutes. All images were taken with the 100X objective of a Leica (TCS SP5) confocal microscope.

Whole-cell electrophysiology. Whole-cell recordings were performed as described previously. The pipette solution contained 147 mM Cs,120 mM methane-sulfonate, 4 mM NaCl, 10 mM EGTA, 2 mM Na2-ATP, 2 mM MgCl2, and 20mM HEPES (pH 7.2; free [Ca2+]i < 10 nM). The standard extracellular bath solution (modifiedTyrode's solution) contained 153 mM NaCl, 5 mM KCl, 2 mM CaCl2, 1 mM MgCl2, 20 mMHEPES, and 10 mM glucose (pH 7.4). BMMs were incubated with IgG-RBCs at 4 °C for 20 minutes then placed at 37°C with 5% CO2 for 5~10 minutes before whole-cell recordings. Dynasore (100 μM) was added when the RBCs were applied to BMMs.

Fura-2 Ca^{2+} imaging. Cells were loaded with 5 μM Fura-2 AM in the culture medium at 37 °C for 60 minutes. Fluorescence was recorded at different excitation wavelengths using an EasyRatioPro system (PTI). Fura-2 ratios (F_{340}/F_{380}) were used to monitor changes in intracellular [Ca^{2+}] upon stimulation. Ionomycin (1 μM) was added at the conclusion of all experiments to induce a maximal response for comparison.

H&E Staining. Hematoxylin and eosin (H&E) staining was performed in 5 μm slice sections prepared from paraffin-embedded spleen tissues using microtome. The tissues were fixed with 4% PFA upon heart perfusion in 10 -12 week old WT and ML1 KO mice.

Cell death analysis in brain slices. Brain slices were stained with propidium iodide (PI; membrane impermanent dye only enters the dying cells) and analyzed with confocal microscopy. Briefly, fresh mouse brains were sectioned into 300 μm thick slices with a vibratome sectioning system. Immediately after cutting the sections, slices were washed with cold (4°C) HBSS solution, then

incubated with PI (20µg/ml) at 37°C for 15 minutes, fixed in 4% paraformaldehyde for another 30 minutes, then mounted on the glass slides. To avoid damage caused by tissue preparation, images were taken 100 µm underneath the surface of the slice sections.

Measurement of splenic iron content. Spleens were completely digested in 3M hydrocholoric acid/10% tricholroacetic acid at 65°C overnight. Samples were then centrifuged in order to precipitate any non-digested materials. The ionic composition of the supernatant was analyzed using a Thermo Scientific Finnigan Element inductively coupled with a plasma-high resolution mass spectrometer (ICP-HRMS).

Data analysis. Data are presented as the mean ± standard error of the mean (SEM). Statistical comparisons were made using analysis of variance (ANOVA). A P value < 0.05 was considered statistically significant.

Results

Expression of TRPML1 is necessary for efficient uptake of large particles in macrophages.

Among the professional phagocytes, I chose macrophages to study the effect of TRPML1 on particle uptake. Unlike other professional phagocytes, such as neutrophils, macrophages have a much longer life cycle and reside in several tissues through the body. More importantly, they actively participate in removing apoptotic bodies in different tissues, such as spleen and brain, and they have a dynamic role in inflammatory responses in those tissues (Chawla 2010). Thus, I hypothesized that macrophages must have established machinery for the uptake of large particles. To study the role of TRPML1 in particle uptake/ingestion, I isolated monocytes from the bone marrow of wild-type (WT) and TRPML1 knockout (KO) mice. Monocytes were incubated with macrophage specific growth factors for 5 days at 37°C to allow for the maturation

of monocytes to bone marrow derived macrophages (BMMs) (Chow, Downey et al. 2004). The initial characterization of TRPML1 KO macrophages was shown in chapter II (**Fig. 2.1**).

To investigate the role of TRPML1 in particle ingestion, WT and TRPML1 KO BMMs were exposed to IgG-opsonized sheep red blood cells (IgG-RBCs), all about 5 μm in size, for different periods of time (15-90 min; **Fig. 3.1A-C**). IgG-RBC uptake was quantified for at least 150 BMMs per time point for each genotype. Un-ingested IgG-RBCs were hypotonically lysed by briefly (1-2 min) incubating the cells in 4ºC water. Ingested IgG-RBCs were counted individually by experimenters who were blind to the genotypes and experimental conditions. Distribution histograms were created at each time point for each genotype based on the number of ingested particles per cell. Thresholds were set (4 to 10 or more particles per cell) based on the cell type and particle size in order to compare the phagocytic capability (**Fig. 3.1B**). Based on a threshold of 10 or more (10+) IgG-RBCs per BMM (**Fig. 3.1B**), a significant difference in particle uptake was noted between WT and TRPML1 KO BMMs. Uptake defects were more severe as time progressed. After 90 minutes, approximately 50% of WT, but less than 20% of TRPML1 KO BMMs contained 10+ internalized IgG-RBCs (**Fig. 3.1A-C**)**.** The progressive inhibition of uptake caused by TRPML1 deficiency suggested that TRPML1 is necessary for the ongoing uptake of large particles, which is consistent with the reported, preferential requirement of lysosomal membrane delivery for large particle uptake.

To further probe this possibility, BMMs were tested for their ability to ingest different-sized IgG-opsonized polystyrene beads. Interestingly, while the internalization of 3 μm beads (a threshold of 10+ 3μm beads set for BMMs) was similar for WT and TRPML1 KO BMMs, uptake of 6μm beads (a threshold of 4+ 6-μm-beads for BMMs) was significantly reduced in TRPML1 KO BMMs at all-time points. Uptake of zymosan particles (diameter = 2-3 μm) was

also normal for TRPML1 KO BMMs (**Fig. 3.1D**). These observations are reminiscent of the particle size-dependent uptake defect seen in SytVII KO BMMs. Taken together, these results suggest that TRPML1 is required for efficient uptake of large particles, i.e., when the need for membranes from internal sources is high.

The channel activity of TRPML1 induces large particle uptake in macrophages.

Next, we investigated whether increasing the expression/activity of TRPML1 can facilitate particle uptake in macrophages. Incubating WT BMMs with a TRPML agonist, ML-SA1 (1-10 μM), for 15 minutes caused more than a two-fold increase in the percentage of cells containing 10+ IgG-RBCs. In contrast, the increase was negligible for TRPML1 KO BMMs (**Fig. 3.2A**). Moreover, heterologous expression of TRPML1-GFP in addition to ML-SA1 treatment in TRPML1 KO BMMs was sufficient to restore the uptake efficiency to the same level as WT BMMs. Meanwhile, the expression of TRPML1-KK-GFP, a non-conducting pore mutant of TRPML1, failed to restore the particle uptake capacity in TRPML1 KO BMMs (**Fig. 3.2B**). These results established a positive correlation between the channel activity of ML1 and IgG-RBC uptake.

We also examined particle uptake in RAW 264.7 macrophage cell lines, as well as RAW cell lines stably expressing TRPML1 (TRPML1 overexpression or O/E) or TRPML1-specfic RNAi (TRPML1 knockdown or KD) (Chapter II**, Fig. 2.4**). Interestingly, particle uptake efficiency in these lines correlated with their respective expression levels of TRPML1 with an even greater correlation in the presence of ML-SA1 (**Fig. 3.2C**). The threshold of 5+ ingested IgG-RBCs was set to reflect the smaller size of RAW cells compared to BMMs. While approximately 30% of the ML1 O/E cells ingested 5+ IgGRBCs, fewer than 10% of ML1 KD cells contained 5+ IgG-RBCs (**Fig. 3.2C**). Collectively, these data suggest that the efficiency of

particle uptake in macrophages is positively-correlated with the expression level and channel activity of TRPML1.

The inhibition of TRPML1 activity inhibited large particle uptake in macrophages.

To further investigate the role of TRPML1 in particle uptake, we employed pharmacological tools to acutely inhibit the channel function of TRPML1. Using a Ca^{2+} imaging-based high-throughput screening method, we identified a synthetic small molecule inhibitor for TRPML1 (Mucolipin Synthetic Inhibitor 1 or ML-SI1). Using whole-endolysosome patch-clamp recordings, we confirmed that ML-SI1 strongly inhibited basal, ML-SA1 or $PI(3,5)P_2$-activated I_{ML1} (**Fig. 3.3A&B**). In contrast, ML-SI1 failed to inhibit $PI(3,5)P_2$-activated whole-endolysosome TPC2 currents (**Fig. 3.3C**), demonstrating a relative specificity. Additionally, similar results were obtained using GCaMP3-ML1based Ca^{2+}-imaging system (Shen, Wang et al. 2012) where ML-SI1 was able to completely block ML-SA1 induced lysosomal Ca^{2+} release (**Fig. 3.3D**). In addition, ML-SI1 was able to mostly inhibit TRPML1 current at very low concentrations, but it completely inhibited TRPML1 current at 10 μM (**Fig. 3.3E**). In correlation with these data, ML-SI1 (10 μM) treatment was sufficient to reduce IgG-RBC uptake in WT BMMs to the same level as TRPML1 KO BMMs without significantly affecting the uptake in TRPML1 KO cells (**Fig. 3.3F**). Collectively, these results illustrate that the channel activity of TRPML1 is required for large particle uptake in macrophages.

TRPML1 is rapidly recruited to phagocytic cups and nascent phagosomes of large particles

To investigate the mechanisms by which TRPML1 contributes to particle uptake, I performed time-lapse confocal microscopy of live RAW cells during the particle uptake process. I observed that TRPML1-GFP was rapidly (within 1-3 min) recruited to the site of phagosome

formation during the uptake of 6 μm beads (**Fig. 3.4A**). Strikingly, in contrast to large particle uptake, TRPML1-GFP was not recruited to the site of phagosome formation during the uptake of 3 μm beads (**Fig. 3.4B**). These data clearly demonstrate that different signaling mechanisms are involved in the uptake of different size particles.

Next, I compared the localization of TRPML1 with other lysosomal membrane proteins known to be involved in phagosome formation and maturation. As mentioned before, SytVII is a lysosomal Ca^{2+} sensor shown to be involved in lysosomal exocytosis (Rodriguez, Webster et al. 1997; Rodriguez, Martinez et al. 1999; Reddy, Caler et al. 2001). In macrophages, SytVII has been shown to be recruited to the nascent phagosomes upon particle binding (Czibener, Sherer et al. 2006). BMMs isolated from SytVII KO mice exhibit a similar phenotype as TRPML1 KO BMMs; they have been shown to be defective in large particle uptake and the defect is proportional to the particle size (Czibener, Sherer et al. 2006). Within 2–3 minutes after exposing the RAW cells to IgG-RBCs, both TRPML1-GFP and SytVII-mCherry appeared on the membranes of nascent phagosomes (**Fig. 3.4C**). TRPML1-GFP and SytVII-mCherry positive (lysosomal) tubules were then observed wrapping themselves around the newly formed phagosomes. The recruitment kinetics was similar for both proteins (**Fig. 3.4C**).

Next I compared the dynamics of TRPML1 to other known proteins involved in phagosome maturation (Vieira, Botelho et al. 2002). Similar to TRPML1 and SytVII, lysosome-associated membrane protein 1 (Lamp-1) was also rapidly recruited to newly formed large-particle-containing phagosomes in RAW macrophages BMMs (**Fig. 3.5**). The recruitment of TRPML1 and Lamp1 to forming phagosomes occurred prior to the recruitment of Rab5, an early phagosome maturation marker, and Rab7, a late phagosome maturation marker (Vieira, Botelho et al. 2002) (**Fig. 3.5**). In correlation with this, the recruitment of lysosomal membrane proteins

TRPML1 and Lamp-1 occurred prior to lysosomal acidification, as illustrated using acid sensitive dye LaysoTraker (**Fig. 3.5**). Consistently, during large particle uptake, the newly formed phagosomes (5 minutes after particle binding) in WT BMMs, compared with TRPML1 KO BMMs, contained significantly more Lamp-1 proteins (**Fig. 3.6A**). Phagosomes are still wrapped with polymerized actin within 5–10 minutes after particle binding (**Fig. 3.6A**) suggesting that TRPML1 and Lamp-1 are recruited to the newly formed phagosomes before the phagosomes enters the phagosomal maturation pathway (Vieira, Botelho et al. 2002). Collectively, these results suggest that during large particle uptake, recruitment of TRPML1 and other lysosomal membrane proteins occurred in the very early stages of phagosome formation, prior to Rab5- mediated early phagosome maturation.

To further confirm the presence of TRPML1 on the newly formed phagosomes, we developed a patch-clamp method to directly record from phagosomal membranes (**Fig. 3.7A-B**). Phagosomes were isolated from Lamp1-GFP or TRPML1-GFP-transfected RAW cells after exposure to IgG-RBCs or beads for 5 min. In Lamp1-GFP-transfected RAW cells, bath application of $PI(3,5)P_2$ (100 nM) or ML-SA1 (25 μM) readily activated endogenous whole-phagosome TRPML1-like currents (**Fig. 3.7C**). Much larger whole-phagosome ML-SA1-activated currents were seen in TRPML1-GFP-transfected RAW cells. In WT BMMs, whole-phagosome I_{TRPML1} was activated by ML-SA1, and inhibited by ML-SI1 (**Fig 3.7D**). These results thus provide functional evidence that TRPML1 is recruited to nascent phagosomes.

TRPML1 mediates large particle uptake by regulating lysosomal Ca^{2+} release

TRPML1 is a lysosomal Ca^{2+} channel suggested to be involved in the release of Ca^{2+} from the lysosomal luminal side into the cytoplasm (Cheng, Shen et al. 2010). Additionally,

large particle uptake in macrophages has suggested to be Ca^{2+} dependent (Czibener, Sherer et al. 2006). Therefore, I hypothesized that TRPML1 could regulate large particle uptake by mediating lysosomal Ca^{2+} release, thus, regulating lysosomal exocytosis. Consistent with this idea pretreatment of BMMs with a membrane-permeable, fast Ca^{2+} chelator, BAPTA-AM, significantly inhibited particle uptake in WT macrophages after 90 minutes, but to a lower degree in TRPML1 KO cells (**Fig. 3.8A**). In a separate experiment, large particle uptake was evaluated after exposing macrophages to different concentrations of the fast Ca^{2+} chelator BAPTA-AM and the slow Ca^{2+} chelator EGTA-AM (**Fig. 3.8B**). BAPTA-AM was able to inhibit large particle uptake at lower concentrations, however, EGTA-AM failed to block large particle uptake even at higher concentrations (**Fig. 3.8B**). This illustrated that the Ca^{2+} required for large particle uptake is most likely provided from a local source very close to the sites of particle uptake and very close to the site of lysosomal exocytosis.

Although lysosomal membrane fusion events are presumed to be dependent on lysosomal Ca^{2+} release in the close vicinity of fusion spots, direct evidence has yet to be reported (Pryor, Mullock et al. 2000; Piper and Luzio 2004; Czibener, Sherer et al. 2006; Luzio, Bright et al. 2007). To directly observe lysosomal Ca^{2+} during particle uptake we used a lysosome-targeted genetically encoded Ca^{2+} indicator, GCaMP3-TRPML1, to specifically measure lysosomal Ca^{2+} release in intact cells (Shen, Wang et al. 2012). Transient and localized Ca^{2+} increases, measured with GCaMP3 fluorescence changes, were observed preferentially at the uptake sites of SytVII-mCherry-positive lysosomes within several minutes of particle binding for both IgG-RBCs (**Fig. 3.9A**). In contrast, little or no GCaMP3 fluorescence increase was seen in other areas of the phagocytosing macrophages within the same time course. These results suggest that particle binding induces TRPML1-mediated lysosomal Ca^{2+} release locally at the site of

uptake. In contrast, in RAW264.7 cells doubly transfected with SytVII-mCherry and GCaMP3-TRPML1-KK (a non-conducting pore mutation), no Ca^{2+} release was observed at the site of particle uptake (**Fig 3.9B**). These results, for the first time, illustrated that particle binding induces TRPML1-mediated lysosomal Ca^{2+} release locally at the site of particle uptake.

TRPML1 regulates particle uptake via lysosomal exocytosis

Lysosome fusion with the plasma membrane (lysosomal exocytosis) has been shown to be required for the uptake of large particles in macrophages (Braun, Fraisier et al. 2004; Braun and Niedergang 2006; Czibener, Sherer et al. 2006; Huynh, Kay et al. 2007). Also, TRPML1 has been shown to be involved in lysosomal exocytosis in macrophages (Chapter II). I sought to evaluate particle induced lysosomal exocytosis by directly investigating the insertion of TRPML1 onto the plasma membrane during particle uptake. Because current antibodies are inadequate for detecting endogenous TRPML1 proteins, we developed a whole-cell patch-clamp method to ‘‘detect’’ the plasma membrane insertion of TRPML1 during particle uptake. This electrophysiology-based ‘‘exocytosis assay’’ provides temporal resolution far superior to other exocytosis/secretion assays. In order to facilitate detection (by decreasing the turnover time of TRPML1 at the plasma membrane), we used dynasore, a cell permeant dynamin inhibitor (Macia, Ehrlich et al. 2006), to block endocytosis presumed to be coupled with focal exocytosis (Braun and Niedergang 2006). Large ML-SA1-induced whole-cell TRPML1-like currents were observed upon exposure of WT BMMs to IgG-RBCs for 10 minutes in the presence of dynasore (**Fig. 3.10A&B**). In contrast, no significant ML-SA1-induced whole-cell currents were observed in RBC-treated TRPML1 KO BMMs, or WT BMMs treated with dynasore alone (**Fig. 3.10A&B**). IgG-RBC-induced whole-cell I_{ML1} was completely inhibited by BAPTA-AM

pretreatment (**Fig. 3.10B)**, suggesting that TRPML1 insertion in to the plasma membrane is Ca^{2+} dependent.

To further investigate the role of TRPML1 in lysosomal exocytosis and particle uptake, BMMs were exposed to IgG-RBCs for various lengths of time and lysosomal enzyme acid phosphatase (AP) release into the surrounding media was measured as the readout for lysosomal exocytosis. Compared with WT BMMs, TRPML1 KO cells exhibited significantly less IgG-RBC-induced AP release (**Fig. 3.10C).** This difference was abolished by either BAPTA-AM or inhibition of TRPML1 using ML-SI1 (**Fig. 3.10C)**.

To directly investigate whether the involvement of TRPML1 in large particle uptake is mediated by lysosomal exocytosis, I assessed particle uptake upon increasing the expression level and channel activity of TRPML1 while simultaneously blocking lysosomal exocytosis. Three approaches were employed to block lysosomal exocytosis. First, lysosomal exocytosis and particle uptake were inhibited by dominant-negative (DN) forms of SytVII (Reddy, Caler et al. 2001). I found that ML-SA1-induced large particle uptake was significantly reduced in SytVII-DN-transfected TRPML1 O/E RAW cells (**Fig. 3.11A**). Second, VAMP7 is a lysosomal SNARE protein required for lysosome-plasma membrane fusion (Braun, Fraisier et al. 2004). VAMP7 belongs to the Longin family of SNARE proteins characterized by the presence of an auto-inhibitory domain at their N terminus (Martinez-Arca, Rudge et al. 2003). Overexpression of the Longin domain of VAMP7 alone in macrophages is known to exert a dominant negative effect on both lysosomal exocytosis and particle uptake (Braun, Fraisier et al. 2004). ML-SA1 treatment failed to enhance particle uptake in cells transfected with Longin-GFP, including ML1 O/E RAW cells (**Fig. 3.11B**), whereas overexpression of VAMP7-GFP had no inhibitory effect. Third, lysosomal exocytosis can also be reduced by treating the cells with colchicine, a known

inhibitor of microtubule polymerization (Lee, Mason et al. 2007). I found that colchicine treatment significantly inhibited ML-SA1-induced large particle uptake (**Fig. 3.11C**) in TRPML1 O/E RAW cells. Taken together, these data suggest that TRPML1 participates in large particle uptake by regulating Ca^{2+}-dependent lysosomal exocytosis in macrophages. The residual particle uptake in TRPML1 KO BMMs was further inhibited by tetanus toxin (TeNT, an inhibitor of several VAMP proteins including VAMP3), which is consistent with an additional contribution of membranes/exocytosis from recycling endosomes as reported previously (**Fig. 3.11D**).

TRPML1 deficiency results in defective clearance of senescent and apoptotic cells *in vivo*.

Senescent RBCs are normally phagocytosed by macrophages in the red pulp region of the spleen, followed by the degradation of their haemoglobin and recycling of iron into the circulating blood (Bratosin, Mazurier et al. 1998). Considering that TRPML1 KO BMMs were defective in the uptake of large cellular particles, we investigated RBC clearance in the spleens of TRPML1 KO mice. In TRPML1 KO spleens, in correlation with other LSDs, Lamp1 expression was elevated as detected by western blot (**Fig. 3.12A**) and tissue immunostaining (**Fig. 3.12B**). Additionally, TRPML1 KO mice exhibited enlarged spleens, but had normal kidney size compared with WT controls (**Fig. 3.12C**). This is suggestive of compensatory changes secondary to defective clearance of senescent RBCs. Consistently, hematoxylin and eosin (H&E) staining of spleen sections revealed an accumulation of RBCs in both white and red pulps of TRPML1 KO but not WT spleens (**Fig. 3.12D**). Accumulation of RBCs in the spleen reportedly leads to a buildup of splenic iron stores (Kohyama, Ise et al. 2009). Indeed, Perl's Prussian blue staining (for ferric iron) revealed an accumulation of iron stores in the spleens of TRPML1 KO mice, which was largely confined to the red pulp region (**Fig. 3.12E**).

Consistently, inductively-coupled plasma mass spectrometry (ICP-MS) analysis revealed that iron content was selectively increased in the TRPML1 KO spleens (**Fig. 3.12F**). Taken together, these results suggest that RBC clearance is defective in TRPML1 KO mice. Defective phagocytosis in the brain may lead to inflammation and microglia (macrophage like cells in the brain) activation. Consistently, Iba1, a 17-kDa EF hand protein that is specifically expressed in activated macrophage/microglia, was up-regulated in the brain of TRPML1 mice (**Fig. 3.13A&B**) in addition to massive cell death observed in the cerebral cortex and hippocampus of TRPML1 mice brain (**Fig. 3.13C**).

Discussion

Using pharmacological, genetic, and biochemical approaches, I demonstrate that the channel activity of TRPML1 is necessary for efficient uptake of large particles in macrophages. Live imaging revealed that TRPML1 is rapidly recruited to the membrane extensions surrounding the particles in the process of phagocytic internalization. Our results are compatible with the following working model: large particle binding to macrophages triggers the activation of TRPML1 which induces TRPML1-mediated lysosomal Ca^{2+} release and lysosomal exocytosis at the site of uptake (**Fig. 3.14**).

The involvement of Ca^{2+} in particle uptake and phagosome formation has been unclear and rather controversial (Nunes and Demaurex 2010). Early studies demonstrated that the activation of IgG Fc receptors during phagocytosis induces a transient increase in intracellular Ca^{2+} in neutrophils (Tapper, Furuya et al. 2002; Nunes and Demaurex 2010), but not macrophages (Young, Ko et al. 1984; Hishikawa, Cheung et al. 1991). However, recent data illustrating the importance of Ca^{2+} induced lysosomal exocytosis in large particle uptake (Braun, Fraisier et al. 2004; Braun and Niedergang 2006; Czibener, Sherer et al. 2006) dramatically

changed our understanding of the role of Ca^{2+} in this process. Ca^{2+} is the only known trigger that has been identified for lysosomal exocytosis, with SytVII being the primary Ca^{2+} sensor and VAMP7 being the SNARE protein required for lysosomal exocytosis. Consistent with the role of lysosomal exocytosis in particle uptake, macrophages lacking VAMP7 or SytVII exhibit defects in both lysosomal exocytosis and particle uptake, but preferentially under high particle loads. This suggests that a small amount of Ca^{2+} release from non-conventional internal stores, that might have escaped detection when using conventional Ca^{2+} imaging methods, may play a crucial role in macrophage phagocytosis.

Using our recently established lysosome-specific Ca^{2+} imaging method with lysosome-targeted genetically encoded Ca^{2+} sensor GCaMP3, which is more sensitive in detecting lysosomal Ca^{2+} release than conventional methods, we indeed found that particle binding to macrophages also induces Ca^{2+} increase, but exclusively at the site of the particle uptake. Furthermore, the present study has extended the earlier observations by demonstrating that transient Ca^{2+} release from the lysosomes through TRPML1 is responsible for triggering lysosomal exocytosis during the uptake of large particles. Additionally, acidic granules in neutrophils (equivalent to lysosomes in macrophages) have been shown to redistribute toward the site of particle uptake, suggesting a source of membrane (Stendahl, Krause et al. 1994; Theler, Lew et al. 1995). Using time-lapse live imaging, I have demonstrated that lysosomes and their resident proteins are also redistributed toward the site of uptake in macrophages. Thus, here I showed that lysosomes serve uniquely as sources not only for membranes, but also for Ca^{2+} that is required for SytVII activation/recruitment with TRPML1 being the Ca^{2+} channel releasing the lysosomal Ca^{2+} (**Fig. 3.14**).

Our results in the present study are consistent with previous reports showing that the clearance of late apoptotic neurons is impaired in the *Drosophila* TRPML (Venkatachalam, Long et al. 2008), suggesting that TRPML1 channels play a role in eliminating pathogenic extracellular particles. Extracellular accumulation of large particles, such as apoptotic cells, may cause brain inflammation and microglia activation, which are common features in most neurodegenerative LSDs (Jeyakumar, Dwek et al. 2005). It is possible that defective phagocytosis of large particles is a general pathogenic factor for many LSDs, with TRPML1 channel deregulation in phagocytes being a primary cause. Collectively, I have provided innovative links between a lysosomal Ca^{2+} channel, lysosomal exocytosis, large particle uptake, and LSDs, and have developed new approaches and chemical reagents to study phagocytosis. Given the pivotal role of phagocytosis in clearance of apoptotic cells, our findings may lead to new therapeutic approaches for a wide spectrum of neurodegenerative and immune diseases.

It is not clear how large particle uptake induces the activation machinery for TRPML1 on the lysosomes. $PI(3,5)P_2$ is the only known endogenous activator for TRPML1 (Dong, Shen et al. 2010). However, the biological cues that lead to $PI(3,5)P_2$ production and TRPML1 activation are not clear. Interestingly, phosphatidylinositol 3-kinase (PI3K) activity has been shown to be necessary for the uptake of large, but not small particles (Cox, Tseng et al. 1999). PI3K activity is mediated through two different isoforms: PI3K type I and III. While type I PI3K has been linked to an effect on cytoskeleton rearrangement during large particle uptake (Cox, Tseng et al. 1999; Hoppe and Swanson 2004), type II PI3K could contribute to large particle uptake via the production of PI3P, the precursor of $PI(3,5)P_2$ (Michell, Heath et al. 2006), which in turn is the endogenous activator of TRPML1. This possibility is explored more in details in the next chapter.

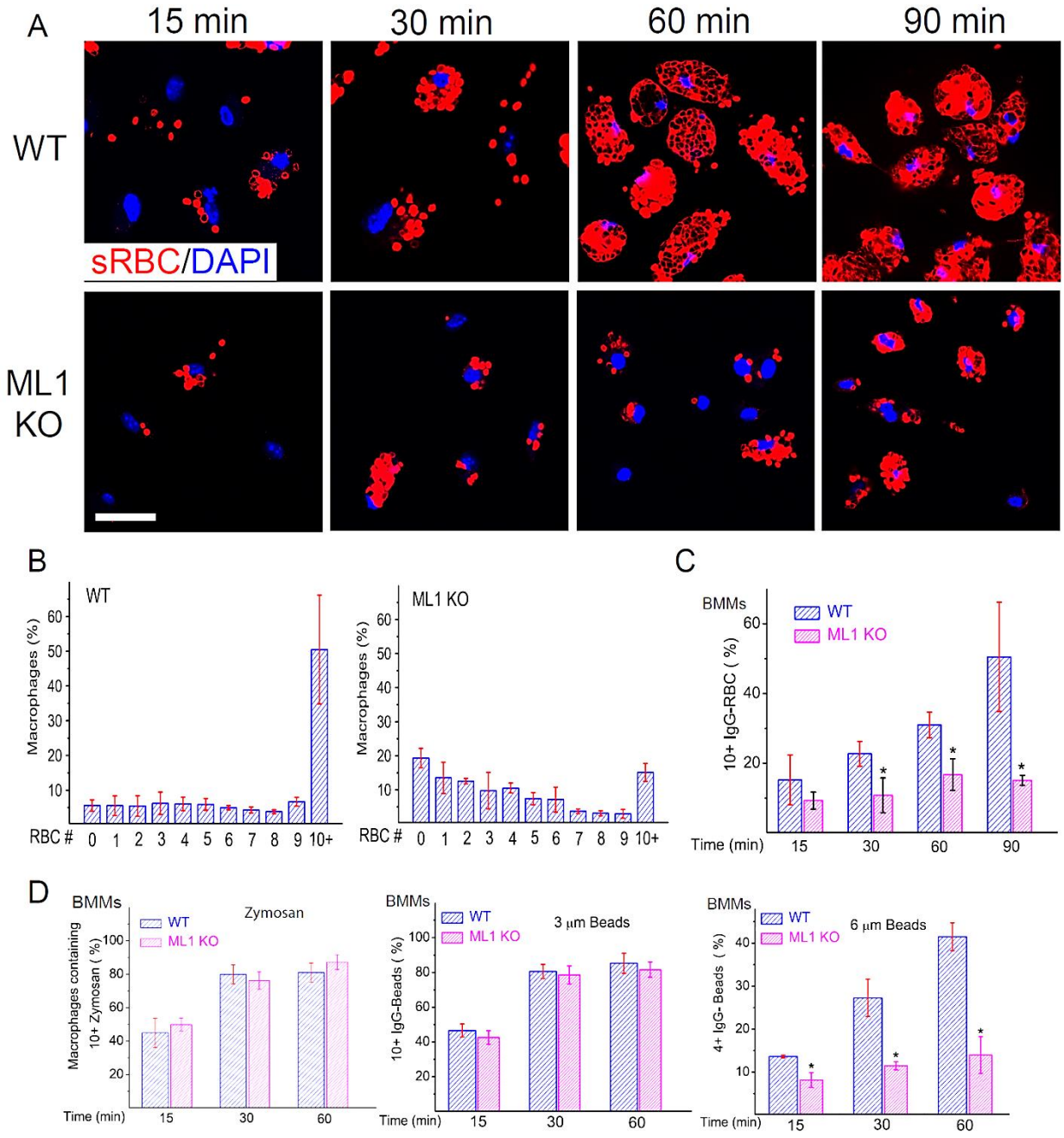
A
15 min
30 min
60 min
90 min
WT
ML1 KO
sRBC/DAPI
B
WT
ML1 KO
Macrophages (%)
RBC #
0 1 2 3 4 5 6 7 8 9 10+
C
BMMs
WT
ML1 KO
10+ IgG-RBC (%)
Time (min)
15
30
60
90
D
BMMs
Zymosan
Macrophages containing 10+ Zymosan (%)
3 μm Beads
10+ IgG-Beads (%)
6 μm Beads
4+ IgG- Beads (%)

Figure 3.1 TRPML1 is necessary for optimal phagocytosis of large particles in bone marrow macrophages

(A) WT and TRPML1 KO BMMs were exposed to IgG-opsonized red blood cells (IgG-RBCs; red colored) at a ratio of 50 RBCs/BMM for time periods indicated (15, 30, 60, and 90 min). Non-ingested IgG-RBCs were lysed by briefly (1–2 min) incubating the cells in water at 4°C. Samples were then fixed and processed for confocal microscopy. (B) Histograms represent the distribution (in percentage) of WT and ML1 KO BMMs containing different numbers of ingested RBCs (x-axis) after 90 minutes. (C) Average particle ingestion for WT and TRPML1 KO BMMs. Ingested IgG-RBCs were quantified for 150–200 BMMs per experiment, by experimenters who were blind to the genotype. (D) Particle-size-dependent phagocytosis defect of TRPML1 KO BMMs. BMMs were exposed to 2 μm zymosans and 3 or 6 μm IgG-coated polystyrene beads for indicated periods of time. Samples were washed extensively and briefly trypsinized to dissociate non-ingested beads attached to the cell surface or coverslips. The number of ingested particles was determined as described in (B). For all panels, unless otherwise indicated, the data represent the mean ± SEM from at least three independent experiments.

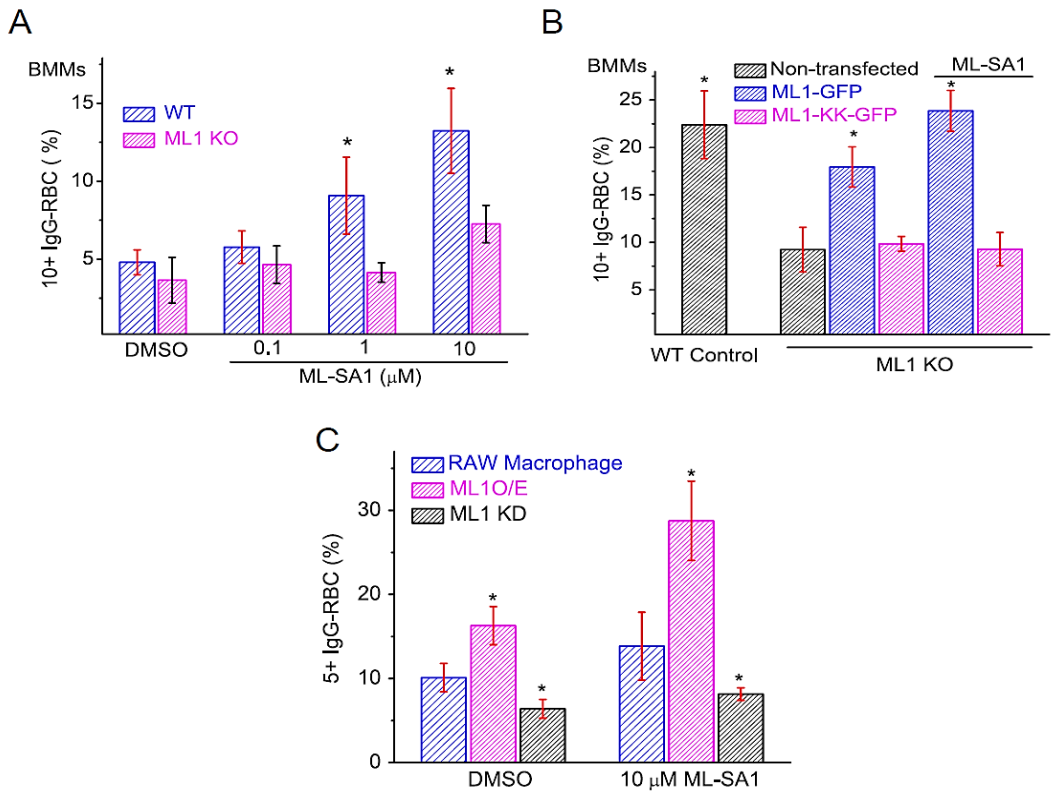

Figure 3.2 The expression level and channel activity of TRPML1 regulate particle Ingestion in macrophages.

(A) Micromolar concentrations of ML-SA1 (0.1, 1, and 10 mM; preincubation for 15 min) increased particle uptake in WT, but not TRPML1 KO BMMs. BMMs were exposed to IgG-RBCs in the presence of ML-SA1 for 15 minutes. (B) Transfection of TRPML1-GFP, but not TRPML1-KK-GFP (nonconducting pore mutation), rescued the uptake defect in TRPML1 KO BMMs. BMMs were exposed to IgG-RBCs for 30 minutes in the presence or absence of the small molecule TRPML agonist, ML-SA1 (10 mM). (C) Particle uptake in RAW 264.7, TRPML1 O/E, and TRPML1 KD RAW macrophages in the presence or absence of TRPML1 specific activator ML-SA1.

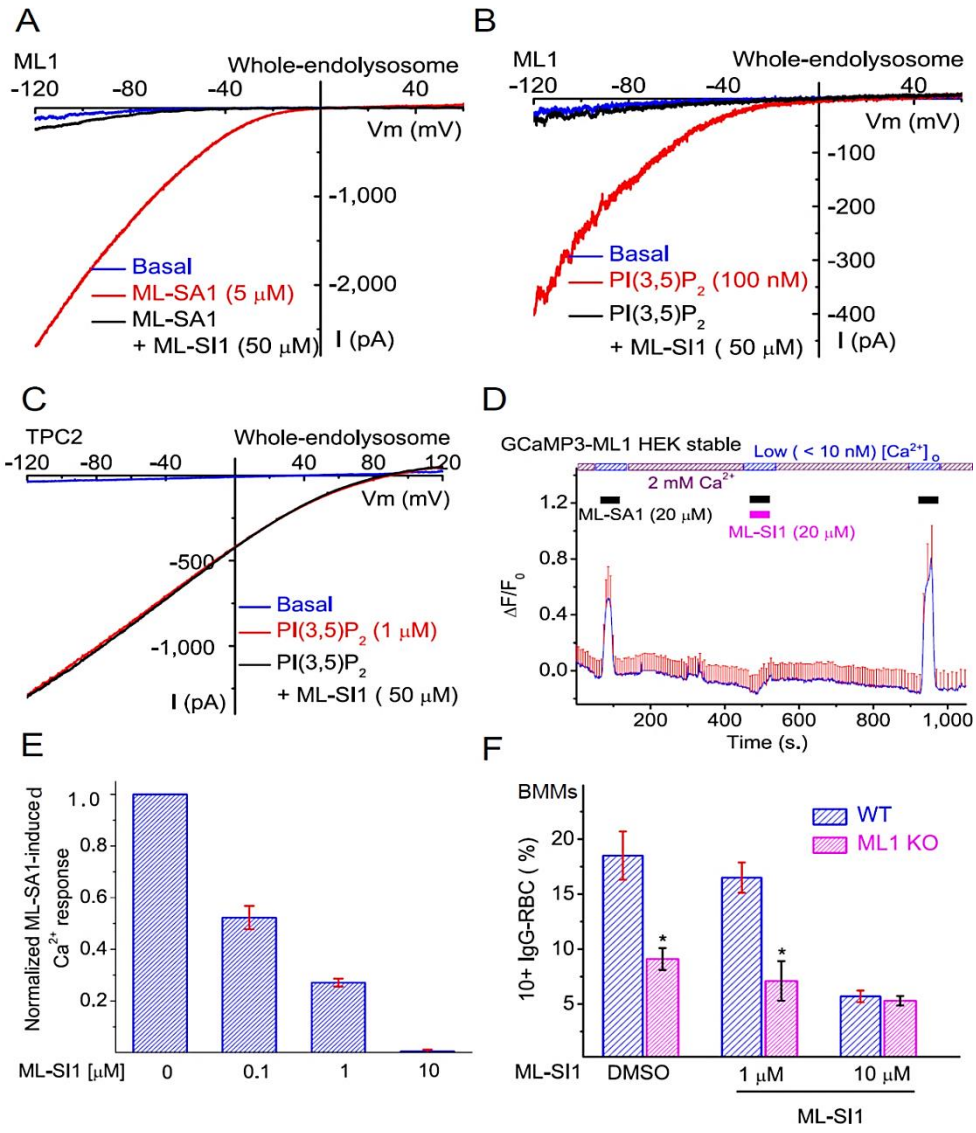

Figure 3.3 Phagocytosis of large particles in macrophages is inhibited by TRPML1 antagonists.

(A & B) ML-SI1 inhibited ML-SA1 or $PI(3,5)P_2$-activated whole-endolysosome currents (C) ML-SI1 did not inhibit $PI(3,5)P_2$ induced TPC2 current. (D) ML-SA1 induced rapid increases in GCaMP3 fluorescence (measured as change of GCaMP3 fluorescence ΔF over basal fluorescence F0; ΔF/F0) under low (<10 nM) external Ca^{2+} in GCaMP3-TRPML1 stable cell lines. Co-application of ML-SI1 abolished the ML-SA1-induced lysosomal Ca^{2+} release. (E) The dose-dependent inhibition of Ca^{2+} increase by ML-SI1 in the micromolar range. (F) ML-SI1 (10 μM; preincubation for 15 min) inhibited particle ingestion in WT BMMs to a similar level of that in TRPML1 KO BMMs. Electrophysiology experiments in sections A, B, and C were performed in collaboration with Xiang Wang and Xiaoli Zhang. Ca^{2+} imaging experiment in section D was performed in collaboration with Abbie Garrity.

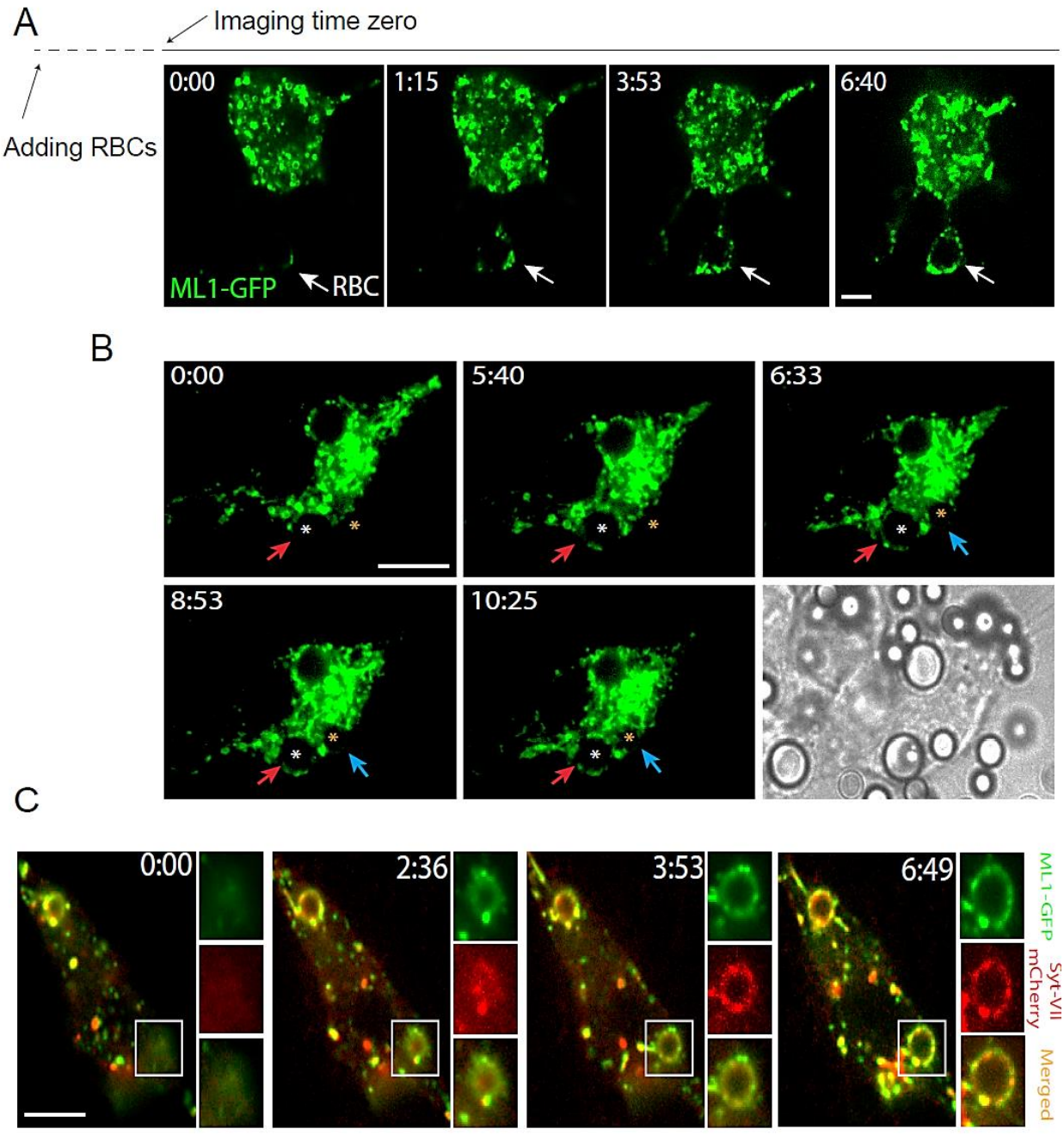
A
Imaging time zero
Adding RBCs
0:00
1:15
3:53
6:40
ML1-GFP
RBC
B
0:00
5:40
6:33
8:53
10:25
C
0:00
2:36
3:53
6:49
ML1-GFP
Syt-VII mCherry
Merged

Figure 3.4 Particle binding to macrophages rapidly recruits TRPML1-GFP to the phagocytic cups and nascent phagosomes.

(A) Rapid recruitment of TRPML1-GFP to the site of particle ingestion (white arrow) and to expanding membrane extensions. Selected frames from time-lapse confocal microscopy of a TRPML1-GFP transfected RAW 264.7 macrophage that was exposed to 6 μm IgG-coated polystyrene beads. Approximately 1 minute after the attachment of beads to the cell surface, TRPML1-GFP was recruited to the membrane extension surrounding the particle (Frame 1 min 15 s; Movie S1). Note that phagocytosis may have been initiated before the imaging time zero due to a technical difficulty in identifying phagocytosing macrophages and capturing phagocytosing events, which typically took 5–10 minutes after particles were added to the recording chamber. Scale bar represents 5 μm. (B) Particle-size-dependent recruitment of TRPML1-GFP to the uptake site. Time-lapse imaging of a TRPML1-GFP-transfected RAW 264.7 macrophage that was exposed to both large (6 μm) and small (3 μm) IgG-coated beads simultaneously. Approximately 5 minutes after the attachment of large beads to the cell surface (phagocytosis initiation), TRPML1-GFP was present at the membrane extensions surrounding a newly formed phagosome (red arrow, frame 5 min 40 sec). In contrast, for small beads, no significant TRPML1-GFP accumulation was seen surrounding the forming phagosome (blue arrow, frame 6 min 33 sec). The center of the particle is indicated with an *. Scale bar = 10 μm. (C) TRPML1-GFP and SytVII-mCherry were simultaneously recruited to nascent phagosomes. Selected frames from time-lapse confocal microscopy showed a RAW cell doubly transfected with TRPML1-GFP and SytVII-mCherry that was exposed to IgG-RBCs. White box indicates the site of particle ingestion; both TRPML1-GFP and Syt VII-mCherry were concurrently recruited to the site of phagosome formation. Scale bar represents 10 μm.

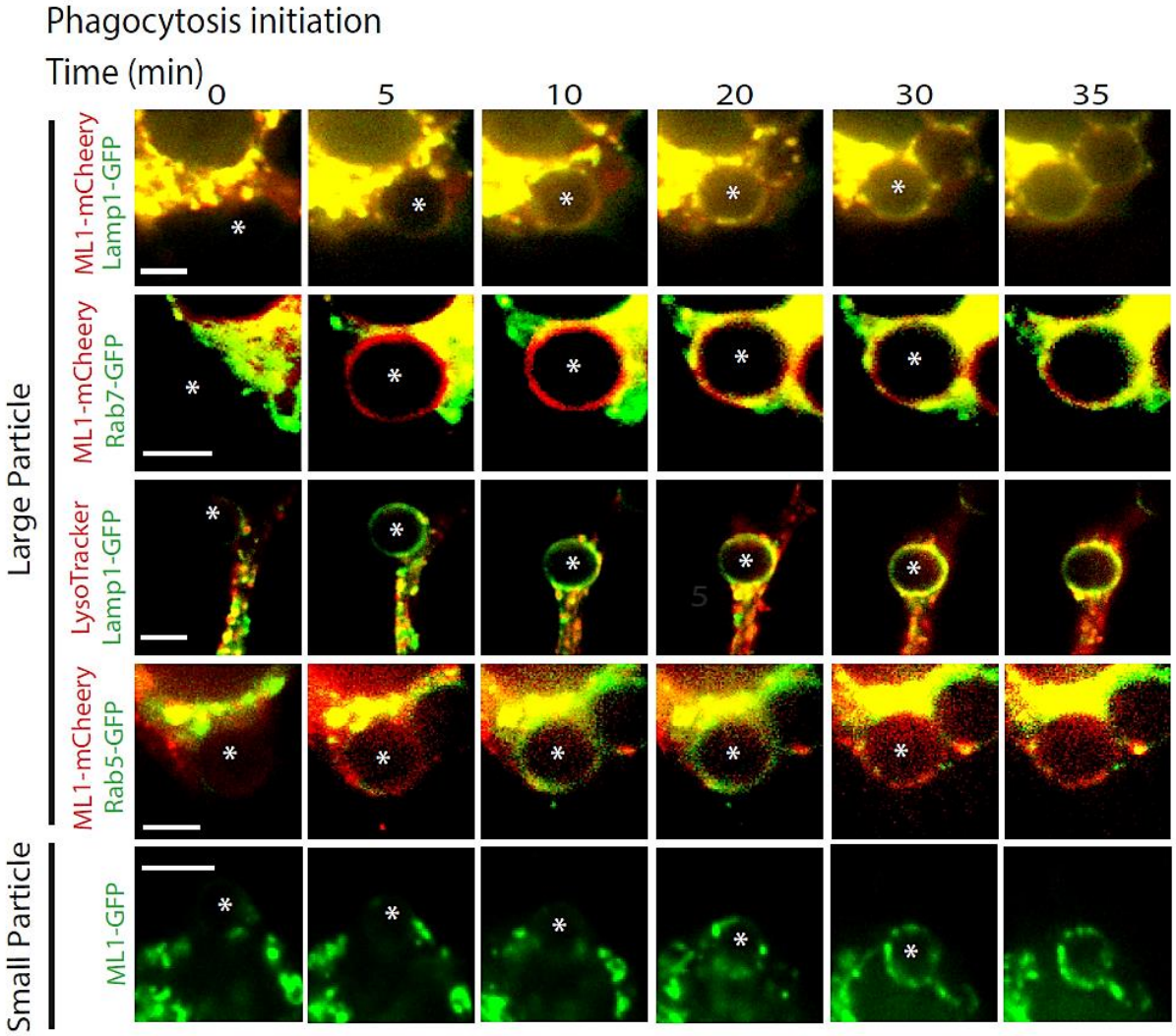

Figure 3.5 The recruitment kinetics of different endolysosomal markers to the particle-containing phagosomes.

RAW macrophage cells were transfected with various molecular endosomal and lysosomal markers. Upon particle binding, the recruitment of these markers to phagosomes was monitored using live-cell imaging over the course of 40 min. For large particles, TRPML1-mCherry and Lamp1-GFP were recruited to the forming phagosomes within 5 min after phagocytosis initiation; Rab7-GFP and LysoTracker were observed in the phagosomes 20 minutes after phagocytosis initiation; Rab5-GFP appeared on the phagosomes 10 minutes after phagocytosis initiation and then disappeared 10 -15 minutes later. For small particles (bottom row), ML1-GFP was recruited to the small particle-containing phagosomes 15–20 minutes after phagocytosis initiation. The center of the particle is indicated with an *. Scale bars represent 5 μm.

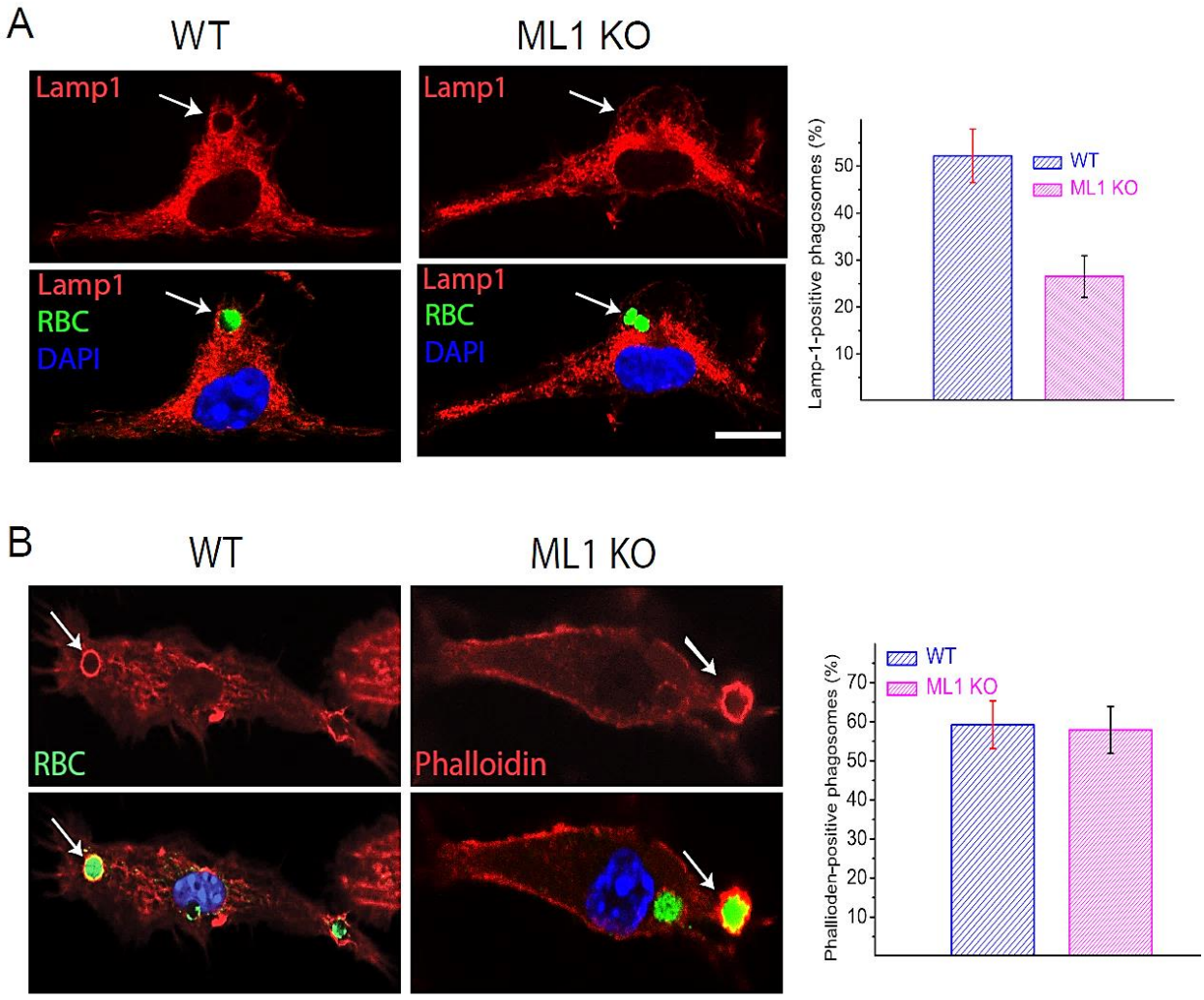

Figure 3.6 Early recruitment of Lamp1 to nascent phagosomes was defective in TRPML1 KO BMMs.

BMMs were exposed to IgG-RBCs for 5 min, fixed, and stained with an anti-Lamp1 antibody (ID4B). Images represent the morphological criteria used to determine phagosome formation. Scale bar = 10 µm. Right panel: percentage of newly-formed phagosomes (5 min after particle binding) in WT and TRPML1 KO BMMs that were Lamp1-positive. Scale bar = 10 µm. (F). Actin polymerization of newly formed phagosomes, shown with phalloidin staining, was comparable in WT and TRPML1 KO BMMs. WT and TRPML1 KO BMMs were exposed to IgG-RBCs for 5 minutes, fixed, and labeled with phalloidin- Alexa-Fluor633 for 30 minutes. Left panel images represent the morphological criteria that were used to determine phagosome formation. The arrows point to RBC-containing phagosomes surrounded by phalloidin-stained polymerized actin.

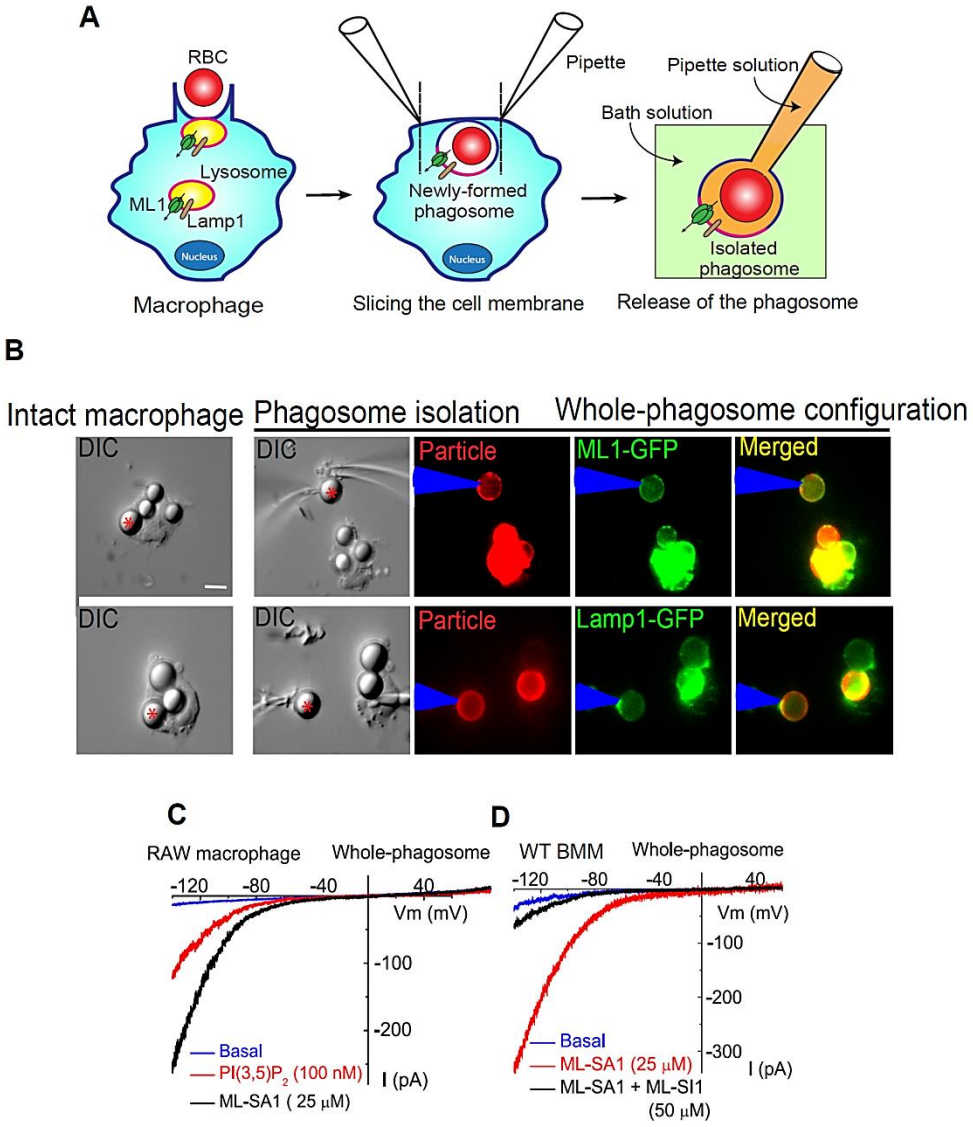

Figure 3.7 Whole-phagosome recording of TRPML1 channels in the isolated nascent phagosomes.

(A) Cartoon illustrations of whole-phagosome recording procedures. Upon RBC uptake (left panel), patch electrodes are used to slice open the phagocytosing macrophage within 5 min of particle binding and ingestion. After RBC-containing phagosomes are isolated, a patch pipette is used to achieve the whole-phagosome configuration. (B) An illustration of whole-phagosome configuration. Cells were transfected with Lamp-1-GFP or ML1-GFP and then exposed to IgG-coated beads on ice for 20 minutes; after phagocytosis was induced by transferring the cells to 37°C for 5 minutes, the newly formed phagosomes were isolated for electrophysiology. (C) ML-SA1- or $PI(3,5)P_2$-activated endogenous whole-phagosome TRPML-like currents in RAW 246.7 cells. (D) Whole-phagosome I_{ML1} in WT, but not ML1 KO BMMs. ML-SA1 (25 μM) - activated I_{ML1} was inhibited by ML-SI1 (50 μM) in WT phagosomes (left panel). No ML-SA1- activated I_{ML1} was seen in ML1 KO phagosomes. Electrophysiology experiments were performed in collaboration with Xiang Wang.

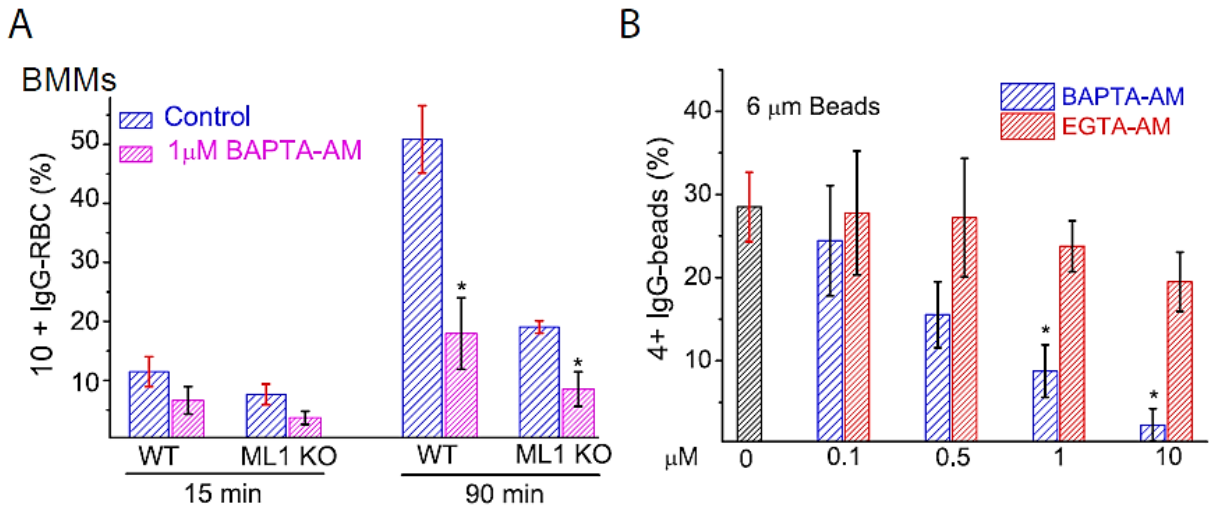

Figure 3.8 Particle uptake is sensitive to intracellular Ca^{2+}

(A) BMMs were pre-incubated with the membrane-permeable fast Ca^{2+} chelator BAPTA-AM (1 μM; 15 min) prior to IgG-RBC exposure for 15 or 90 minutes. After 90 minutes, large particle uptake significantly decreases in WT BMMs. Particle uptake was quantified similar as Figure 3.1. (B) Dose-dependent inhibition of large bead (6 μm) uptake in WT BMMs by low dosage of BAPTA-AM, but not slow Ca^{2+} chelator EGTA-AM at 30 minutes upon particle binding.

A

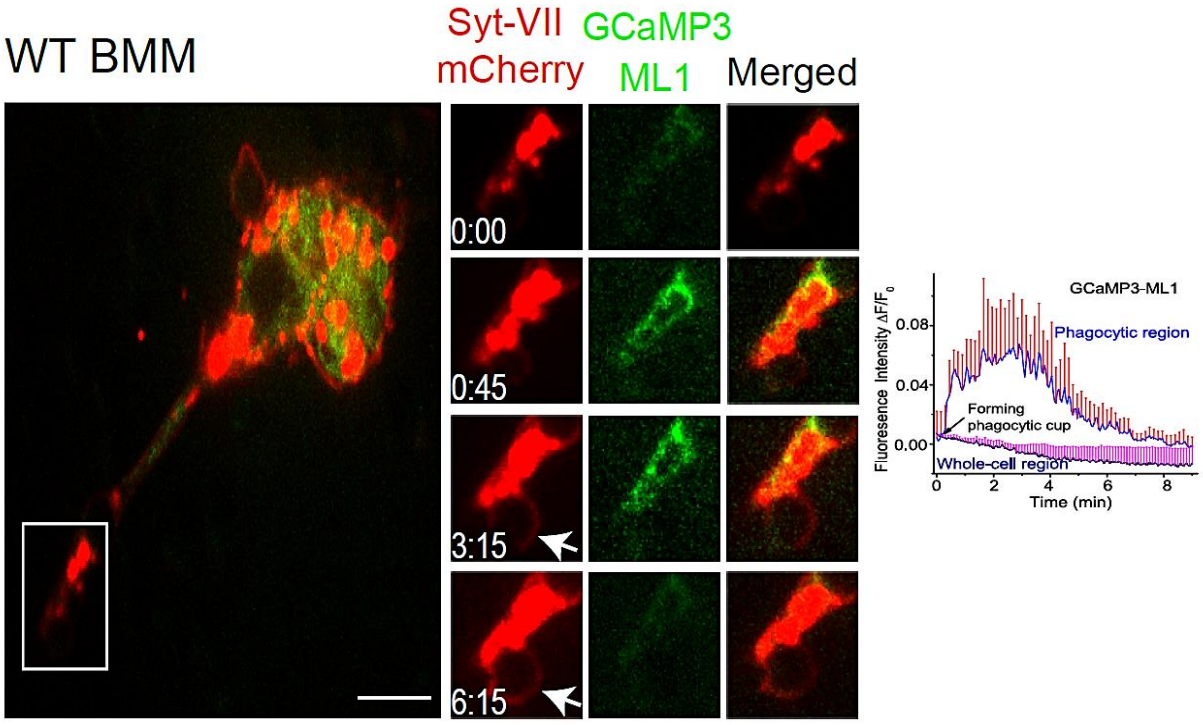
WT BMM
Syt-VII mCherry
GCaMP3 ML1
Merged
0:00
0:45
3:15
6:15
GCaMP3-ML1
Phagocytic region
Forming phagocytic cup
Whole-cell region
Fluoresence Intensity ΔF/F0
0.08
0.04
0.00
0
2
4
6
8
Time (min)

B

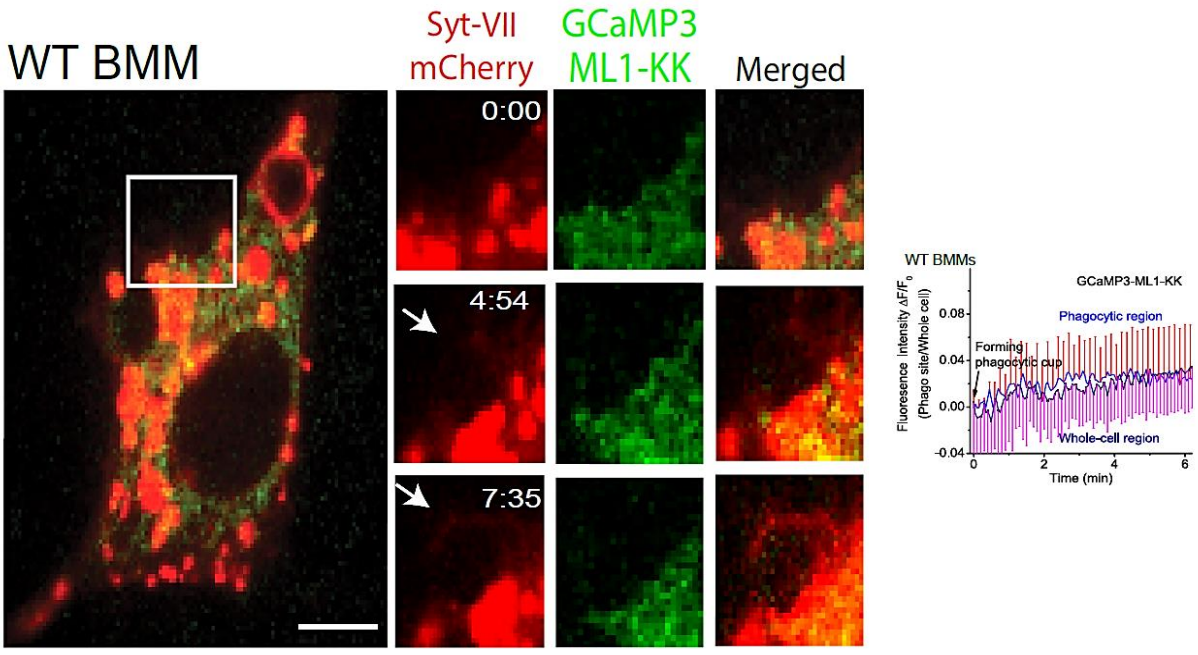
WT BMM
Syt-VII mCherry
GCaMP3 ML1-KK
Merged
0:00
4:54
7:35
WT BMMs
GCaMP3-ML1-KK
Phagocytic region
Forming phagocytic cup
Whole-cell region
Fluoresence intensity ΔF/F0 (Phago site/Whole cell)
0.08
0.04
0.00
-0.04
0
2
4
6
Time (min)

Figure 3.9 Particle binding induce TRPML1 mediated lysosomal Ca^{2+} release in macrophages

(A) IgG-RBC binding triggered a localized Ca^{2+} increase at the site of uptake, shown with selected image frames of a RAW cell doubly-transfected with GCaMP3-TRPML1 and SytVII-mCherry. Upon IgG-RBC binding, GCaMP3-TRPML1 fluorescence increased rapidly (frame 0 min 45 sec) near the site of uptake and around the SytVII-mCherry-positive compartments in the membrane extension, and then decreased after phagosome formation (frame 6 min 15 sec). Right: The time-dependent changes of GCaMP3-TRPML1 fluorescence upon particle binding at the site of uptake (white box) and in the cell body (whole-cell region). White box indicates the site of particle uptake. Scale bar = 10 μm. (B) Selected image frames of a RAW cell doubly-transfected with GCaMP3-TRPML1-KK and SytVII-mCherry. No significant GCaMP3 fluorescence increase was observed at the site of IgG-RBC uptake and cell body (whole-cell region). Right: Time-dependent change of the GCaMP3-TRPML1-KK fluorescence signal upon particle binding. For all panels, scale bars = 10 μm. For all panels, unless otherwise indicated, the data represent the mean ± the standard error of the mean (SEM) from at least three independent experiments.

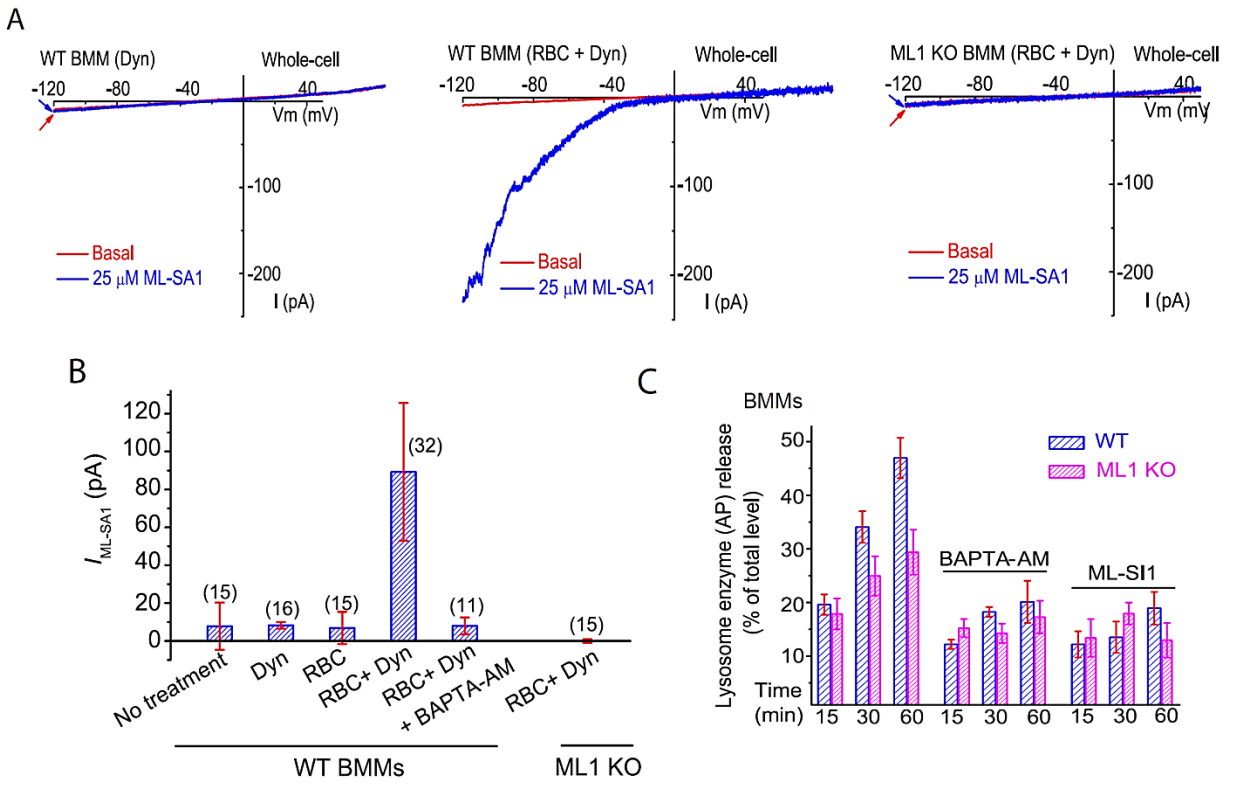

Figure 3.10 TRPML1 is involved in particle uptake induced lysosomal exocytosis.

(A) Whole-cell TRPML1-like currents in WT BMMs exposed to IgG-RBCs for 10 minutes. Dynasore (Dyn, 100 μM) was used to block dynamin-dependent endocytosis in order to facilitate the detection of whole-cell TRPML1 current. No significant whole-cell TRPML1 current was detected in TRPML1 KO BMMs (IgG-RBCs for 10 min). (B) Summary of whole-cell TRPML1 current under different experimental conditions. For all panels, unless otherwise indicated, the data represent the mean ± SEM from at least three independent experiments. (C) RBC-ingestion-induced lysosomal acid phosphatase (AP) release in WT BMMs was reduced by treatment of BAPTA-AM (500 nM, pre-incubation for 15 min) or ML-SI1 (10 μM, pre-incubation for 10 minutes) to the same levels as TRPML1 KO BMMs. Electrophysiology experiments were performed in collaboration with Xiang Wang.

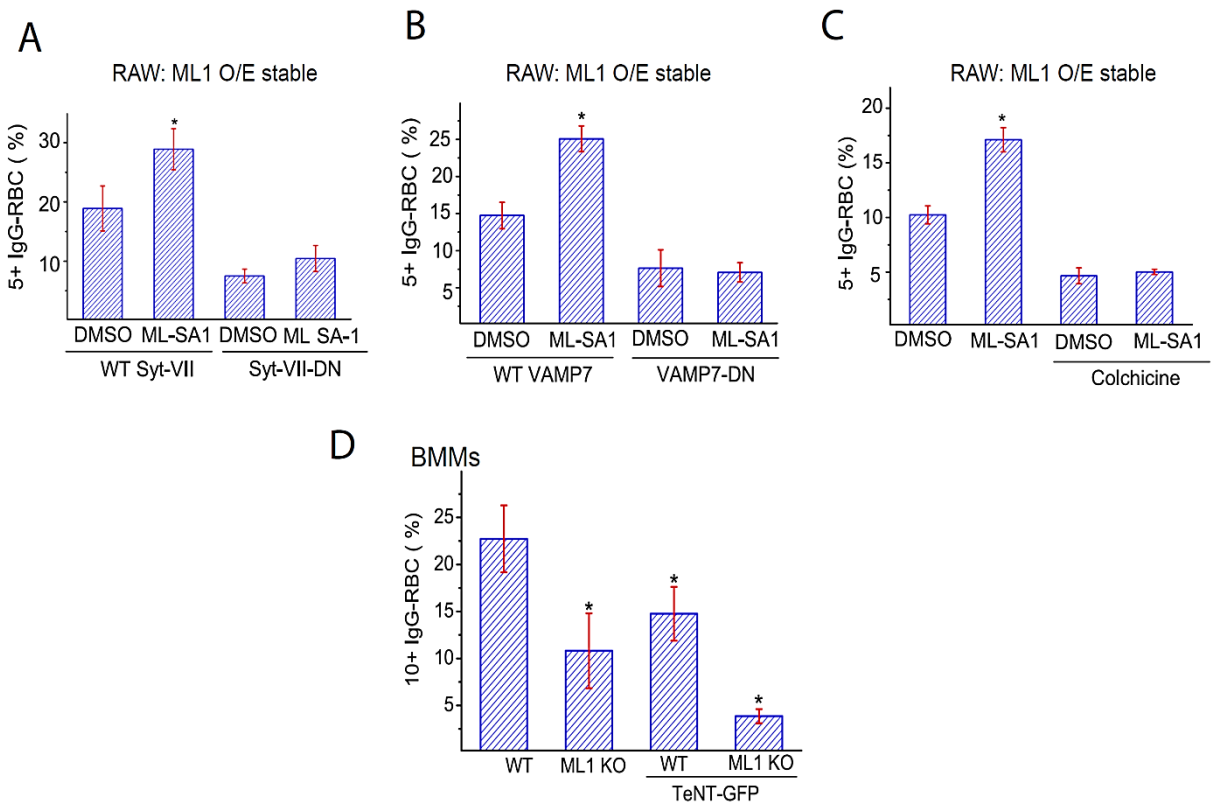

Figure 3.11 TRPML1 mediates particle uptake via the induction of lysosomal exocytosis.

(A) ML-SA1 (10 µM) failed to increase particle ingestion in TRPML1 O/E RAW cells transfected with a SytVII dominant-negative (DN) construct. Cells were pre-incubated with DMSO or ML-SA1 for 15 minutes before they were exposed to IgG-RBCs for 30 minutes. (B) ML-SA1 (10 µM) failed to increase particle ingestion in TRPML1 O/E RAW cells transfected with a VAMP7 dominant-negative (VAMP7-DN) construct. (C) A microtubule-disrupting agent colchicine (10 µM) inhibited ML-SA1-enhanced particle ingestion in WT BMMs. (D) TeNT toxin reduced particle uptake in both WT and ML1 KO BMMs.

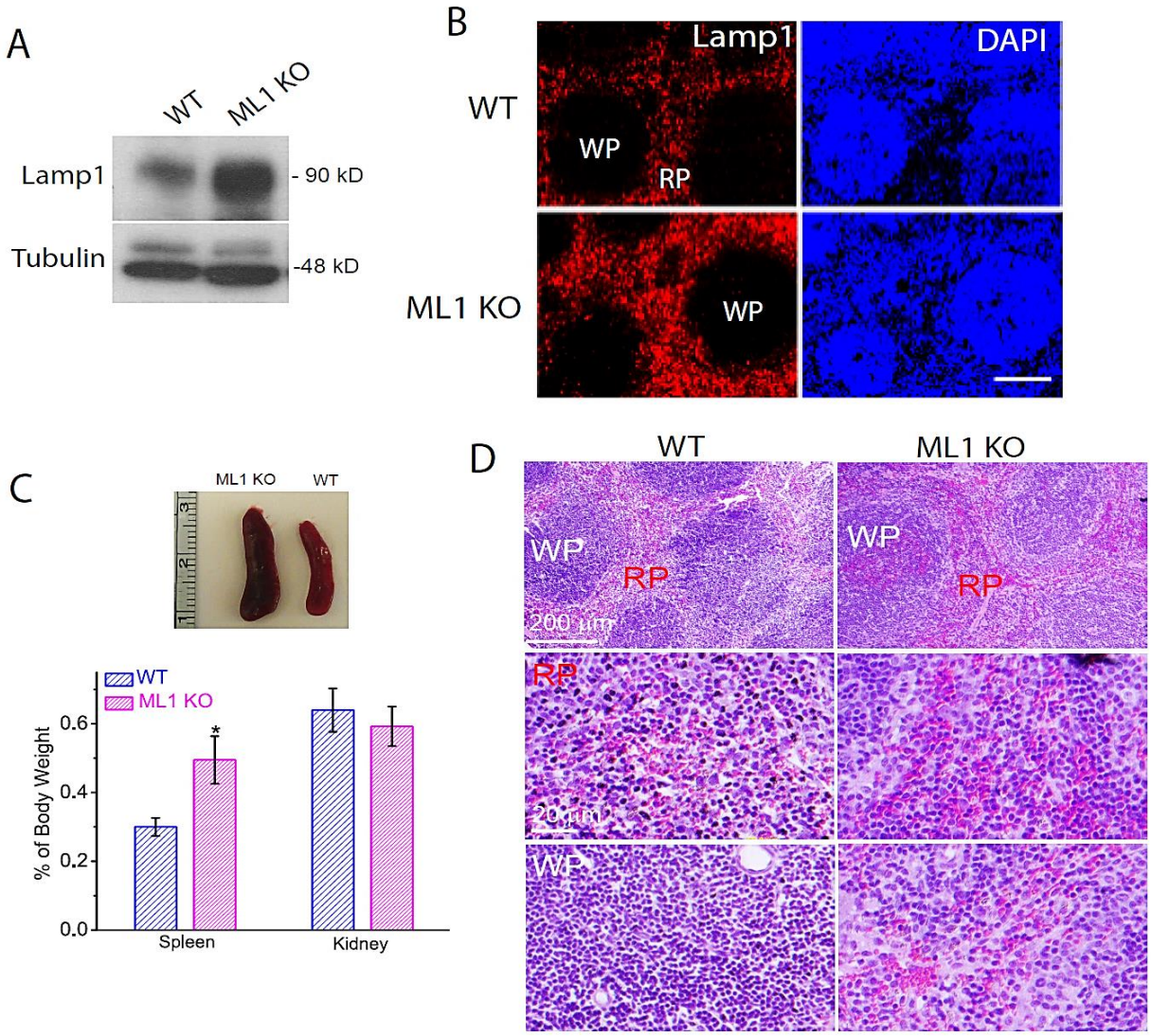
A
WT
ML1 KO
Lamp1
- 90 kD
Tubulin
-48 kD
B
Lamp1
DAPI
WT
WP
RP
ML1 KO
WP
C
ML1 KO
WT
WT
ML1 KO
% of Body Weight
0.0
0.2
0.4
0.6
*
Spleen
Kidney
D
WT
ML1 KO
WP
RP
200 μm
RP
WP
E
WT
ML1 KO
WP
RP
WP
RP
F
WT
ML1 KO
Ion Ratio
0.0
0.1
0.2
0.3
*
Fe/Na
Mg/Na
Ca/Na

Figure 3.12 TRPML1 deficiency results in defective clearance of senescent red blood cells in the spleen

(A) An increased expression of Lamp1 proteins in TRPML1 KO spleens (B) Lamp1 levels increased in the spleen sections of WT and TRPML1 KO mice as released by Immunofluorescence staining . (C) Normalized weight of spleens and kidneys from 4-month-old mice (N=5 animals for each). Inset: Representative images of spleens from 4-month-old WT and ML1 KO mice. (D) Accumulation of RBCs in the red (RP) and white (WP) pulps of a TRPML1 KO spleen revealed by H&E staining. (E) Perl's (Prussian blue) staining for ferric iron in the splenic red pulp (RP) from 4-month-old mice. Scale bar = 200 μm. (F) ICP-MS analysis of the splenic iron content using digested whole spleens from WT and TRPML1 KO mice. Data were presented as ratios of different ions. For all panels, unless otherwise indicated, the data represent the mean ± SEM from at least three independent experiments.

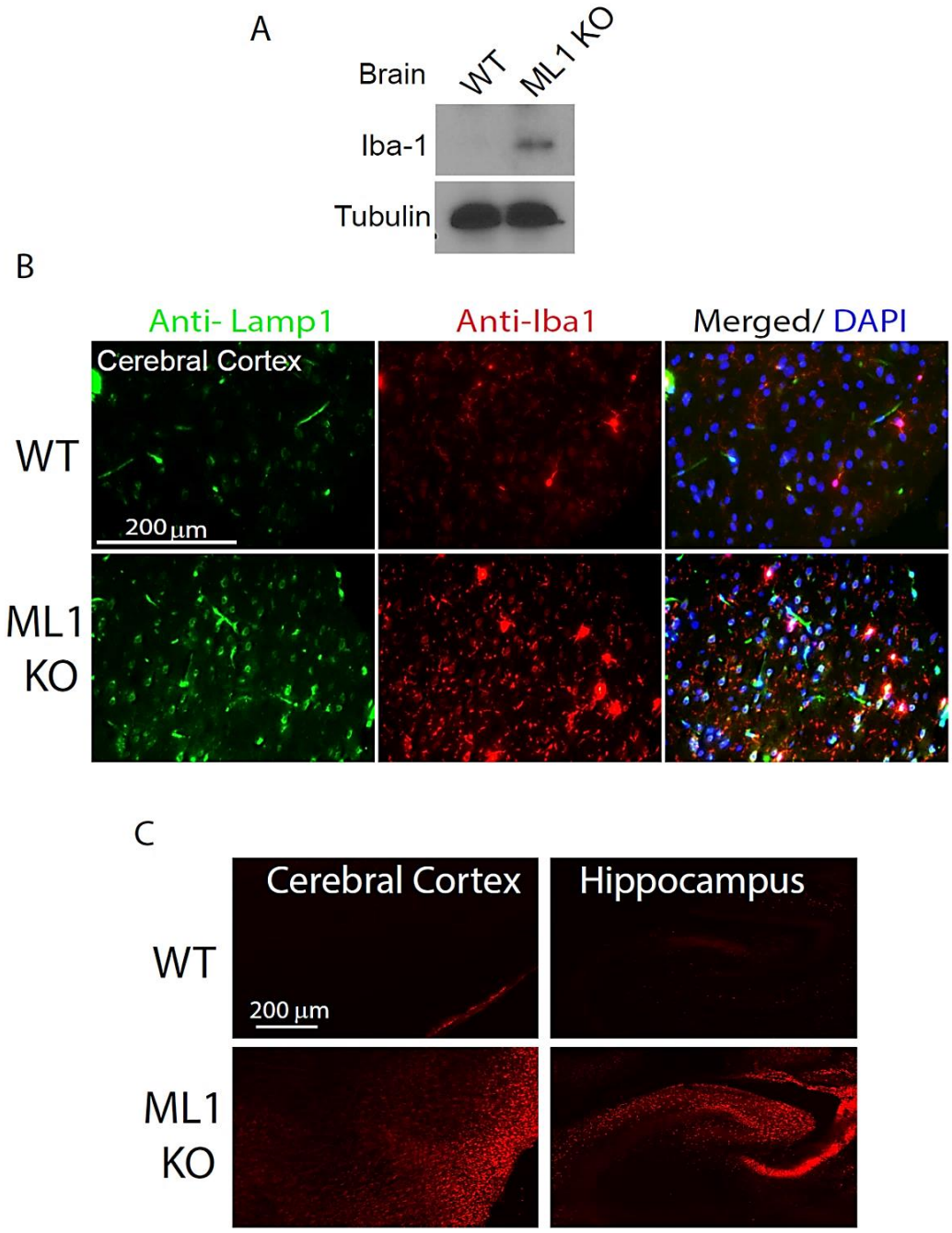

Figure 3.13 Microglia activation and the accumulation of dead cells in the brain of TRPML1 KO mice.

(A) Iba1 was up-regulated in the whole-brain lysates of TRPML1 KO mice. (B) Iba1-positive cells were up-regulated in the sections of the brain cortex of TRPML1 KO mice. (C) Propidium iodide (PI, 20 μg/ml) -labeled cells in the cerebral cortex and hippocampus of WT and TRPML1 KO mouse brain sections.

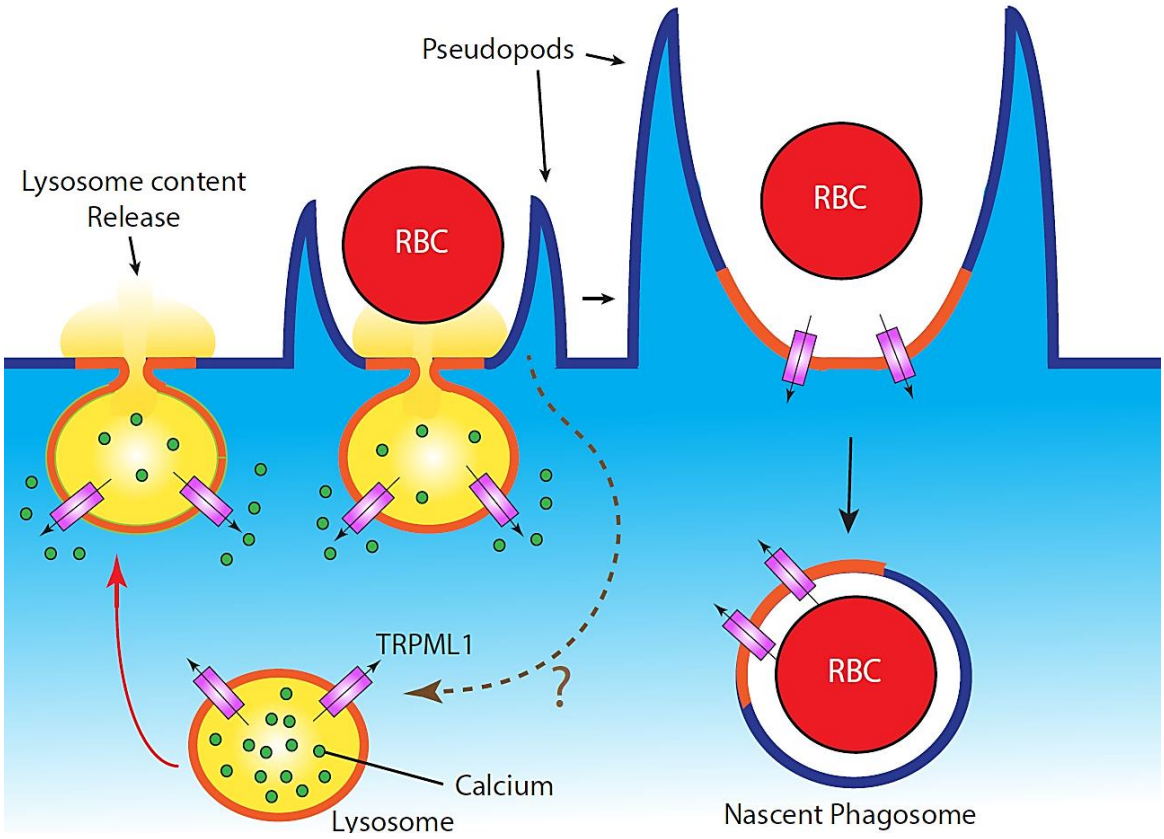

Figure 3.14 Particle binding activates lysosomal TRPML1 to initiate Ca^{2+}-dependent lysosomal exocytosis.

Large particle (IgG-RBC) binding induces the activation of TRPML1 on the surface of lysosomes to induce lysosomal Ca^{2+} release. Juxtaorganellar Ca^{2+} can then trigger lysosome-plasma membrane fusion, which provides substantial amount of lysosomal membranes for the pseudopod extension around IgG-RBCs. As a result, lysosomal membrane proteins, such as TRPML1, are inserted into the plasma membrane and become part of the phagocytic cup. Pseudopod extension continues until the IgG-RBCs are completely internalized. Phagocytic cups are then closed, and nascent phagosomes are formed which contain lysosomal membrane proteins. The signaling events that lead to TRPML1 activation in macrophages are not clear, but it could be through signaling molecules such as phosphoinositides.

CHAPTER IV

PI(3,5)P_2 IS INVOLVED IN PARTICLE UPTAKE IN MACROPHAGES

Abstract

Recent evidence indicates that membrane extension and pseudopod formation in macrophages depends on the delivery of lysosomal membranes (lysosomal exocytosis) to the site of particle uptake through the activation of the lysosomal Ca^{2+} channel TRPML1. Thus, lysosomal membrane can compensate for the plasma membrane used during phagosome formation. However, the TRPML1 activation mechanism during this process is currently unknown. Phosphatidylinositol 3,5-bisphosphate [PI(3,5)P_2] is a low-abundance phosphoinositide shown to be localized on the endosomes and lysosomes. On the surface of the lysosomes, PI(3,5)P_2 is the only known endogenous activator for TRPML1 and is suggested to be involved in TRPML1 induced lysosomal exocytosis. Here I show that during particle uptake, PI(3,5)P_2 levels increase on the lysosomes adjacent to the particle ingestion site and at the phagocytic cup. Moreover, inhibiting PI(3,5)P_2 production through genetic and pharmacological approaches blocked particle ingestion in macrophages, indicating that PI(3,5)P_2 synthesis on the lysosome is necessary for TRPML1 activation and efficient particle ingestion in macrophages.

Introduction

Phosphoinositides (PIs) are signaling molecules involved in a variety of cellular trafficking events in different cell types (Di Paolo and De Camilli 2006). In macrophages PIs are involved in different signaling events essential for efficient phagocytosis (Gillooly, Simonsen et al. 2001; Cosio and Grinstein 2008). During phagocytosis initiation, actin rearrangement is required at the site of particle ingestion in order to facilitate pseudopod formation (Allen and Aderem 1996). This process has been shown to be dependent on $PI(4,5)P_2$ production, followed by the local production of $PI(3,4,5)P_3$, which is required for phagosome sealing (Botelho, Scott et al. 2004). The production of both $PI(4,5)P_2$ and $PI(3,4,5)P_3$ are transient and localized at the phagosomal cup. Their cellular levels have been shown to decrease after phagosome formation (Botelho, Scott et al. 2004). PI3P is known to be important for phagosome maturation and it accumulates on phagosomes once phagosomes fuse with the early endosomes. Cells deficient in PI3P production have been shown to be defective in phagosomal maturation (Botelho, Scott et al. 2004).

Among the PIs, $PI(3,5)P_2$ is the least characterized and its role in phagocytosis remain elusive. Recent data have shown that $PI(3,5)P_2$ is localized on the surface of lysosomes and activates the lysosomal Ca^{2+} channel TRPML1 (Dong, Shen et al. 2010). As shown in the previous chapter, TRPML1 activity is required for large particle uptake in macrophages. TRPML1 was shown to regulate large particle uptake by mediating lysosomal exocytosis and therefore regulating the delivery of lysosomal membrane to the site of particle uptake in order to provide excess membrane for phagosome formation (Chapter III). Here, I hypothesized that TRPML1 activation during particle uptake is regulated through the production of $PI(3,5)P_2$ on the lysosomes adjacent to the site of particle uptake. By using a recently established fluorescent

tagged PI(3,5)P_2 probe developed in our lab, I was able to characterize the dynamics of PI(3,5)P_2 during particle ingestion and reveal that, during particle ingestion PI(3,5)P_2 is synthesized on the phagocytic cup and is required for the efficient uptake of large particles in macrophages.

Methods

Fluorescence and time-lapse imaging Live imaging of RBC uptake by BMMs was performed on a heated stage using a Spinning Disk confocal imaging system consisting of an Olympus IX81 inverted microscope, a 100X Oil objective NA 1.49 (Olympus, UAPON100XOTIRF), a CSU-X1 scanner (Yokogawa), an iXon EM-CCD camera (Andor), and MetaMorph Advanced Imaging acquisition software v.7.7.8.0 (Molecular Devices). The PI(3,5)P_2 probe was generated with the tandem repeats of the TRPML1 N-terminal segment (residues 1–68) fused with a GFP tag (Li, Wang et al. 2013). All images were taken with the 100X objective of a Leica (TCS SP5) confocal microscope.

HPLC measurement of phosphoinositide levels. Raw macrophage cell lines were grown in 6 well plates to 20-30% confluence. Cells were then rinsed twice with PBS and incubated for 48 hours with the inositol labeling medium, contained inositol-free DMEM, 10 μCi/mL of myo-[2-^{3}H] inositol (GE Healthcare), 10% (vol/vol) dialyzed FBS, 20 mM Hepes, 5 μg/mL transferrin, and 5 μg/mL insulin (Zolov, Bridges et al. 2012). Afterwards, a solution (pre-warmed to 37°C) of IgG-coated 6 μM polystyrene beads was prepared in a 1:50 ratio (macrophage:beads). After RAW cells were rinsed with PBS once, 4 ml of beads were added to each well. The plates were centrifuged briefly for 1 minute at 3,000 RPM and then placed in the 37°C incubator for 1, 2, 5, and 10 minutes. After each time point, the un-ingested beads were removed and RAW cells were treated with 500 μl of ice-cold 4.5% (vol/vol) perchloric acid for 15 minutes at room temperature. The plates were

rotated gently every 2 minutes in order to prevent cells from drying. RAW cells were then scraped off, spun at 12,000 × g for 10 minutes at 4 °C, and then processed for HPLC measurement. The data were analyzed as described previously (Zolov, Bridges et al. 2012).

Results

$PI(3,5)P_2$ is up-regulated at the site of particle uptake

$PI(3,5)P_2$ is the only known endogenous activator of TRPML1 (Dong, Shen et al. 2010) and TRPML1 activation has been shown to be required for efficient large particle uptake in macrophages (Chapter III). Thus, I hypothesized that $PI(3,5)P_2$ levels are elevated during particle ingestion in order to mediate the activation of TRPML1. To directly test the possibility that an elevation of $PI(3,5)P_2$ is locally triggered by large particle binding, I used the newly generated $PI(3,5)P_2$-specific probe, ML1-2N-GFP, made by the fusion of GFP to the phosphoinositide-binding domain of TRPML1 (Li, Wang et al. 2013), to detect dynamics of $PI(3,5)P_2$. Strikingly, ML1-2N-GFP was rapidly recruited to the forming phagosomes (**Fig. 4.1A**) in RAW cells that were doubly transfected with ML1-2N-GFP and SytVII-mCherry. A transient and localized increase in ML1-2N-GFP fluorescent intensity was observed preferentially at the uptake sites of SytVII-mCherry-positive lysosomes within three minutes of particle binding (**Fig. 4.1A**, frame 2 min and 54 sec). In contrast, no increase in GFP fluorescence was observed in cells transfected with ML1-7Q-2N-GFP (a $PI(3,5)P_2$ unbinding control probe) (**Fig. 4.1B**), indicating the specificity of the probe.

We also measured the radio-labeled phosphoinositides using high-performance liquid chromatography (HPLC). We found that $PI(3,5)P_2$ levels increased significantly during the first 5 minutes of phagocytosis upon particle binding, which corresponds to the time necessary for

phagosome formation (**Fig. 4.2**). Interestingly, PI3P levels also increase with similar kinetics to PI(3,5)P_2 (**Fig. 4.2).** This wasn't unexpected because on the lysosomal compartments PI(3,5)P_2 is generated from PI3P on the endosomes, so it make sense for PI3P levels to increase with similar kinetics as PI(3,5)P_2 since it's the precursor for PI(3,5)P_2 production (Zolov, Bridges et al. 2012)**.** The levels of other PIs, such as PI4P, PI5P, and PI(4,5)P_2, did not change during the same time point suggesting that localized PI(3,5)P_2 generation may be one of the initial steps during large particle ingestion (**Fig. 4.2**).

PI(3,5)P_2 activity is required for efficient large particle uptake in macrophages

PI(3,5)P_2 is generated from PI3P by a protein complex that contains PIKfyve, a PI kinase that is localized on the late endosomes and lysosomes (Jefferies, Cooke et al. 2008). The activity of PIKfyve is dependent on the FIG4 protein in the complex (Lenk, Ferguson et al. 2011). Thus, macrophages isolated from FIG4 KO mice are predicted to have a reduced PI(3,5)P_2 level compared with WT cells (Chow, Zhang et al. 2007). FIG4 KO BMMs contained enlarged Lamp1-positive compartments (**Fig. 4.3A**), as seen in other cells types from FIG4 KO mice (Chow, Zhang et al. 2007). Similar to TRPML1 KO BMMs, FIG4 KO BMMs were also defective in IgG-RBC uptake (**Fig. 4.3B**) and IgG-RBC-induced lysosomal AP release (**Fig. 4.3C**), illustrating that cells deficient in PI(3,5)P_2 exhibit similar characteristics as TRPML1 deficient macrophages. Additionally, I evaluated large and small particle uptake in WT macrophages after exposing them to PIKfyve specific inhibitor YM201636 (Jefferies, Cooke et al. 2008). Interestingly, large (6 μm), but not small (3 μm) bead uptake, was defective in WT BMMs treated with YM201636 similar to macrophages isolated from FIG KO mice (**Fig. 4.4A-**

C). Collectively, these data suggest that PI(3,5)P_2 participates in large particle uptake and lysosomal exocytosis, a phenotype similar to TRPML1 KO macrophages.

PI(3,5)P_2 levels increase during particle uptake prior to phagosome maturation

PI(3,5)P_2 has been shown to exist on the surface of lysosomes (Li, Wang et al. 2013). Lysosomes are traditionally believed to be delivered to phagosomes through the phagosomal maturation process in order to facilitate the degradation of the ingested particle (Aderem and Underhill 1999; Flannagan, Jaumouille et al. 2012). However, in previous chapters I illustrated that lysosomes get delivered to the site of particle ingestion via lysosomal exocytosis in order to provide excess membrane for phagosome formation. Our data indicated that PI(3,5)P_2 levels are increased at the site of particle uptake (**Fig. 4.1**), so I sought to determine at what stage of phagosome formation P(3,5)P_2 levels are increased.

I analyzed the kinetics of two other PIs known to accumulate on the surface of phagosomes at different stages. PI3P accumulates on phagosomes after formation and before the final delivery to lysosomes, this was detected using the 2X-FYVE-GFP probe. On the other hand, PI(3,4,5)P_3 has been shown to accumulate to the forming phagosomes before closure and was detected using the AKT-PH-GFP probe (Yeung, Ozdamar et al. 2006). Consistent with this, the AKT-PH-GFP probe accumulated rapidly on forming phagosomes, but quickly disappeared upon closing of phagocytic cups within several minutes (**Fig. 4.5A**). The time course of PI(3,4,5)P_3 production matches phagosome formation and closure as shown previously(Yeung, Ozdamar et al. 2006). In contrast, the PI3P probe accumulated on the early phagosomes approximately 10 minutes after phagosome initiation (**Fig. 4.5B**), which was similar to Rab5 recruitment to early phagosomes (**Fig. 3.5**). Note that PI3P increase occurred after SytVII

recruitment (**Fig. 4.5B**). Because PI(3,5)P_2 accumulates at the phagocytic site with a time course similar to PI(3,4,5)P_3 and prior to PI3P, it is very likely that PI(3,5)P_2 increase occurs during phagosome formation.

Discussion

PIs have been extensively studied in macrophages and in the course of phagocytosis (Gillooly, Simonsen et al. 2001; Yeung, Ozdamar et al. 2006; Cosio and Grinstein 2008). However, the localization and dynamics of PI(3,5)P_2 in macrophages remained largely unknown, mainly due to the lack of a direct method to visualize this low-abundance phosphoinositide. By using a recently established fluorescent tagged PI(3,5)P_2 probe, I illustrated that PI(3,5)P_2 gets synthesized on the lysosomes adjacent to the site of particle uptake (**Fig. 4.6**) and its production is required for lysosomal exocytosis and large particle uptake in macrophages. These phenotypes are reminiscent of TRPML1 KO macrophages. PI(3,5)P_2 is the only known endogenous activator for TRPML1 (Dong, Shen et al. 2010). Therefore, it is possible that PI(3,5)P_2 regulates large particle uptake through the activation of TRPML1 in macrophages.

What differentiates the uptake of large vs. small particles is not clear. A small increase in the diameter of particles may result in a much larger demand for membranes, receptors, signaling molecules, and cytoskeleton machinery. It is known that the uptake of large (> 4.5 μm) IgG-coated particles depends on phosphatidylinositol 3-kinase (PI3K) activity, whereas the uptake of smaller (< 3 μm) particles does not require PI3K activity (Cox, Tseng et al. 1999). For example, wortmannin and LY294002, two non-specific type I & II PI3K inhibitors, preferentially inhibit the uptake of large particles(Cox, Tseng et al. 1999; Hoppe and Swanson 2004). While type I PI3K has been linked to an effect on cytoskeleton rearrangement during large particle uptake

(Cox, Tseng et al. 1999; Hoppe and Swanson 2004), type II PI3K could contribute to large particle uptake via the production of PI3P, the precursor of $PI(3,5)P_2$, which in turn acts as the endogenous activator of TRPML1.

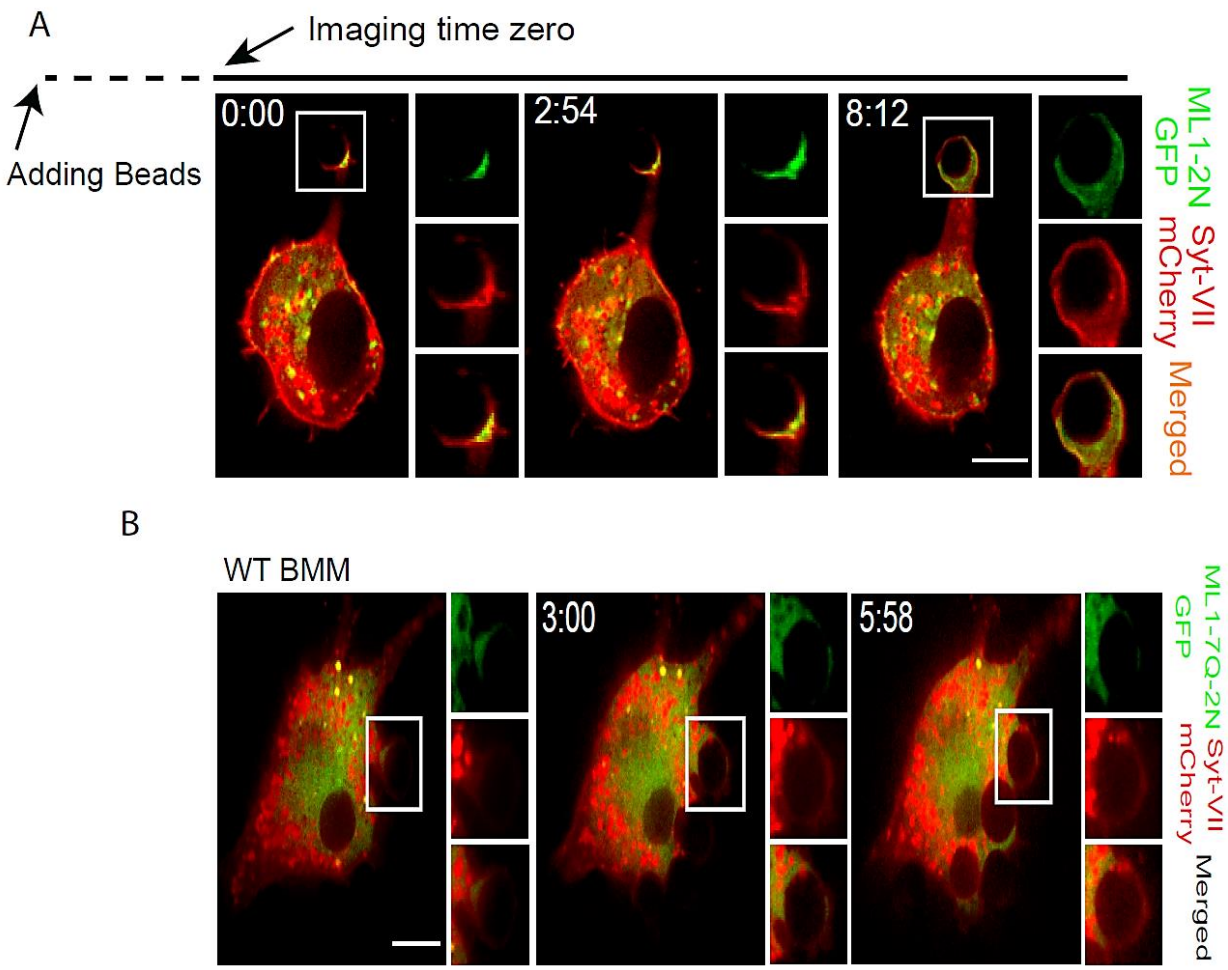

Figure 4.1 PI(3,5)P_2 levels are elevated adjacent to the site of particle uptake.

(A) Upon particle binding, ML1-2N-GFP and SytVII-mCherry accumulated at the site of uptake within minutes. Note that phagocytosis initiation may have occurred before the imaging time zero due to a technical difficulty in identifying macrophages undergoing phagocytosis. Scale bar = 10 µm (B) Lack of ML1-7Q-2N-GFP accumulation at the site of uptake. Scale bar = 5 µm.

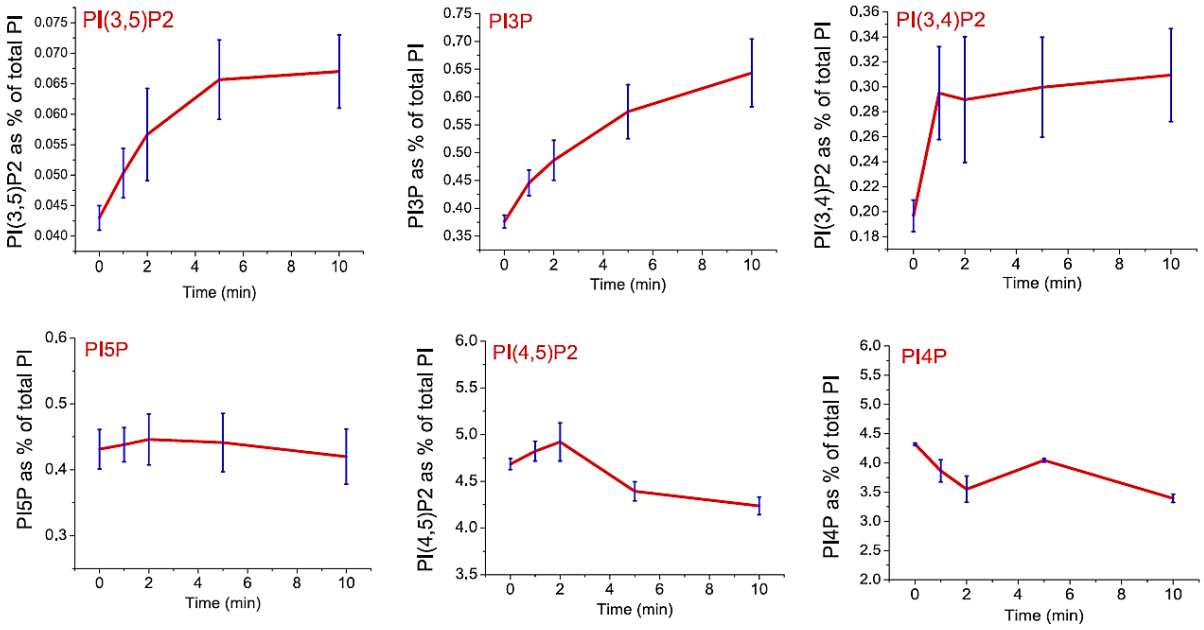

Figure 4.2 HPLC analysis of the levels of different PIs during phagosome formation.

Myo-[2-3H] inositol-labeled RAW cells were exposed to IgG-coated beads (6 μm) in a 1:50 ratio (macrophage:beads) and then centrifuged at 4°C to synchronize the phagocytosis event. After centrifugation, cells were placed at 37°C for 0, 1, 2, 5, and 10 minutes. After each time point, cells were harvested and prepared for HPLC analysis. Data is from three independent experiments. HPLC experiments were performed in collaboration with Sergey Zolov and Lois Weisman from the LSI at the University of Michigan.

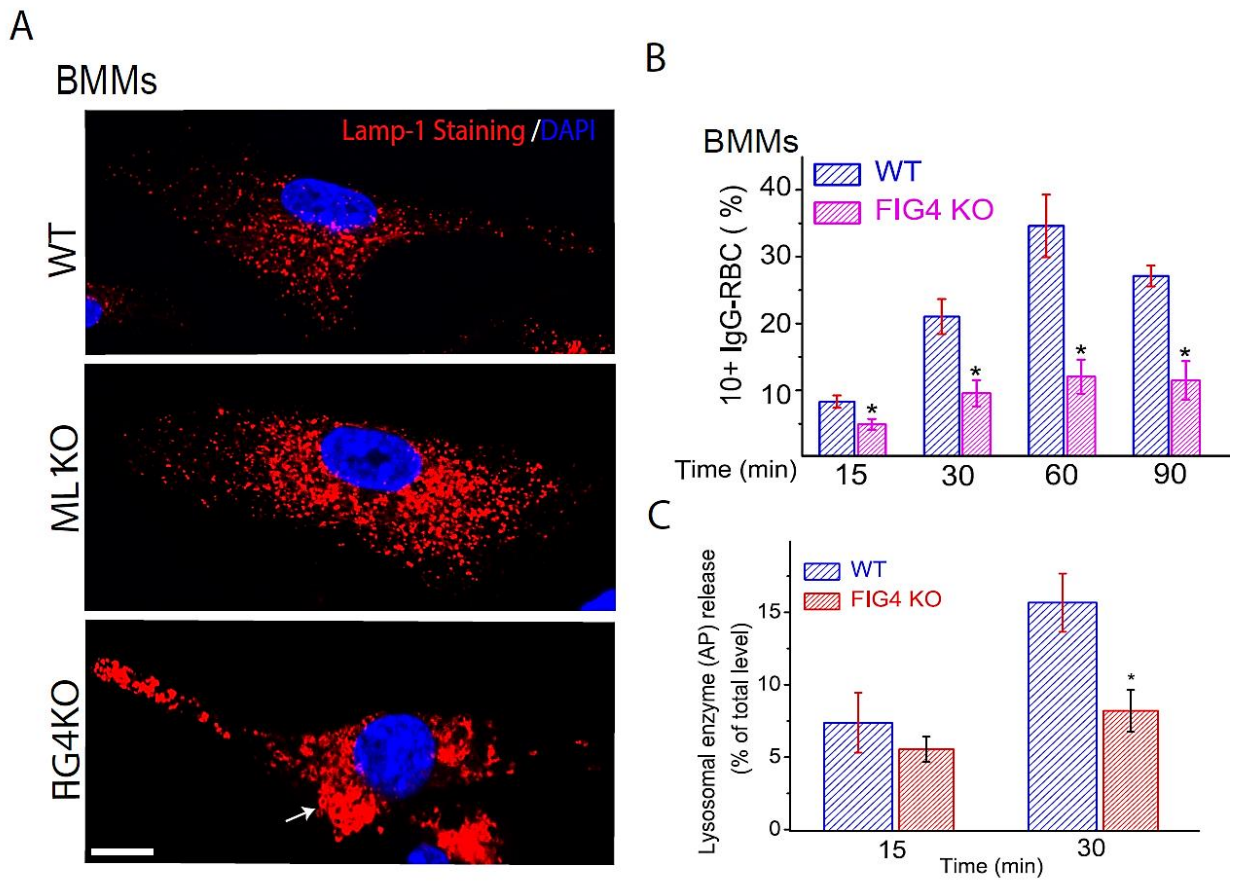

Figure 4.3 FIG4 KO macrophages are defective in large particles.

(A) Enlargement of Lamp1-positive compartments in FIG4 KO BMMs. Scale bar = 5 µm. (B) FIG4 KO macrophages were defective in IgG-RBC ingestion. WT and FIG4 KO BMMs were exposed to IgG-RBCs for the time periods indicated. (C) IgG-RBC (30 min)-induced lysosomal AP release was reduced in BMMs from FIG4 KO mice.

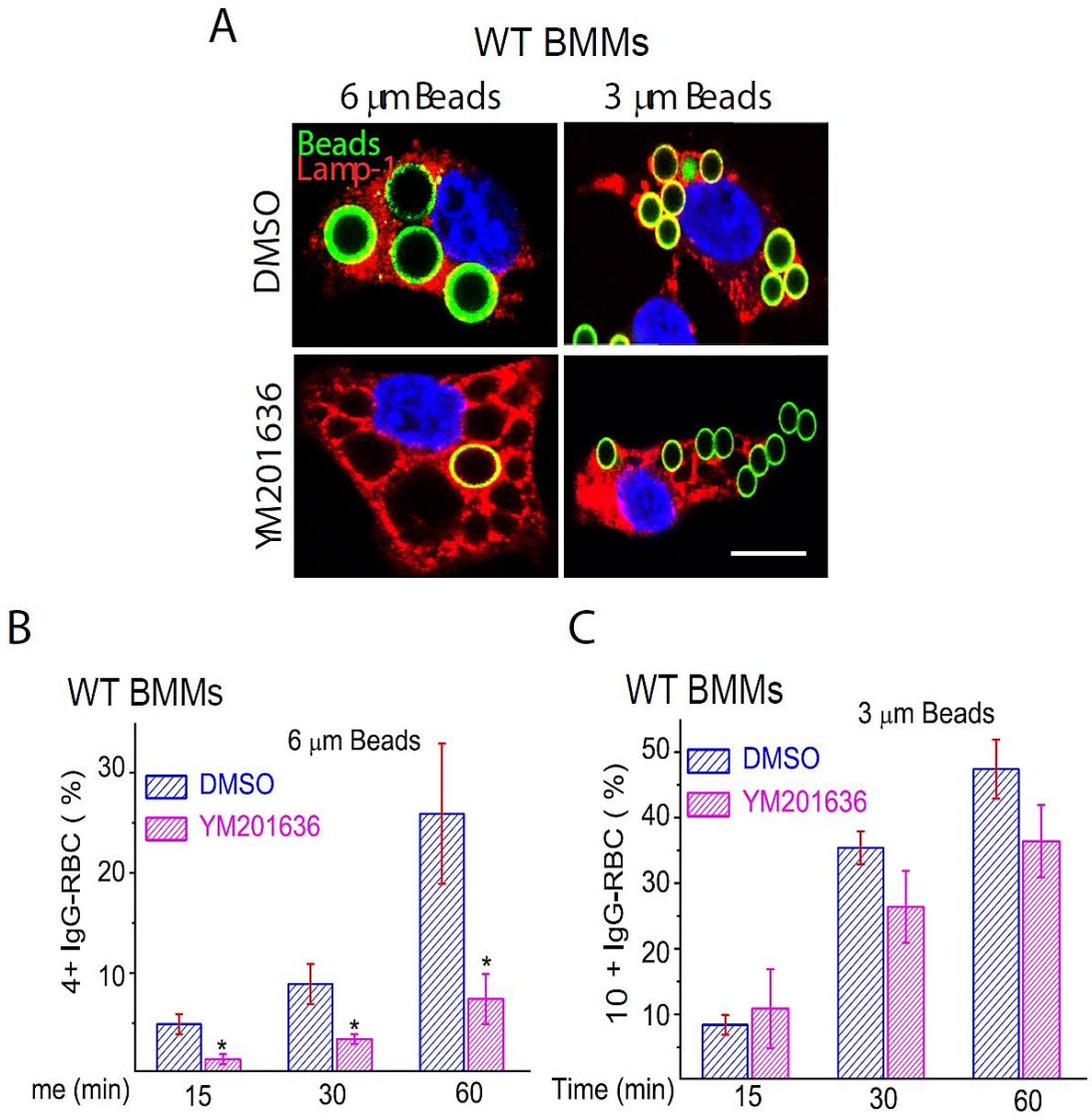

Figure 4.4 PIKfyve activity is required for the efficient uptake of large particles.

(A) DMSO (control) or YM0201636 (1 μM for 1 hour) treated macrophages were exposed to IgG-opsonized small (3 μm) or large (6 μm) beads for 30 minutes. Samples were then fixed and processed for confocal microscopy. YM0201636 treated cells exhibited large vacuoles (B) Average particle ingestion for DMSO (control) or YM0201636 macrophages.

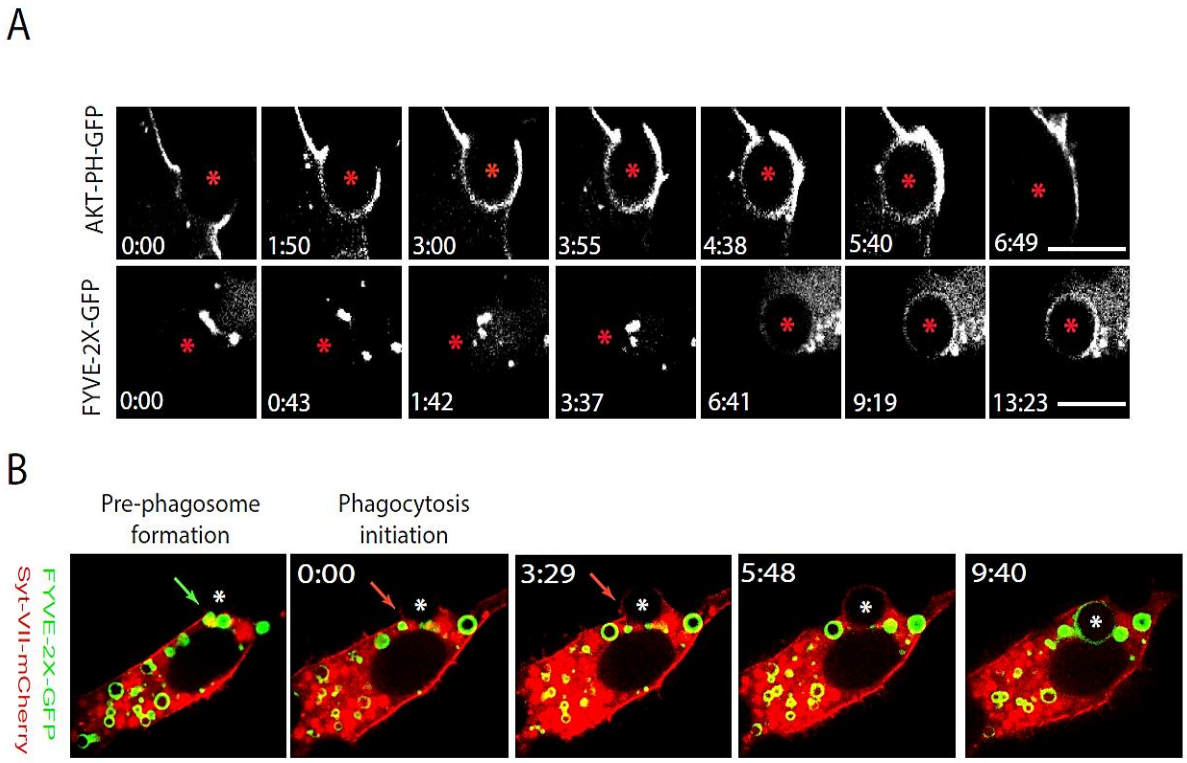

Figure 4.5 PI(3,5)P2 up-regulation occurs prior to phagosomal maturation.

(A) Distinct recruitment kinetics of AKT-PH-GFP (PI(3,4,5)P3/PI(3,4)P2 probe) and 2X-FYVE-GFP (PI3P probe) to forming phagosomes. AKT-PH-GFP probe is up-regulated during the formation of new phagosome, while 2X-FYVE-GFP gets synthesized on the phagosomes 10 minutes after formation. Scale bars = 10 µm. (B) While SytVII-mCherry appeared on the forming phagosomes within 3-5 minutes of phagocytosis initiation, 2X-FYVE-GFP (PI3P probe) appeared on phagosomal membranes several minutes later (9 min 40 sec). The center of the particle is indicated with an *.

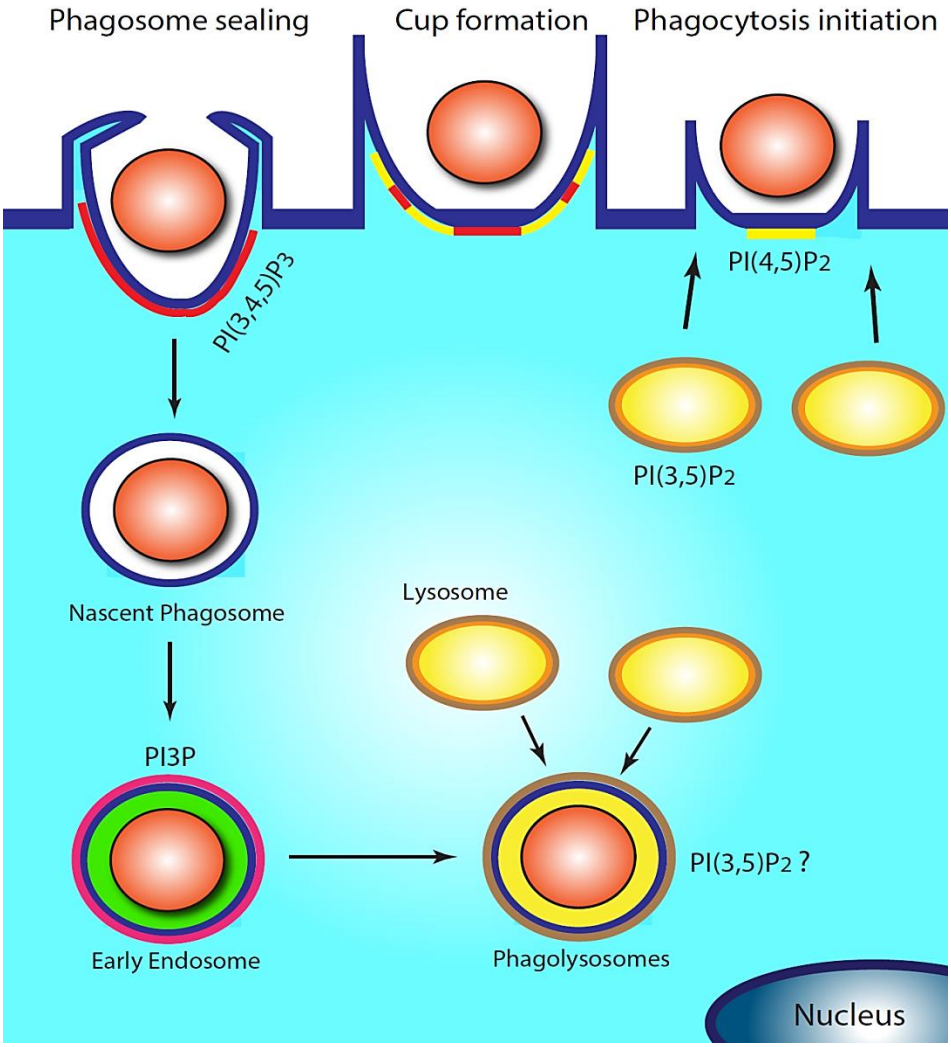

Figure 4.6 phosphoinositides dynamics during phagocytosis.

The changes in the relative abundance of each PI are illustrated in the figure. PI(3,5)P_2 is up-regulated on the lysosomes adjacent to the site of particle uptake and regulates the activity of TRPML1 (not shown), which is required for lysosomal fusion with the plasma membrane in order to provide excess membrane for particle ingestion. PI(4,5)P_2 is synthesized on the phagocytic cup and is involved in actin polymerization. During particle ingestion and pseudopod extensions, PI(4,5)P_2 mainly gets converted to PI(3,4,5)P_3, which is required for phagocytic cup closure and the final step of particle ingestion. Once the phagosomes are formed they go through the phagosomal maturation pathway where PI3P gets synthesized on the surface of phagosomes after they are delivered to early endosomes.

CHAPTER V

TRPML1 MEDIATES THE DEGRADATION OF INTRACELLUALR PATHOGENS IN MACROPHAGES

Abstract

Inhibiting phagosome-lysosome fusion is crucial for intracellular survival and replication of many intracellular pathogens within the macrophages. Here, I found that the lysosomal cation channel Mucolipin TRP channels 1 (TRPML1) limits the intracellular replication of photogenic bacteria. I observed that bacteria elimination in macrophages is inhibited by synthetic TRPML1 blockers and is defective in macrophages isolated from TRPML1 knockout mice. Using time-lapse confocal imaging I observed that TRPML1 facilitates the fusion of phagosomes containing bacteria with lysosomes in a calcium dependent manner. In addition, TRPML1 was also shown to deplete lysosomes from the iron shown to be necessary for bacteria growth within the lysosomal compartments. Therefore, TRPML1 potentially has a dual role in macrophage bactericidal activity; mediating the lysosomal fusion and depleting lysosomes from the nutrients required for bacteria growth.

Introduction

Salmonella is an intracellular pathogen responsible for a variety of diseases in humans such as typhoid fever, paratyphoid fever, and gastroenteritis (Haraga, Ohlson et al. 2008). Macrophages are one of the main immune cells responsible for ingestion and elimination of *Salmonella* (Haraga, Ohlson et al. 2008). However, *Salmonella* have developed a set of mechanisms to alter and hijack the trafficking and signaling pathways of macrophages for their own benefit and survival (Radtke and O'Riordan 2006). Within macrophages, *Salmonella* replicate in membrane-bound vacuoles referred to as *Salmonella*-containing vacuoles (SCVs) (Haraga, Ohlson et al. 2008; Figueira and Holden 2012). Once formed, SCVs interact with endoctytic compartments and exhibit characteristics closely resembling the late endosomes, however, they avoid fusion with lysosomes by targeting evolutionary conserved proteins involved in lysosomal fusion (Drecktrah, Knodler et al. 2007). In addition, once SCVs survive lysosomal fusion they utilize nutrients they receive from endocytosis, such as iron, in order to replicate within the host cells (Puschmann and Ganzoni 1977).

TRPML1 is a non-selective cation channel on the surface of the late endosomes/lysosomes responsible for mediating the release of cations, such as Ca^{2+} and Fe^{2+}, from the luminal side of lysosomes into the cytoplasm (Dong, Cheng et al. 2008; Cheng, Shen et al. 2010; Dong, Shen et al. 2010). Human mutations of TRPML1 cause Mucolipidosis type IV (MLIV), a childhood neurodegenerative disorder with lysosomal trafficking defects at the cellular level (Amir, Zlotogora et al. 1987; Bach 2001; Altarescu, Sun et al. 2002). Since late endosome-lysosome fusion has been suggested to be regulated by Ca^{2+} release from the compartments themselves (Luzio, Rous et al. 2000; Luzio, Bright et al. 2007), it has been suggested that TRPML1 regulates the late endosome/lysosomes fusion. In correlation with this,

TRPML1 activity has been shown to be regulated by the lysosomal phosphoinositide $PI(3,5)P_2$, which is required for late endosome/lysosome trafficking events (Jefferies, Cooke et al. 2008). Interestingly, macrophages deficient in $PI(3,5)P_2$ have been shown to be defective in restricting intracellular survival of *Salmonella* (Kerr, Wang et al. 2010) suggesting that $PI(3,5)P_2$ could possibly influence the intracellular growth of *Salmonella* in macrophages through TRPML1. In addition to its role in membrane trafficking, TRPML1 KO fibroblasts have also been known to accumulate Fe^{2+} in their lysosomes (Dong, Cheng et al. 2008). Iron is a critical nutritional element and essential for *Salmonella* metabolism (Puschmann and Ganzoni 1977). Collectively these data suggest that TRPML1 could potentially play a double role against *Salmonella* growth; it can promote lysosome fusion and deplete lysosomes from the iron necessary for their survival. Here I provide evidence that TRPML1 is involved in the efficient elimination of intracellular *Salmonella* in macrophages.

Methods

Macrophage cell culture. Murine bone marrow derived macrophages (BMMs) were prepared and cultured as described previously (Link, Park et al. 2010). Briefly, bone marrow cells from mouse femurs and tibias were harvested and cultured in macrophage differentiation medium (RPMI-1640 medium with 10% fetal bovine serum (FBS) and 100 unit/ml recombinant colony stimulating factor (PeproTech, Rocky Hill, NJ). After 7 days in culture at 37 °C with 5% CO_2, the adherent cells (> 95% are expected to be macrophages) were harvested for assays. RAW 264.7, RAW cells stably expressing TRPML1 (ML1 overexpression or O/E), and RAW cells stably expressing TRPML1-specific RNAi (ML1 knockdown or KD) (Thompson, Schaheen et

al. 2007) were kindly provided by Dr. Hanna Fares (University of Arizona) and cultured in DMEM/F12 media supplemented with 10% FBS at 37°C with 5% CO_2.

***Salmonella* infection**. Salmonella infection was performed as shown before (Roy, Liston et al. 2004). Briefly, BMMs from WT and TRPML1 KO mice were seeded at 1 X 10^6/well on a 6 well tissue culture plate 24 hours prior to experiments. A 1:30 dilution of overnight *Salmonella* culture was grown in LB broth for 3 hours at 37°C while shaking at 300 rpm (a condition that minimizes induction of cytotoxicity in macrophages). Bacteria re-suspended in tissue culture medium was added to cells at a multiplicity of infection (MOI) of 10, dishes were centrifuged (50g, 2 min) and incubated at 37°C for 45-60 minutes. Then they were washed, and incubated with fresh medium containing gentamicin at 100 μg/ml for the desired infection period. For determining colony forming units (CFU), infected monolayers were washed and lysed in PBS containing 0.1% Triton X-100. The lysates were serially diluted and spread on LB agar plates containing the appropriate antibiotics, and incubated at 37°C. The number of colonies was counted the next day.

Antibodies and fluorescence microscopy. After bacterial infection, cells were washed, fixed with 4% paraformaldehyde in PBS at 4°C for 1 hour, permeabilized in PBS 1% BSA 0.1% and 0.3% Triton X, and incubated with Lamp-1 primary(1D4B) and secondary antibodies. For co-localization of bacteria with dextran-containing lysosomes, cells were incubated with 0.5 mg/ml lysinefixable dextran-Texas red (10 kDa, Molecular Probes) for 1hour and chased for 3 hour in fresh media, prior to infection. The number of intracellular bacteria associated with >200 cells (determined by antibody staining or GFP expression in the presence of extracellular gentamicin) was determined visually in triplicate. Phagolysosome fusion was quantified by examining all

phagosomes in approximately 5 randomly acquired optical images for each experimental condition. TUNEL assays for *in situ* detection of apoptotic macrophages were performed according to the manufacturer's instructions (Roche).

Lysosome isolation by subcellular fractionation. Lysosomes were isolated as described previously with modifications (Kim, Soyombo et al. 2009). Briefly, cell lysates were obtained by Dounce homogenization in a homogenizing buffer (HM buffer; 0.25 M sucrose, 1 mM EDTA, 10 mM HEPES, and pH 7.0), and then centrifuged at 1900 *g* (4, 200 rpm) at 4°C for 10 min to remove the nuclei and intact cells. Post-nuclear supernatants then underwent ultracentrifugation through a Percoll density gradient using a Beckman L8-70 ultracentrifuge. An ultracentrifuge tube was layered with 2.5 M sucrose and 18% Percoll in HM buffer. Centrifugation speed was 67,200 *g* at 4°C for 1 hour using a Beckman Coulter 70.1 Ti Rotor. Samples were fractionated into light, medium, and heavy membrane fractions. Heavy membrane fractions contained concentrated bands of cellular organelles and were further layered over a discontinuous iodixonal gradient. The iodixonal gradient was generated by mixing iodixonal in the HM buffer with 2.5 M glucose (in v/v; 27%, 22.5%, 19%, 16%, 12%, and 8%); the osmolarity of all solutions was ~ 300 mOsm. After centrifugation at 4°C for 2.5 hours, the sample was divided into 10 fractions (0.5 ml each) for biochemical and atomic absorption analyses. Note that the ionic composition of the lysosome was largely maintained due to the low rate of ion transport across the lysosomal membrane at 4°C. Antibodies used for western blots: anti-Lamp1 (Iowa Hybridoma bank), 1:5000 dilution; anti-Annexin V (Abcam), 1:2000 dilution; anti-GM130 (Abcam), 1:2000 dilution; anti-EEA1 (Santa Cruz Biotechnology), 1:500 dilution; anti-Complex II (Abcam), 1:5000 dilution; anti-GFP (Covance), 1:5000 dilution.

Inductively Coupled Plasma Mass Spectrometry (ICP-MS)

Lysosomal fractions were prepared for atomic absorption by diluting the samples at a 1:1 ratio with concentrated nitric acid. After digestion (10min, 60ºC), the ionic composition was measured using a Thermo Scientific Finnigan Element inductively coupled with a plasma-high resolution mass spectrometer (ICP-HRMS) (Seby, Gagean et al. 2003).

Results

Macrophages lacking TRPML1 are defective in restricting intracellular *Salmonella* growth

In order to determine whether TRPML1 plays a role in *Salmonella* infection, WT and TRPML1 KO macrophages were infected with *Salmonella* WT strain SL1344 expressing GFP (GFP-SL1344) as described in the methods section for different time periods (**Fig. 5.1A&B**). The initial amount of ingested *Salmonella* was comparable between WT and TRPML1 KO macrophages (time 0; **Fig. 5.1A&B**). However, in TRPML1 KO macrophages, bacterial growth started shortly after entry, as the intracellular growth of *Salmonella* was significantly enhanced in TRPML1 KO macrophages after about 2 hours of infection and continued to increase vigorously with time (**Fig. 5.1B**). In contrast, *Salmonella* growth not only did not increase in WT macrophages, but instead decreased initially for the first 10 hours and increased modestly after 24 hours (**Fig. 5.1B**), most likely due to the bactericidal activity of WT macrophages. Interestingly, similar results were also obtained using different concentrations of TRPML1 specific inhibitor ML-SI1 (**Fig. 5.1A&B and Fig 5.2A**) and PIKfyve specific inhibitor YM201636 (Jefferies, Cooke et al. 2008) (**Fig. 5.1B**), confirming the results obtained previously showing that PIKfyve inhibition enhances the intracellular growth of *Salmonella* in macrophages (Kerr, Wang et al. 2010). Similar results were also obtained in macrophage cell lines with altered

expression levels of TRPML1 (Chapter II, **Fig. 2.4**) where *Salmonella* growth enhanced significantly in macrophage cell lines with lower expression levels of TRPML1 (**Fig. 5.2B).** This increase in intracellular growth of *Salmonella* in TRPML1 KO macrophages was not related to *Salmonella*-induced macrophage cytotoxicity. Under the growth conditions used, *Salmonella* induced similar low levels of programmed cell death on both WT and TRPML1 KO macrophages and did not cause differential cell loss between 2 and 6 hours after infection, as shown by TUNEL staining (**Fig. 5.2C)**. Collectively, these data suggest that TRPML1 is involved in restricting the intracellular growth of Salmonella in macrophages.

TRPML1 influence the fusion of *Salmonella* with lysosomes in a Ca^{2+} dependent manner.

The knockdown of TRPML1 using shRNA against the *TRPML1* gene in macrophage cell lines and fibroblasts isolated from MLIV patients demonstrated a delay in lysosomal delivery and subsequent delay in the degradation of endocytosed proteins, such as BSA and platelet-derived growth factor receptors (PDGF-R) (Thompson, Schaheen et al. 2007; Vergarajauregui, Oberdick et al. 2008). Considering these data, I hypothesized that TRPML1 could potentially be involved in the delivery of SCVs to the lysosomes by facilitating the release of lysosomal Ca^{2+} and regulating lysosomal fusion (Luzio, Rous et al. 2000; Luzio, Bright et al. 2007); therefore, lack of TRPML1 will enhance *Salmonella* survival in macrophages.

I investigated whether the fusion of lysosomes with phagosomes containing *Salmonella* is defective in TRPML1 KO macrophages. As mentioned before, *Salmonella* reside in compartments exhibiting late endosome characteristics, but they avoid fusion and degradation by lysosomes (Drecktrah, Knodler et al. 2007). Late endosome/lysosome membrane protein, Lamp-1, was used to label late endosomes/lysosomes, while fluorescent conjugated dextran was used to

label lysosomes (**Fig. 5.3A&B**). Macrophages were infected with *Salmonella* for 6 hours and the extent to which *Salmonella*-containing phagosomes colocalized with Lamp-1 or dextran preloaded into lysosomes was quantified in WT and TRPML1 KO macrophages from images obtained from confocal microscopy (**Fig. 5.3A&B**). The percentage of *Salmonella*-containing phagosomes positive for Lamp-1 and dextran was comparable in WT cells. However, TRPML1 KO macrophages or macrophages treated with ML-SI1 contained a significantly higher percentage of *Salmonella*-containing phagosomes positive for Lamp-1 compared to dextran, indicating the late endosome/lysosomes fusion was defective (**Fig. 5.3A&B**). Similar results were also obtained by using live confocal microscopy where lysosomal fusion was blocked using ML-SI1 and YM 201636 compound (**Fig. 5.4)**. Interestingly, treating cells with the fast Ca^{2+} chelator BAPTA-AM also resulted in similar results (**Fig. 5.3A&B**) suggesting that TRPML1 potentially regulates the fusion of *Salmonella*-containing phagosomes with lysosomes by providing the Ca^{2+} required for lysosomal fusion.

In order to further investigate this possibility, the intracellular survival of *Salmonella* was evaluated after exposing the cells to different concentrations of the fast and slow Ca^{2+} chelators. The survival rate of *Salmonella* was significantly increased in WT macrophages treated with BAPTA-AM, almost to the same level of TRPML1 KO macrophages, in a dose dependent manner, while the slow Ca^{2+} chelator EGTA-AM had a minor effect (**Fig. 5.5**). BAPTA binds to Ca^{2+} approximately 100 times faster than EGTA does, thus EGTA is more likely not able to chelate Ca^{2+} close to the site of Ca^{2+} release (explained in detail in Chapter I) (Pryor, Mullock et al. 2000; Luzio, Bright et al. 2007). Collectively, these data illustrated that TRPML1 potentially provides the Ca^{2+} required for membrane fusion between the SCVs and lysosomes. These data are in agreement with previous findings implicating the importance of intracellular Ca^{2+} in

phagosome-lysosome fusion and pathogen elimination in macrophages (Nunes and Demaurex 2010).

Lack of TRPML1 leads to accumulation of intra-lysosomal iron and increase in *Salmonella* growth

As shown earlier in TRPML1 KO macrophages, bacterial growth started shortly after entry, as the intracellular growth of *Salmonella* was significantly enhanced in TRPML1 KO macrophages after about 2 hours of infection, and continued to increase with time (**Fig. 5.1**). This data suggested that, in TRPML1 KO macrophages, not only are *Salmonella* able to survive lysosomal degradation, but they are also able to replicate dynamically, meaning they most likely have access to nutrients they require for metabolism. Lysosomal iron has been shown to be crucial for microbial growth and replication within macrophages (Schaible and Kaufmann 2004), so it is no surprise that iron accumulation in endosomal/lysosomal compartments is associated with an increased susceptibility to bacterial infections (Wanachiwanawin 2000). Meanwhile, the depletion of lysosomal iron was shown to increase natural resistance against intracellular pathogen (Puschmann and Ganzoni 1977). Nramp-1 is a known iron efflux transporter on the surface of the lysosomes shown to deplete lysosomal iron upon infection in order to prevent bacteria replication within the lysosomes (Gunshin, Mackenzie et al. 1997; Cuellar-Mata, Jabado et al. 2002). Recent studies indicate that TRPML1 is able to conduct iron from the luminal side of the lysosomes into the cytoplasm (Dong, Cheng et al. 2008), Hence, we hypothesized in addition to modulating lysosome-phagosome fusion, TRPML1 can potentially play a similar role as Nramp-1 and restrict intracellular *Salmonella* growth by depleting lysosomal iron.

To explore this possibility, I first evaluated the iron content of lysosomes in TRPML1 KO macrophages. To directly measure the ionic composition of the lysosome lumen, we enriched the lysosome fraction of HEK293T cells using density-gradient centrifugation (**Fig. 5.6A**). The cell homogenate (designated Fraction A in **Fig. 5.6A**) was subjected to two rounds of density-gradient centrifugation steps, which progressively separated lysosomes from other organelles. Centrifugation of the homogenate at 4200 rpm eliminated unbroken cells and the damaged membranes. The supernatant contained significant amounts of most of the cellular organelles (**Fig. 5.6B;** fraction C). Fraction C was then subjected to centrifugation through a discontinuous percoll gradient and yielded three main fractions designated light, medium, and heavy membrane fractions (**Fig. 5.6A**). The heavy membrane fractions contained the lysosomal organelles (**Fig. 5.6B**), but it was still contaminated with mitochondria (**Fig. 5.6B**; fractions F and G). In order to further purify lysosomes, we combined fractions F and G and subjected them to an additional centrifugation step through continuous iodixanol gradient (**Fig. 5.6C**). We were able to obtain pure lysosomes in lower percentage fractions of the iodixanol gradient (**Fig. 5.6C**). After isolating lysosomes, they were subjected to inductively coupled plasma mass spectrometry (ICP-MS) analysis to analyze the ionic composition of the lysosomes. All centrifugation steps were performed at 4°C (1 hour in the Percoll density gradient and 2.5 hour in the iodixanol gradient). At this temperature, the rate of ion transport across the lysosomal membrane is expected to be extremely low. In addition, the sucrose-based homogenization buffer contains few ions. Thus, lysosomal ion transporters/exchangers are not likely to be operative. Hence, we presume that the lysosomal ion composition is largely maintained during the isolation procedure. Although the absolute concentrations of ions could not be accurately measured due to the lack of

information about lysosome volume, this approach allowed us to determine the relative abundance/ratios of the total but not free ions in the lumen.

By using this approach, we were able to isolate lysosomes from macrophages and evaluate their ionic compositions. The basal level of total iron levels was comparable in the lysosomes of WT and TRPML1 KO macrophages (**Fig. 5.7A**). However, after we treated the culture macrophages with iron conjugated dextran overnight (under this condition, endocytosed iron is expected to be localized exclusively in the lysosomes), we observed an accumulation of iron in TRPML1 KO, but not WT macrophages (**Fig. 5.7A**). The total levels of magnesium remain unchanged, indicating that lysosomal iron increases specifically. Additionally, the accumulation of lysosomal iron in cultured macrophages was confirmed by using sulphide-silver method (SSM) staining. Significantly more lysosomal iron staining was seen in TRPML1 KO macrophages compared to WT cells (**Fig. 5.7B**) indicating that iron accumulates within the lysosomes of TRPML1 KO macrophages. Interestingly, Salmonella growth was elevated in the TRPML1KO macrophages after treating the cells with iron dextran overnight (**Fig. 5.7C**) indicating that lack of TRPML1 can enhance *Salmonella* metabolism by providing excess iron essential for *Salmonella* replication.

Discussion

Salmonella can get inside host cells through several different routes such as phagocytosis or macropinocytosis, but no matter how they get into the cell they manipulate the encompassing vacuoles in order to generate a replicative niche that supports its survival and growth (Weber, Ragaz et al. 2009). The invasion and intracellular replication of *Salmonella* is a carefully choreographed interplay between the host cell's molecular machinery and secreted effectors of

the pathogen which hijacks the endogenous host cell machinery for their own benefits (Haraga, Ohlson et al. 2008). One of the key events required for *Salmonella* survival within the host cell is lysosomal fusion avoidance (Drecktrah, Knodler et al. 2007). Here, by using both genetic and pharmacological manipulations, I showed that cells lacking the lysosomal Ca^{2+} channel TRPML1 are defective in restricting intracellular growth of *Salmonella* in macrophages. TRPML1 is a lysosomal Ca^{2+} channel shown to be involved in mediating membrane fusion events in different cell types late in the endocytic/excotytic pathways (Cheng, Shen et al. 2010). By using confocal microscopy, I observed that in TRPML1 deficient macrophages, *Salmonella* avoid fusion with lysosomes and they remain in late endosomal compartments. Therefore, they are able to avoid lysosomal degradation and survive within the cells. Additionally, I showed there is an accumulation of iron in the lumen of the lysosomes in TRPML1 KO macrophages, which could provide additional nutrition required for *Salmonella* growth (Puschmann and Ganzoni 1977; Cuellar-Mata, Jabado et al. 2002; Jabado, Cuellar-Mata et al. 2003). Therefore, here for the first time, I have potenitally identified a cation channel responsible for two fundamental process involved in host cell bactericidal activity; promoting lysosomal fusion and depleting lysosomes from nutrients, such as iron, required for *Salmonella* growth.

Although I have suggested the mechanisms of how TRPML1 restricts intracellular growth of *Salmonella in vitro*, this remains to be tested *in vivo* on animal models. Also, it needs to be discovered if *Salmonella* effectors directly interact and inhibit TRPML1 in the host cells. Moreover, how intracellular iron regulates *Salmonella* replication and its relation to TRPML1 needs further investigation. Exposing WT macrophages to BAPTA-AM was sufficient to induce *Salmonella* replication to the same levels of TRPML1 KO macrophages (**Fig. 5.5**), illustrating that the effect of TRPML1 is independent of intracellular iron and only depends on the

lysosomal Ca^{2+} release. However, the intracellular survival of *Salmonella* was more evident after the addition of exogenous iron (**Fig. 5.7**). Nevertheless, it needs to be noted that exogenous iron could potentially alter lysosomal ionic composition and therefore, *Salmonella* growth observed in these experiments could be due to secondary effects, such as altering lysosomal Ca^{2+} concentration, independent from TRPML1. So, the interplay between Ca^{2+} and iron needs to be separated and investigated more in detailed.

Interestingly, macrophages lacking TRPML1 endogenous activator $PI(3,5)P_2$ also exhibit a similar phenotype as TRPML1 KO macrophages, so it is possible that TRPML1 is a major target for *Salmonella* effectors in order to promote the bacteria growth within the macrophages. With the development of antibiotic resistant bacteria strains, new strategies to combat infection must be devised. Considering the close interplay between host and bacteria cell, new strategies can be developed by targeting host molecules and pathways essential for bacterial replication. Hence, the disruption of TRPML1 activity using its small molecule inhibitors in infected cells may be a viable strategy to combat acute infection.

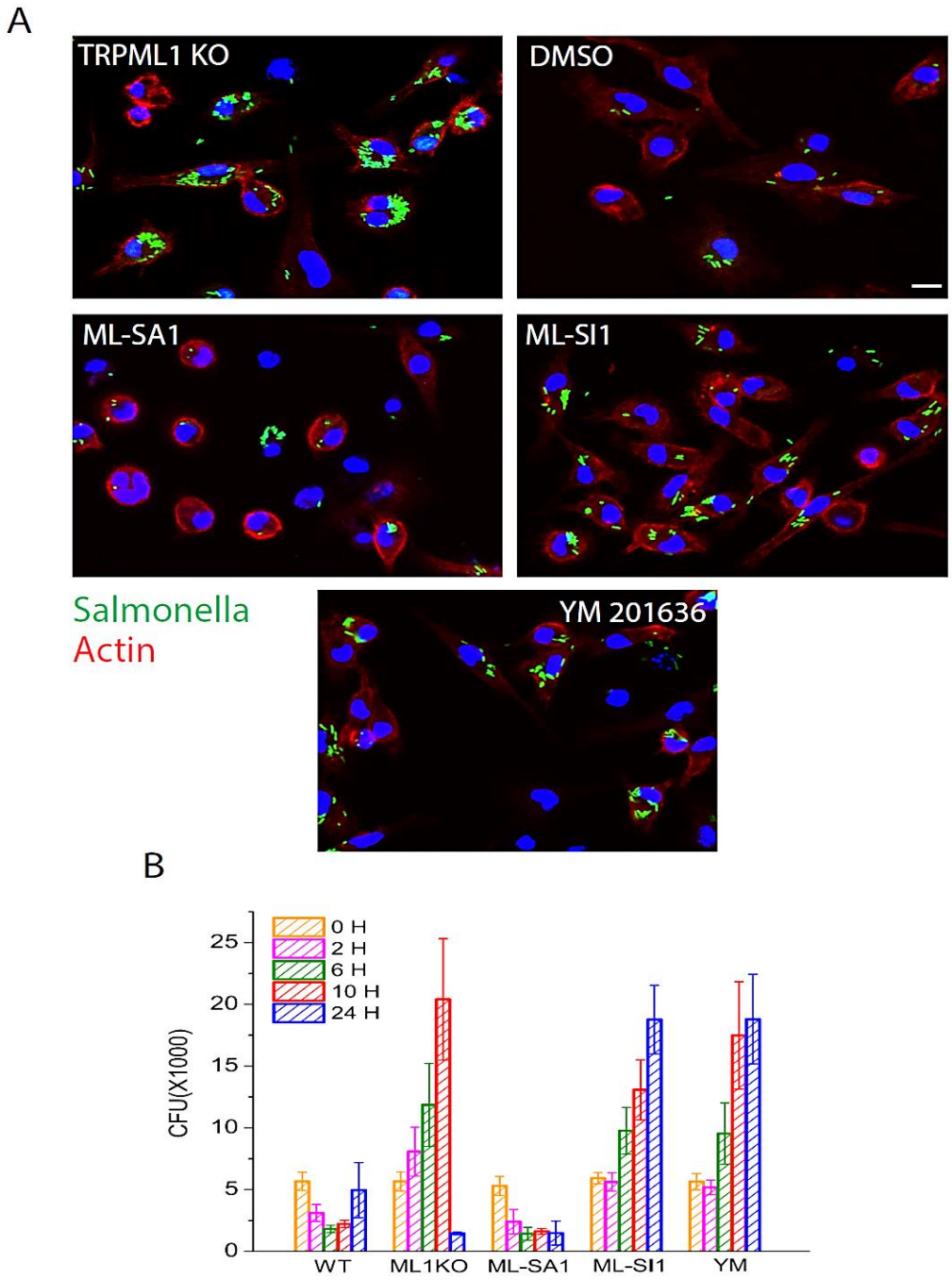

Figure 5.1 Macrophages isolated from TRPML1 KO mice are defective in *Salmonella* elimination

(A) Fluorescent images showing intracellular GFP-expressing *Salmonella* (green) 6 hours after infection in TRPML1KO macrophages and WT macrophages treated with ML-SA1, ML-SI1, and YM201636 compounds. Cell area is demonstrated with actin staining (B) Bone marrow macrophages with different treatments (similar to part (A)) were infected with *Salmonella* for 1 hour and the number of intracellular bacteria was determined by colony factor unit (CFU). The mean of triplicates SEM is shown.

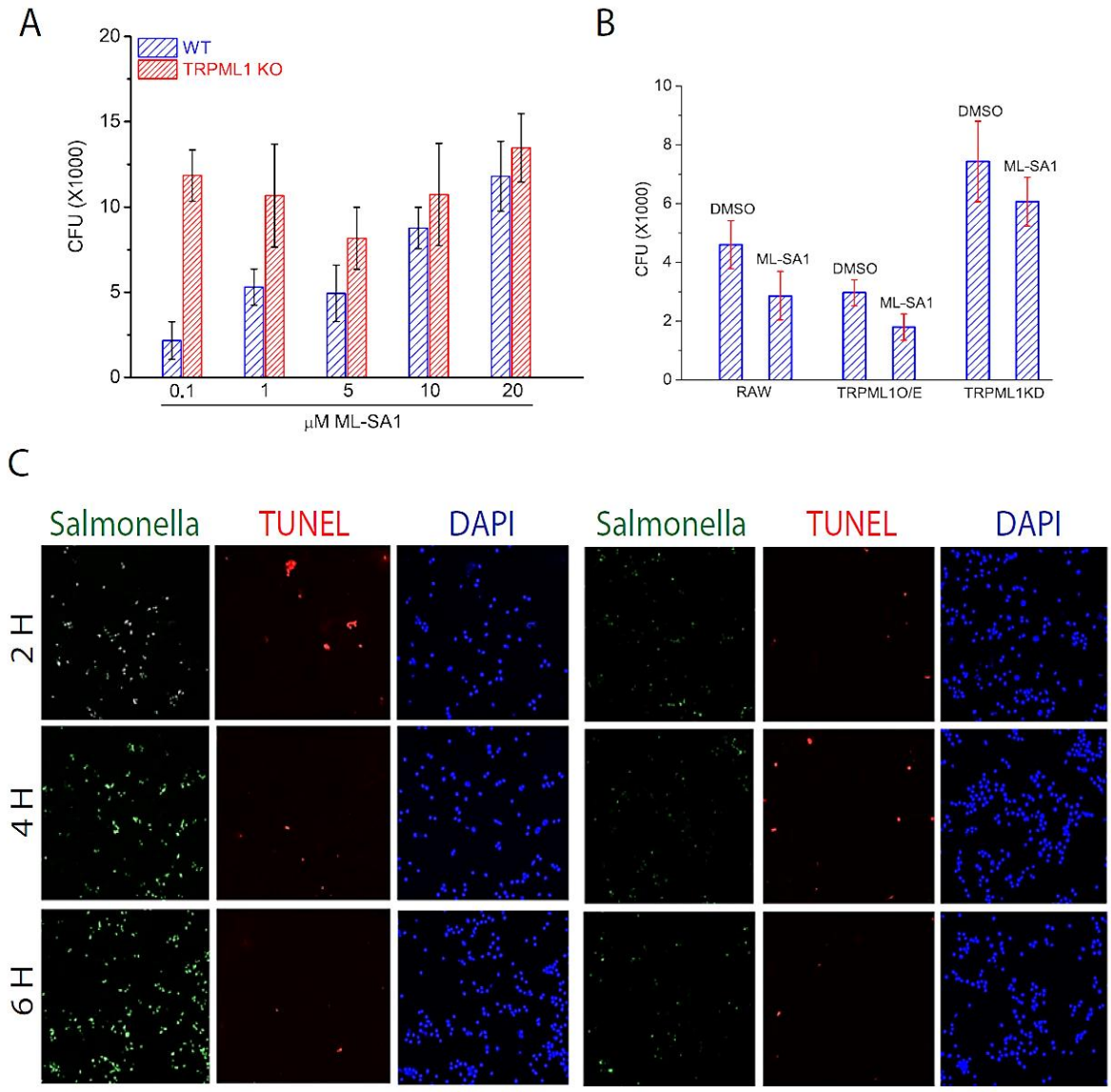

Figure 5.2 TRPML1 function is required for restricting *Salmonella* intracellular survival.

(A) Dose dependent effect of ML-SI1 on *Salmonella* intracellular growth after 6 hours of infection. (B) *Salmonella* growth in macrophage cell lines with higher expression (TRPML1 O/E) or lower expression (TRPML1 KD) of TRPML1. (C) TUBEL staining indicating cell death in response to bacterial infection. For all experiments *N*=3, ± SEM.

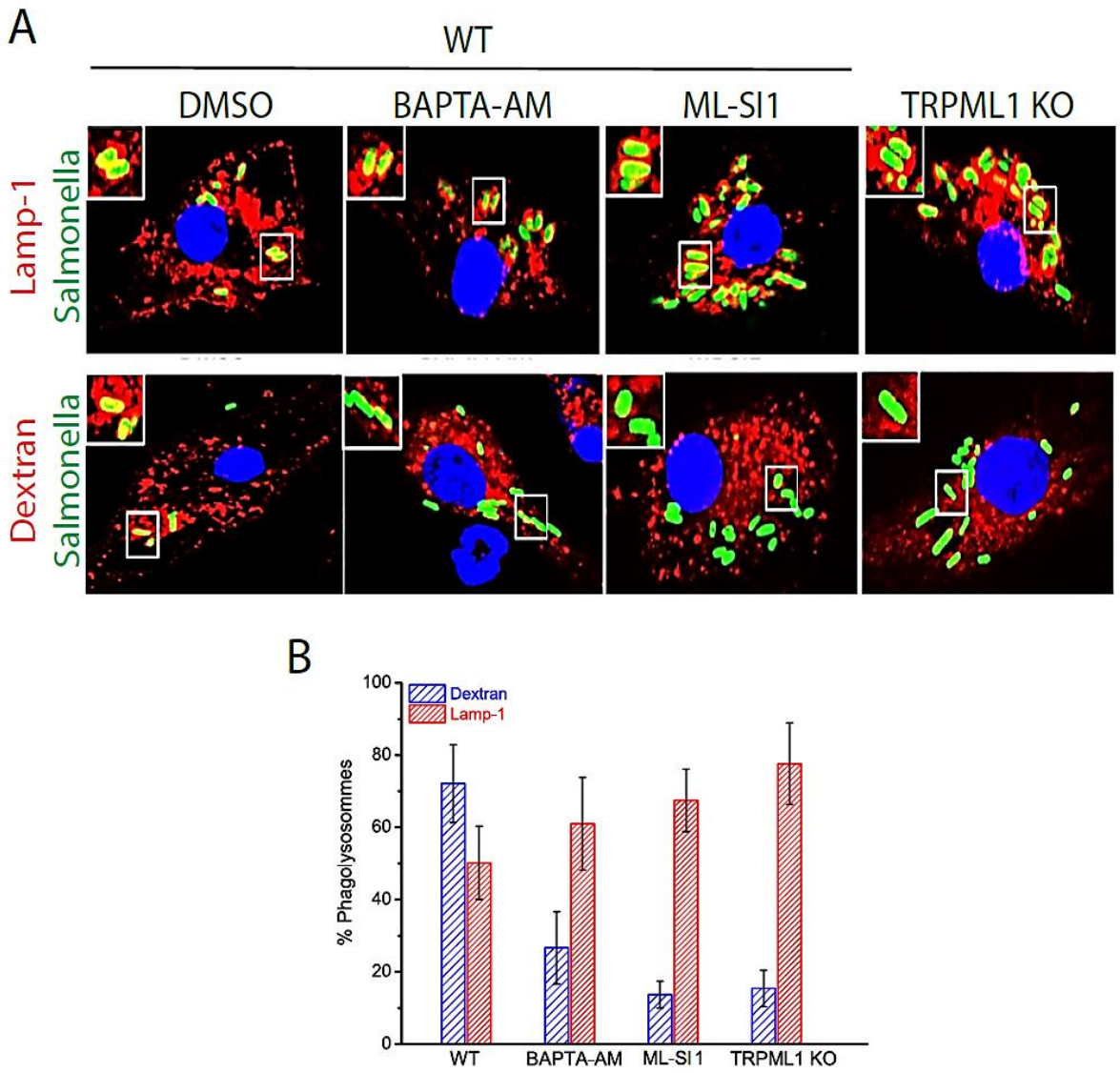

Figure 5.3 TRPML1 promotes the transition of the phagosomes from the late endosomes to the lysosomes.

Macrophages were infected with *Salmonella* for 4 hours and then stained with Lamp-1 to label late endosomes and fluorescent conjugated dextran to label the lysosomes. Images represent the morphological criteria used to determine the percent phagolysosome formation in part (B). *Salmonella* was able to avoid fusion with lysosomes in TRPML1 KO macrophages as well as WT macrophages exposed to TRPML1 specific inhibitor (ML-SI1) and BAPTA-AM. (B) Percent of phagolysosome formation in cells shown in part (A).

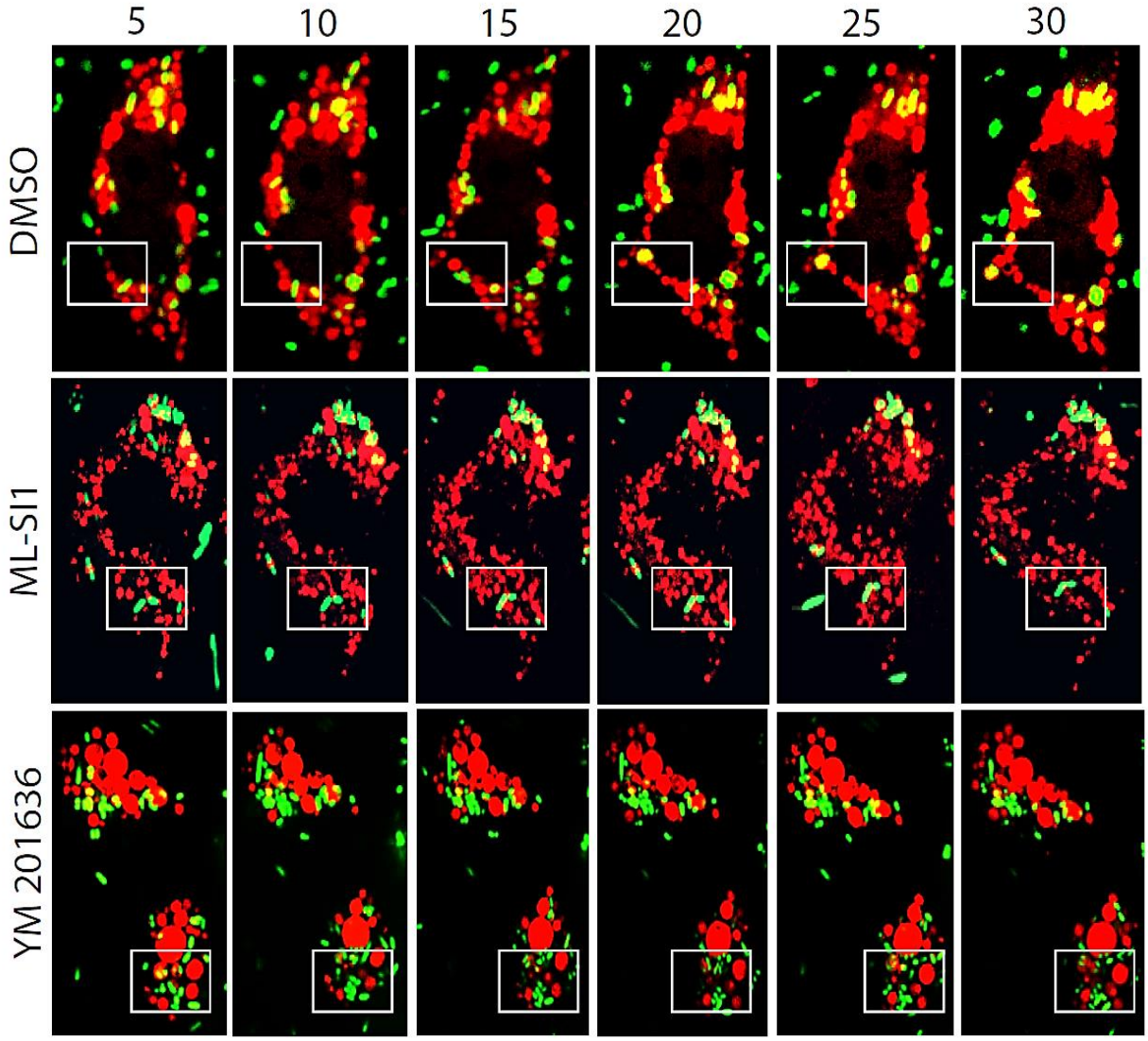

Figure 5.4 TRPML1 promotes the formation of phago-lysosomes.

Live imaging confocal microscopy evaluating phagolysosome formation in WT macrophages and macrophages treated with ML-SI1 and YM 201636 compounds (0-30 miutes). White boxes indicate the site of phagolysosomes formation.

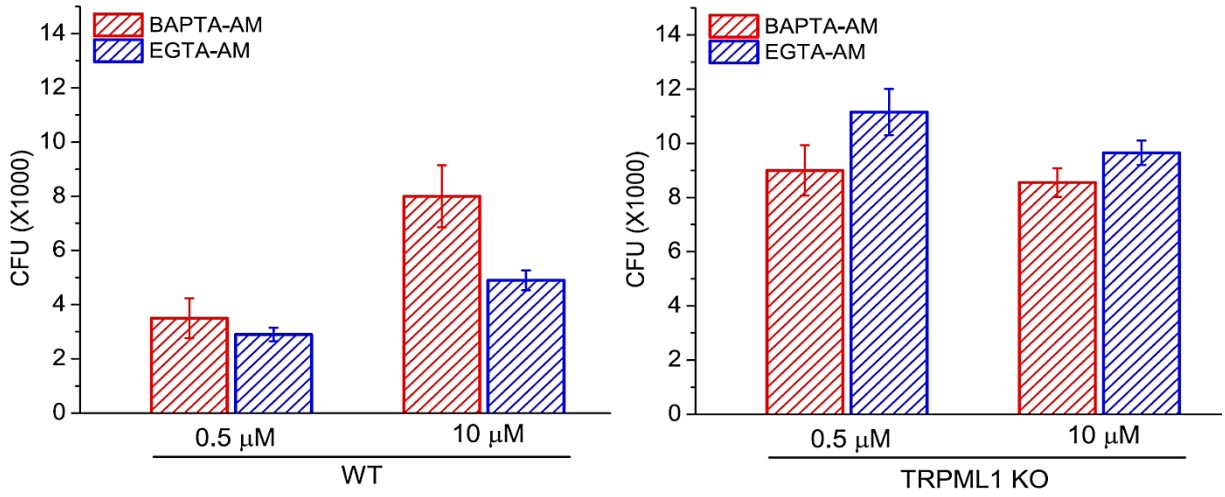

Figure 5.5 Bacteria survival depends on intracellular and localized Ca^{2+} release.

Dose-dependent effect of fast Ca^{2+} chealtor BAPTA-AM on *Salmonella* growth in WT macrophages. The slow Ca^{2+} chelator EGTA-AM had no significant effect. Neither, BAPTA-AM nor EGTA-AM had an effect on TRPML1 KO macrophages. For all experiments *N*=3, ± SEM.

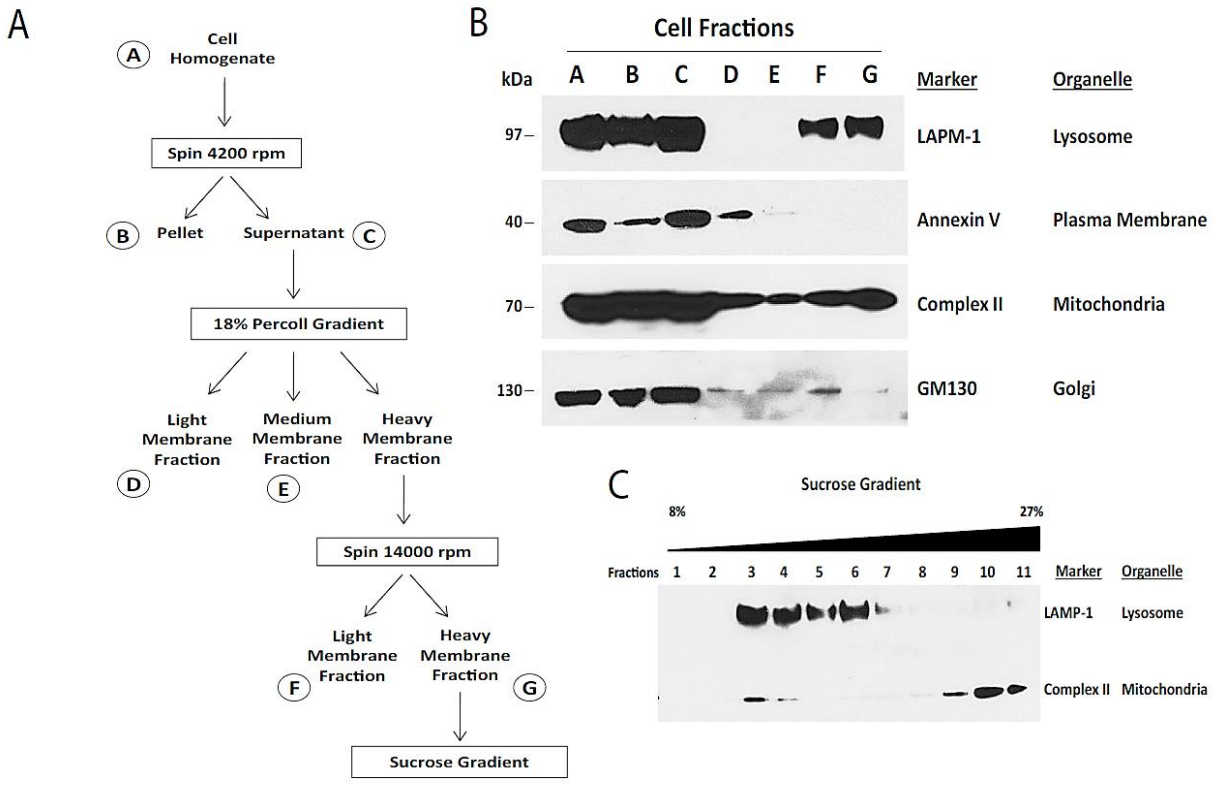

Figure 5.6 Lysosomal isolation procedures

(A) Diagram illustrating the steps of lysosome membrane fractionation. A-G denotes major fractions recovered and analyzed by immunoblot analysis. (B) Cells were treated according to the fractionation scheme as described in the Methods and Results sections and as shown in (A). Cells were disrupted using a ball-bearing homogenizer and centrifuged at 4500 RPM. The supernatant was then loaded at the top of a discontinuous sucrose gradient and centrifuged for 1 hour, yielding three distinct membrane layers which were used for further fractionation. After this step, aliquots representing equal volumes of each fraction (A–G) were subjected to immunoblot analysis for the indicated organelle markers. (C) The heavy membrane fraction obtained after the discontinuous sucrose gradient step was loaded on a continuous 8%–27% iodixanol gradient and centrifuged for 2.5 hours, after which fractions were collected from the top. Equal volumes of each fraction were subjected to immunoblot analysis for the indicated organelle markers.

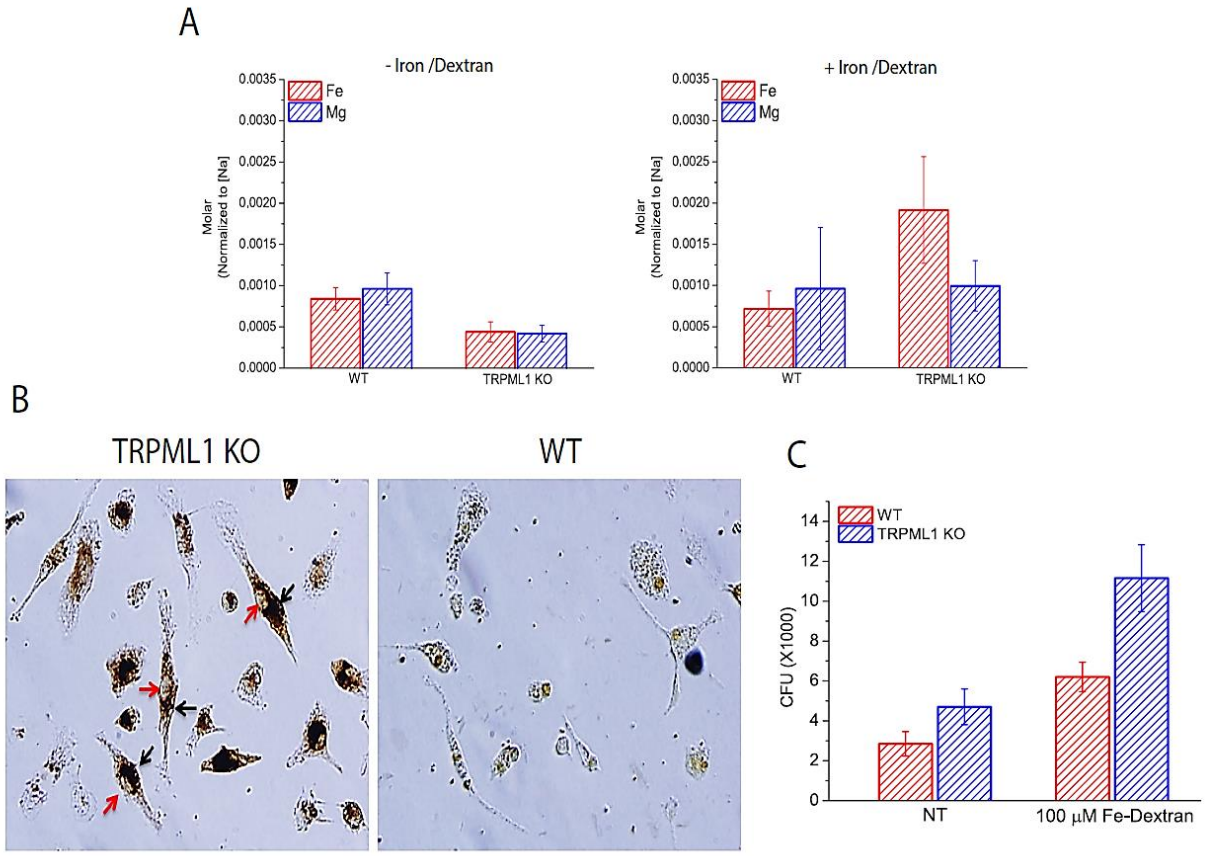

Figure 5.7 Intralysosomal accumulation of iron induces *Salmonella* growth in TRPML1 KO macrophages.

(A) Ionic composition of the isolated lysosomes was quantified by using ICP-MS. There were no difference in the Iron composition of the lysosomes isolated form WT and TRPML1 KO macrophages. However, after treating the cells with iron-dextran overnight, there was a significant increase in the iron content of lysosomes isolated from TRPML1 KO macrophages compared to WT cells. (B) Sulphide-Silver Method (SSM) staining revealed iron accumulation in the lysosomes (black arrows) close to the nucleus (red arrow). (C) Intracellular *Salmonella* survival was significantly increased in TRPML1 macrophages after loading the cells with iron-dextran overnight and infecting macrophages for 6 hours. For all experiments N=3, ± SEM.

CHAPTER VI

DISCUSSION

1. Summary of results and significance

Phagocytosis of large extracellular particles, such as apoptotic bodies, requires a substantial amount of intracellular membrane to surround and ingest the particles (Huynh, Kay et al. 2007). Lysosomes have been proposed as a candidate source of intracellular membranes. Upon particle binding to macrophage surface receptors, lysosomes have been shown to fuse with plasma membrane through lysosomal exocytosis to provide the excess membrane required for phagosome formation (Braun, Fraisier et al. 2004; Braun and Niedergang 2006; Czibener, Sherer et al. 2006). Here I showed that TRPML1 activation is required to mediate lysosomal exocytosis and fusion of lysosomes with plasma membrane in macrophages (Chapter II). Additionally, I identified TRPML1 on the surface of the lysosomes as the key Ca^{2+} channel regulating large particle uptake through the induction of lysosomal exocytosis (Chapter III) and a lysosomal specific phosphoinositide, $PI(3,5)P_2$, as the channel agonist that is produced upon particle binding (Chapter IV). Therefore, our findings illustrate that TRPML1 represents the first Ca^{2+} channel and the first lysosome ion channel regulating two fundamental cellular processes: lysosomal exocytosis and phagocytosis (**Fig. 6.1**). Although the role of Ca^{2+} in lysosomal exocytosis and phagocytosis has been well studied, it remains enigmatic and controversial (Nunes and Demaurex 2010). While lysosomal exocytosis is thought to be Ca^{2+} dependent,

particle uptake during phagocytosis is generally considered to be Ca^{2+}-independent. Yet, lysosomal exocytosis has been reported to be required for phagocytosis (Braun, Fraisier et al. 2004; Braun and Niedergang 2006; Czibener, Sherer et al. 2006; Huynh, Kay et al. 2007). One reason for this inconsistency could potentially be that the conventional techniques for measuring Ca^{2+} lack the sensitivity and resolution needed to detect the small and localized amount of Ca^{2+} required for this process. Indeed, in our study, by using a lysosomal targeted genetically encoded Ca^{2+} sensor, I was able to directly observe lysosomal Ca^{2+} release during phagosome formation in macrophages (**Fig. 3.9**). Additionally, the role of Ca^{2+} in lysosomal exocytosis was suggested largely through the use of non-specific reagents such as the Ca^{2+} ionophore ionomycin, which induces Ca^{2+} flux non-physiologically and independent of any specific ion channels. Our identification of a lysosomal Ca^{2+} channel that regulates both lysosomal exocytosis and phagocytosis has provided definitive evidence at the molecular level for the roles of Ca^{2+} and lysosomal membranes in large particle uptake (**Fig. 6.1**). The Ca^{2+}-dependence of exocytosis is well established in neurotransmitter release in which the voltage-gated Ca^{2+} channels are responsible for Ca^{2+} flux in response to voltage changes. I have now identified the machinery (TRPML1-PI(3,5)P2) for the second, but drastically different, example of the Ca^{2+}-exocytosis link (Chapter II).

In addition to the role of TRPML1 in large particle uptake during phagocytosis, I have potentially discovered another role for TRPML1 during phagosome maturation (Chapter V). I observed that macrophages isolated from TRPML1 KO mice are defective in restricting the intracellular survival of *Salmonella*. By using both genetic and pharmacological approaches, I showed that TRPML1 most likely regulates the fusion of *Salmonella* containing vacuoles with lysosomes, hence, promoting their lysosomal degradation. Therefore, my results illustrated that

TRPML1 mediates the fusion of lysosomes with the plasma membrane during the early stages of phagocytosis in addition to regulating the fusion of lysosomes with the phagosomes through phagosome maturation. I discuss this in more detail in the next section.

2. The dual role of lysosomes during phagocytosis

Throughout years, several different important studies have established lysosomes as the end point of phagocytosis where they fuse with the phagosomes through phagosomal maturation to aid the degradation of ingested particles (Aderem and Underhill 1999; Niedergang and Chavrier 2004; Flannagan, Jaumouille et al. 2012). In addition to the lysosome's role in particle degradation, I have shown that during large particle uptake lysosomal membrane proteins, such as TRPML1, SytVII, and Lamp1, are rapidly delivered to forming phagosomes. Our data suggests that lysosomes play a very dynamic role during phagocytosis and they are delivered to phagosomes through two different stages, phagosomes formation and maturation (Chapters III & V).

Throughout this study, I performed a number of live imaging experiments using a variety of endolysosomal or phagosomal markers (Rab5, PI3P probe, PI(3,4,5)P_3/PI(3,4)P_2 probe, Rab7, SytVII, Lamp1, and LysoTracker) in pairs with TRPML1-GFP or TRPML1-mCherry to gain insight into the dynamics of lysosomes during phagosome formation and maturation (Chapter III, IV & V). During the course of large particle uptake, I found that Rab5-GFP began to appear on newly formed phagosomes 5-10 minutes after phagocytosis initiation, but disappeared after 10 minutes (**Fig. 3.5**). Afterwards, Rab7 appeared on phagosomes 20 min after phagosome initiation (**Fig. 3.5**), reflecting the Rab5 to Rab7 conversion/switch that is required for late phagosome maturation or phagosome-lysosome fusion (Henry, Hoppe et al. 2004; Kitano, Nakaya et al.

2008). In agreement with this time course, LysoTracker Red, a fluorescent dye that labels acidic organelles in live cells, also appeared on phagosomes 20 minutes after phagocytosis initiation (**Fig. 3.5**). Phagosome-lysosome fusion and phagosomal acidification are the key events during late phagosome maturation. Collectively, these results suggest that in our system, consistent with the literature (Henry, Hoppe et al. 2004), Rab5 and Rab7 are sequentially recruited to early and late phagosomes, respectively, for the purpose of phagosome maturation. Interestingly, TRPML1, Lamp1, and SytVII were found to appear on forming phagosomes within 5 minutes after phagocytosis initiation, prior to Rab5 recruitment (**Fig. 3.5**). Although, their fluorescence intensity on phagosomal membranes continued to increase over the time course of the experiments, phagosomal acidification (LysoTracker) failed to occur until Rab7 recruitment. Hence, TRPML1 and Lamp1 are recruited during phagosome formation, prior to Rab5-mediated early phagosome maturation. To further separate these two processes (phagosome formation and maturation), I monitored the TRPML1-GFP recruitment in macrophages that were exposed to small particles. In contrast to large particle uptake, TRPML1-GFP was recruited only after 20 minutes of phagocytosis initiation in small particle uptake (**Fig. 3.5**).

Strikingly, the early recruitment of Lamp1 to the forming large phagosomes was significantly blocked in TRPML1 KO cells (**Fig. 3.6**). These results suggest that the only role that can be attributed to TRPML1-mediated lysosomal exocytosis is Lamp1 recruitment. In connection with this, in chapter V I showed that in macrophages isolated from TRPML1 KO mice the fusion of late endosomes containing *Salmonella* was blocked, as revealed when using fluorescent conjugated dextran. This suggests TRPML1 also mediates the fusion of late endosomes with lysosomes late in the phagosomal maturation process (**Fig. 5.3**)

Collectively, these data suggest that lysosomes are delivered to the phagosomes at two different stages (**Fig. 6.2**). First, for large particles, lysosomes fuse with the plasma membrane at the phagocytic cup, which provides the membranes necessary for phagosome formation. As a result, lysosomal membrane proteins, such as TRPML1 and Lamp1, are delivered to the newly formed phagosomes, prior to or during phagocytic cup closing. This is an indirect (through lysosomal exocytosis) path that occurs early during phagosome formation (**Fig. 6.2**). Second, for both large and small particles, lysosomes are delivered to the late phagosomes through late phagosome maturation (phagosome-lysosome fusion), which is required for the degradation of phagocytic materials. This second stage is accompanied by Rab7 recruitment and phagosomal acidification, as well as further recruitment of lysosomal membrane proteins including TRPML1 and Lamp1. This is a direct path that occurs late during phagosome-lysosome fusion (**Fig. 6.2**). As discussed in previous studies (Czibener, Sherer et al. 2006), the early recruitment of lysosomal membrane proteins may serve as an early preparation of phagosome maturation, but is not essential for phagosome maturation.

3. TRPML1 induced lysosomal exocytosis as a therapeutic approach for LSDs.

Accumulation of lipids in lysosomes has been associated with several human diseases (LSDs, Chapter I). Identification of molecules and processes that could clear the accumulated materials can potentially serve as a novel therapeutic target for LSDs. Several therapeutic approaches have been developed for LSDs including substrate reduction therapy, bone-marrow transplantation, gene therapy, and enzyme replacement therapy (ERT) (Cox and Cachon-Gonzalez 2012). ERT and substrate reduction are the most common therapies, especially for the treatment of Gaucher and Fabry diseases (Eng, Banikazemi et al. 2001; Cox and Cachon-

Gonzalez 2012). In addition, for a subset of mutation causing Gaucher, Fabry, and Tay-sachs diseases that are caused by enzyme misfolding in the ER, chemical chaperones have been proven helpful (Sawkar, Adamski-Werner et al. 2005). For most LSDs, however, an effective therapeutic approach is still lacking. For the currently available approaches, there are various intrinsic limitations, especially the problem of low efficacy. For instance, while the brain is the most commonly affected tissue in LSDs, it is very difficult in ERT to deliver enzymes across the blood-brain barrier. Most importantly, all the current available approaches are disease specific.

There are many different conditions characterized as LSDs resulting from dysfunction of different lysosomal proteins, so developing disease specific therapies could be extremely expensive. Most evidence illustrates many similarities between the mechanisms that lead to lipid storage diseases, suggesting that a common approach targeting specific pathways can potentially rescue the disease phenotype (Schultz, Tecedor et al. 2011). For instance, one similar observation in almost all LSDs is that the dysfunction of the disease associated enzyme is correlated with an increase in expression or activity of other lysosomal proteins such as Lamp-1 (Ballabio and Gieselmann 2009; Schultz, Tecedor et al. 2011). This suggests that the expression of lysosomal proteins are interconnected and related to each other. So it is possible that a common process regulating lysosomal function could also be defected in lipid storage diseases and targeting that common process could potentially be a universal therapeutic strategy.

The discovery of TFEB made this approach very appealing (Chapter I) (Sardiello and Ballabio 2009; Sardiello, Palmieri et al. 2009). Interestingly, the overexpression of TFEB enhanced the clearance of storage materials in several LSDs such as multiple sulfatase deficiency (MSD), mucopolysaccharidosis type IIIA (MPS-IIIA) , Batten, and Pompe's disease (Medina, Fraldi et al. 2011; Settembre, Fraldi et al. 2013; Spampanato, Feeney et al. 2013). Notably,

TFEB overexpression in all these assays reduced lysosomal storage in different LSDs despite the lack of function of the disease specific lysosomal enzyme, so it is not unforeseen that TFEB can also be used to decrease the storage of lipids within the lysosomes in other LSDs.

The beneficial effect of TFEB on various LSDs is dependent on TRPML1 and lysosomal exocytosis (Medina, Fraldi et al. 2011). TFEB-mediated clearance is largely abolished when TRPML1 channel activity is compromised or when lysosomal exocytosis is inhibited (Medina, Fraldi et al. 2011). Additionally, unlike other LSDs, the overexpression of TFEB failed to induce the clearance of stored materials in MLIV cells, indicating that TFEB most likely induces cellular clearance through the activation of TRPML1 (Medina, Fraldi et al. 2011). Considering that TRPML1 is up-regulated by TFEB overexpression (Sardiello, Palmieri et al. 2009), it is likely TFEB may directly up-regulate TRPML1 to promote lysosomal exocytosis. However, TFEB may also mediate the expression of Vac14 (Sardiello, Palmieri et al. 2009), a protein required for $PI(3,5)P_2$ production (Chapter IV) (Duex, Tang et al. 2006). Therefore, it is possible that TFEB promotes substrate clearance in different LSDs by increasing the expression/function of TRPML1 (**Fig. 6.3**). In agreement with this, TRPML1 overexpression and small molecule TRPML1 agonists were shown to promote cholesterol clearance in NPC cells (Shen, Wang et al. 2012). As cholesterol accumulation is commonly seen in many LSDs, "activating" TRPML1 may represent a novel therapeutic approach for many other LSDs (**Fig. 6.3**). As I shown in Chapter II, TRPML-specific agonist ML-SA1 can induce lysosomal exocytosis in macrophages. Thus, ML-SA1 together with the next generation of TRPML-specific activators may be used as a therapeutic strategy for lipid storage disorders.

4. The role of TRPML1 in phagocytic clearance and neurodegeneration.

One of the interesting defects seen in most of the animal models of LSDs (Chapter I) is the massive amount of inflammatory responses in the brain (Jeyakumar, Dwek et al. 2005) that is usually initiated by microglia and macrophages in the innate immune system. These types of inflammatory responses are also seen in common neurodegenerative disease such as Alzheimer's (McGeer and McGeer 2003) and Parkinson's diseases (McGeer and McGeer 2004). This indicates that LSDs, as well as other common neurodegenerative diseases, share similar pathological cascades and molecular pathways.

It is not clear what triggers the enormous inflammatory response in the brain of animal with LSDs. As explained in chapter I, LSDs are usually characterized by the accumulation of undigested lipids in the lysosomes (**Fig. 1.1&1.2)**. These storage materials are structurally normal self-components and should be immunologically silent. However, lipid accumulation leads to the activation of resident microglia and recruited macrophages in the brain which initiate an inflammatory response. How macrophages and microglia are initially activated in response to lipid accumulation in their lysosomes remains unknown. One of the main triggers to initiate an inflammatory response by microglia/macrophages may be the clearance of apoptotic neurons through phagocytosis. Phagocytic clearance in the brain is strongly related to the homeostatic maintenance of the brain. Both microglia and macrophages act as the "garbage trucks" of the brain as they regulate the physical removal of dying cells. This usually occurs quickly and includes the recruitment of the microglia/macrophages to the site of apoptotic cell accumulation and the activation of phagocytosis process by the binding of the apoptotic cells to the surface receptors of the microglia/macrophages. This leads to the clearance of the dying cells and prevents the release of toxic or immunogenic intracellular content from the dying cell into the

extracellular space which can contribute to the inflammation responses. In addition, activated microglia themselves also produce pro-inflammatory compounds that can induce an inflammatory response in the brain. Therefore, the accumulation of both activated microglia and apoptotic cells in the brain collectively induces substantial inflammation in the brain.

How does lipid accumulation in the lysosomes of the microglia lead to inflammation? I showed that in macrophages isolated from mouse models of two different LSDs, MLIV and Charcot-Marie-Tooth (CMT/ALS) diseases (which is caused by deficiency in $PI(3,5)P_2$ production), the uptake of large particle phagocytosis, which resemble apoptotic cells in size, was severely impaired. Consistently, microglia activation was evident in the brains of these mice as well as in the mouse models of other LSDs (Jeyakumar, Dwek et al. 2005). So it is possible that TRPML1 mediated lysosomal exocytosis contributes to microglia activation and the clearance of apoptotic debris in the brain (**Fig. 6.4**). For example, in the *Drosophila* model of MLIV, it is proposed that the defective clearance of late apoptotic neurons contributes significantly to neurodegeneration (Venkatachalam, Long et al. 2008). Thus, this could be the basic phagocytic mechanism that could explain pathogenic accumulation of apoptotic cells and brain inflammation seen in most LSDs and it could demonstrates the first mechanistic link between lysosome storage and inflammatory response. Therefore, the activation of TRPML1 could potentially serve as a therapeutic target for the activation of the phagocytic clearance of microglia/macrophages in the brain and other tissues across the body. This remains to be investigated by evaluating the particle uptake efficiency of microglia/macrophages isolated from other LSDs in response to TRPML1 specific activators such as ML-SA1.

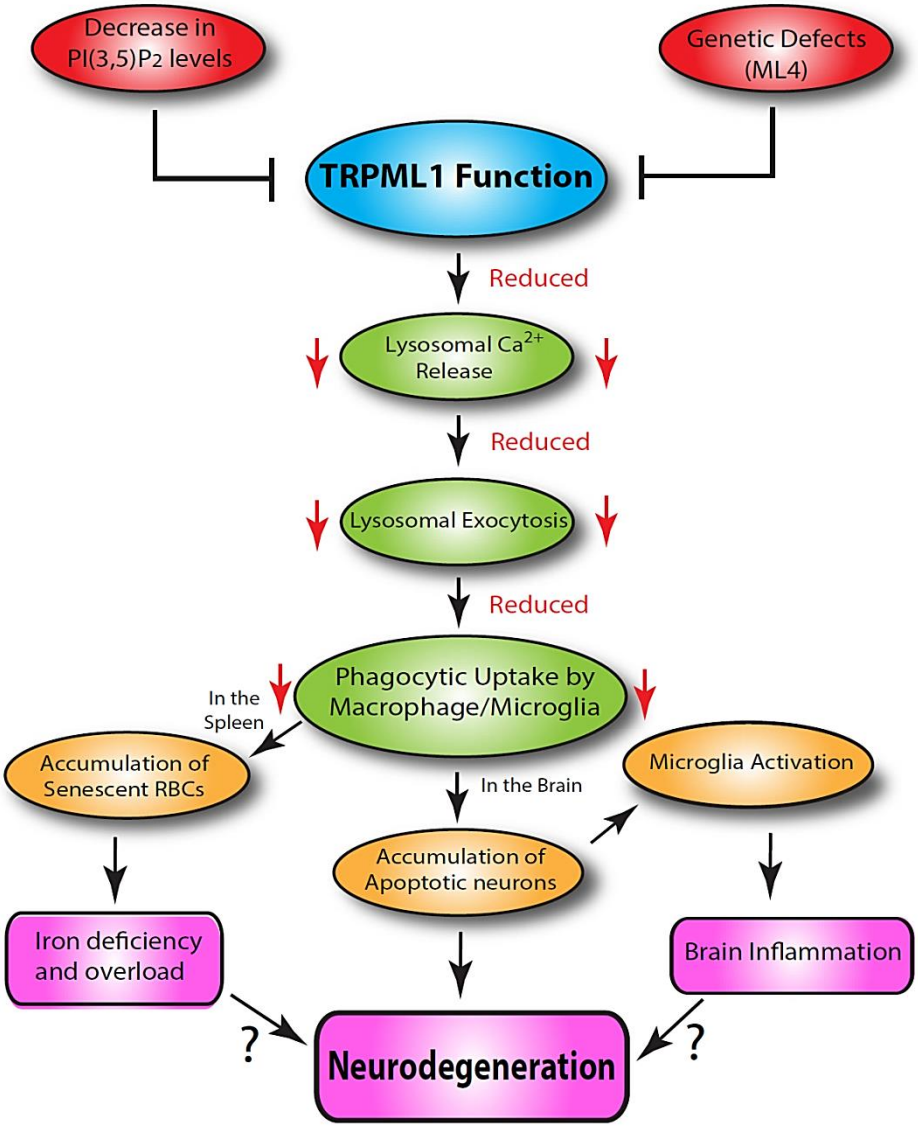

Figure 6.1 Defects in TRPML1function leads to decrease lysosomal exocytosis and defective clearance of apoptotic bodies in different tissues.

Dysfunction of TRPML1, either by genetic manipulations or by lacking its endogenous activator $PI(3,5)P_2$, leads to decrease in lysosomal Ca^{2+} release and subsequent inhibition of lysosomal exocytosis. This leads to defective phagocytic clearance by macrophage/microglia cells which can have several different consequences such as iron deficiency and overload in the spleen and/or the accumulation of apoptotic neurons and microglia activation in the brain. All these can potentially lead to neurodegenration.

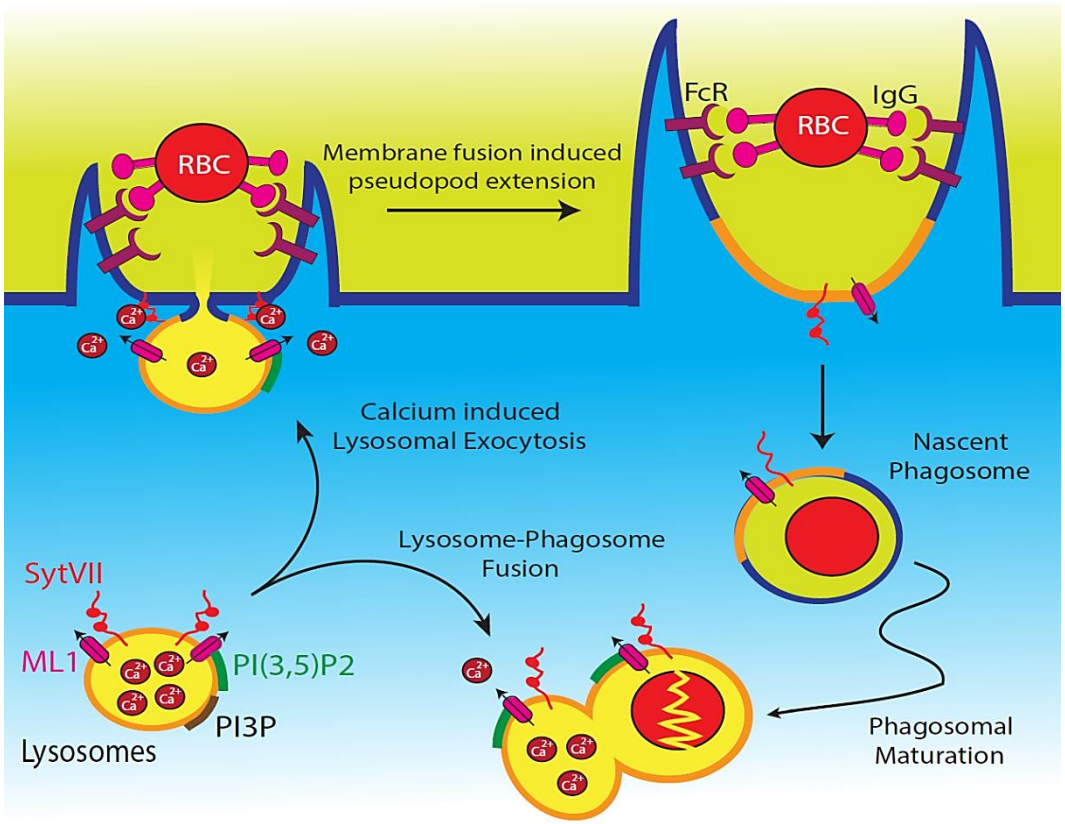

Figure 6.2 The dual role of lysosomes during phagocytosis.

Particle binding activates lysosomal TRPML1 to initiate Ca^{2+}-dependent lysosomal exocytosis. Upon particle (IgG-RBC) binding, the activity of PIKfyve (not shown) is stimulated at the site of particle uptake. The subsequent increase of $PI(3,5)P_2$ level can then activate lysosomal TRPML1 to induce lysosomal Ca^{2+} release. Juxtaorganellar Ca^{2+} can then bind the Ca^{2+} sensor SytVII to trigger lysosome-plasma membrane fusion, which provides substantial amount of lysosomal membranes for the pseudopod extension around IgG-RBCs. As a result, lysosomal membrane proteins, such as TRPML1 and SytVII, are inserted into the plasma membrane. Pseudopod extension continues until the IgG-RBCs are completely internalized. Phagocytic cups are then closed, and nascent phagosomes are formed. Newly formed phagosomes then undergo a series of membrane fusion and fission processes, collectively called phagosome maturation, to become late phagosomes. Lysosomes are also delivered to the late phagosomes through late phagosome maturation (phagosome-lysosome fusion), which is required for the degradation of phagocytic materials.

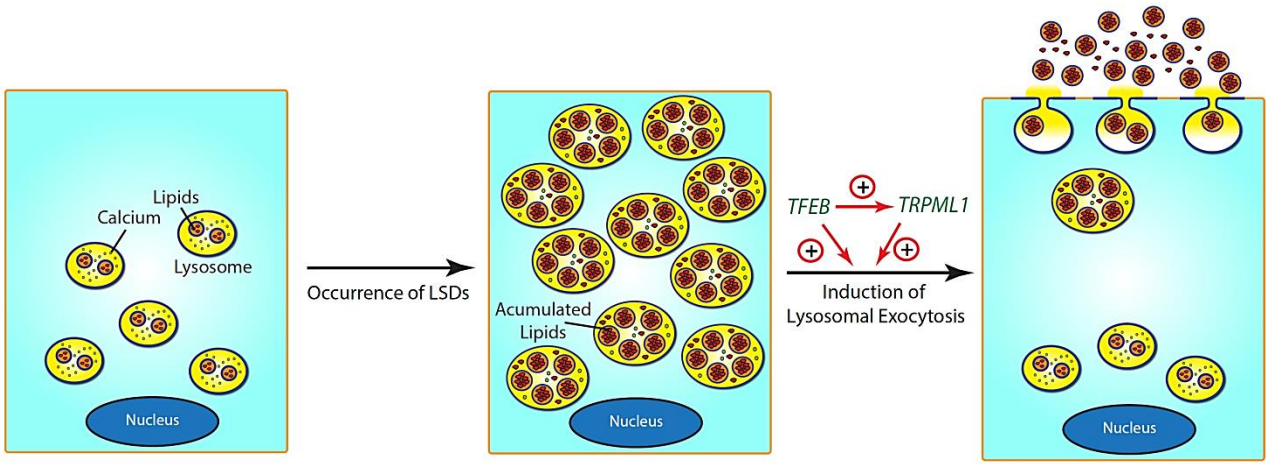

Figure 6.3 Cellular clearance by TFEB and TRPML1-mediated lysosomal exocytosis.

Accumulation of undigested lipids and other materials cause LSDs. Lysosomal exocytosis promotes cellular clearance in LSDs regardless of the primary defects and nature of the accumulated materials. The lysosome biogenesis transcription factor TFEB increases lysosomal docking and up-regulates the expression and/or activity of lysosomal Ca^{2+} channel TRPML1. Activation of TRPML1 by small molecule synthetic agonists induces lysosomal fusion with the plasma membrane. Increasing the activity and expression of TFEB and TRPML1 promote lysosomal exocytosis to induce the clearance of lysosome storage, serving as a potential therapeutic approach for many LSDs.

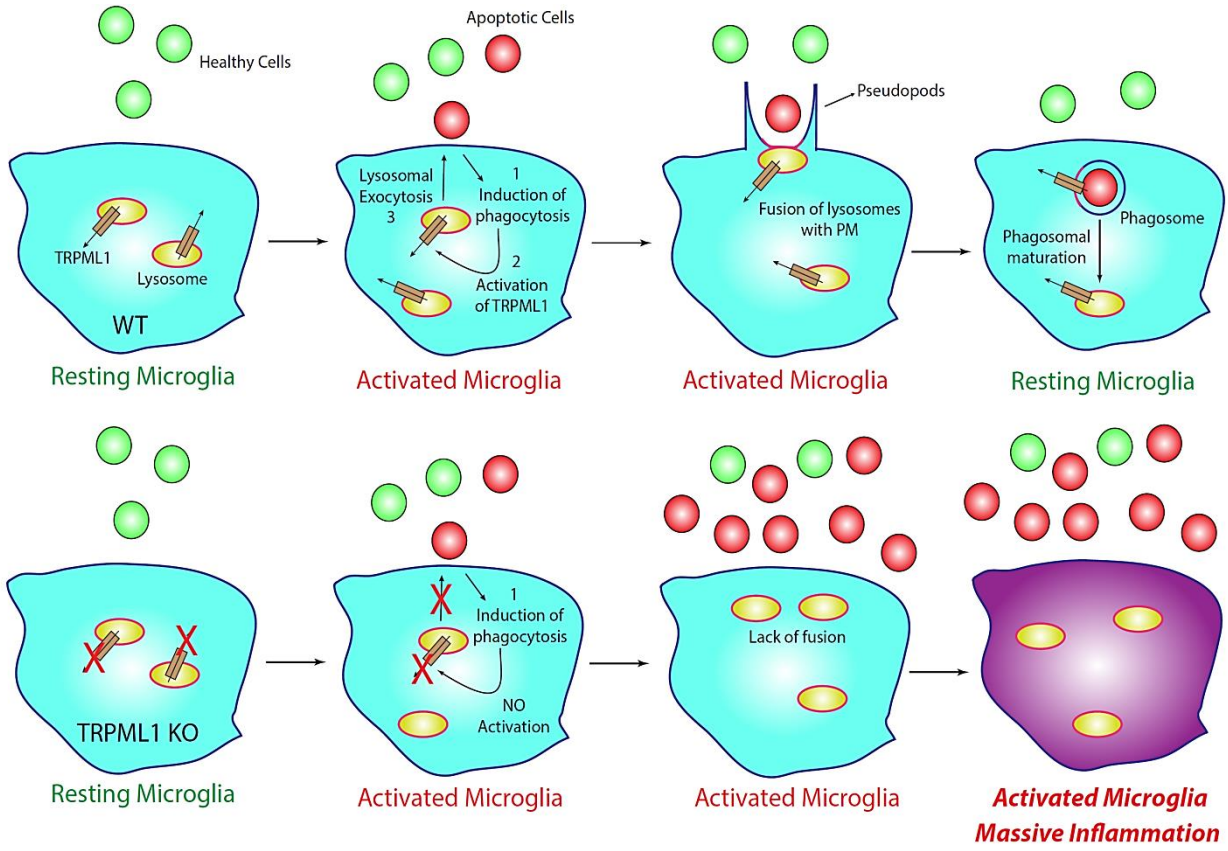

Fig 6.4 TRPML1 induced phagocytic clearance is required to avoid inflammation in LSDs

Under normal conditions apoptotic cells are ingested and eliminated by phagocytic cells, such as microglia, in the brain. Once apoptotic cells interact with the receptors on the surface of the macrophages (not shown) they trigger a series of events that lead to the induction of phagocytosis, including the activation of TRPML1 on the surface of the lysosomes that leads to the recruitment and fusion of lysosomes with the plasma membrane to provide excess membrane for pseudopods formation and particle ingestion. However, lack of TRPML1 activity results in insufficient particle ingestion in activated microglia which results in the accumulation of apoptotic cells in the brain. Accumulated apoptotic cells along with activated microglia produce inflammatory substances that lead to massive inflammation in the brain.

APPENDIX

LIST OF MY PUBLICATIONS DURING MY TENURE AT THE UNIVERSITY OF MICHIGAN

1. **Samie, M.A**., and Xu, H. (2014) Lysosomal Exocytosis and Lipid Storage Disorders. Journal of Lipid Research, manuscript under revision.

   - In this article we have discussed the recent advances and the understandings of lysosomal exocytosis and the potential for using this insight in the development of novel therapeutics for lysosomal storage diseases. Some parts of the Introduction (Chapter I) and Discussion (Chapter VI) are adapted from this article.

2. **Samie, M**., Wang, X. , Zhang, X. ,Goschka, A.,Li, X., Cheng, X., Gregg, E., Azar, M., Zhuo, Y., Garrity, AG,,Gao, Q., Slaugnehaupt, S, Pickel, J., Zolov, S., Weisman, LS., Lenk, G., Titus, S., Bryant-Genevier, M., Southall, N., Juan, M., Ferrer, M., and Xu, H. (2013) A TRP Channel in the Lysosome Regulates Large Particle Phagocytosis via Focal Exocytosis. Developmental Cell 26, Issue 5, 16 September 2013, Pages 511–524

   - In this article we have illustrated the role of TRPML1 in lysosomal exocytosis and large particle uptake in macrophages. The majority of data presented in Chapters II, III, and IV are adapted from this article

3. Wang, X., Zhang, X., Dong, X., **Samie, M**., Li, X., Cheng, X., Goschka, A., Shen., D., Zhou, Y., Harlow, J., Zhu, M.X., Clapham, D.E., Ren, D., and Xu, H. (2012) TPC Proteins are Sodium-selective Ion Channels in the Endosomes and Lysosomes. Cell 151, 373-383, Oct. 12, 2012.

   - In this article we identified the first lysosomal Na^+ channel. In this article I developed the assay to purify lysosomes and characterized the lysosomal ionic composition (*Figure 4 and Supplemental Figure 4*).

4. **Samie, M.A**, and Xu, H. (2010) Studying TRP Channels in Intracellualr Membranes. CRC press, Book chapter, TRP Channels--Methods in Signal Transduction Series. Chapter 19. PMID: 22593956 (Pubmed)

   - In this article we discussed the new emerging methods and techniques to study intracellular ion channels localized on the surface of the cellular compartments. Some parts of the Introduction (Chapter I) are adapted from this article.

5. Cheng, X., Jin, J., Hu, L., Shen, D., Dong, X., **Samie, M.A**, Knoff, J., Eisinger, B., Liu, M., Huang, S.M., Caterina, M.J., Dempsey, P., Michael, L.E., Dlugosz, A., Andrews, N., Clapham DE, and Xu H (2010) TRP Channel Regulates EGFR Signaling in Hair Morphogenesis and Skin Barrier Formation. Cell 2010 10.1016/j.cell.2010.03.013

   - In this article we identified a novel role for TRP channels in hair and skin formation. In this article I evaluated the mRNA and protein expression levels of different genes shown to be involved in skin formation (*Figure 3 and Supplemental Figure 3).*

6. Cheng, X., Shen, D., **Samie, M.A**., and Xu, H. (2010) Mucolipins: Intracellular TRPML1-3 Channels. FEBS Letters 2010 Jan. 12

   - In this article we discussed and summarized the new findings regarding TRPML channel family.

REFERENCES

Aderem, A. and D. M. Underhill (1999). "Mechanisms of phagocytosis in macrophages." Annu Rev Immunol **17**: 593-623.

Allen, L. A. and A. Aderem (1996). "Molecular definition of distinct cytoskeletal structures involved in complement- and Fc receptor-mediated phagocytosis in macrophages." J Exp Med **184**(2): 627-37.

Allen, L. A., C. Yang, et al. (2002). "Rate and extent of phagocytosis in macrophages lacking vamp3." J Leukoc Biol **72**(1): 217-21.

Altarescu, G., M. Sun, et al. (2002). "The neurogenetics of mucolipidosis type IV." Neurology **59**(3): 306-13.

Amir, N., J. Zlotogora, et al. (1987). "Mucolipidosis type IV: clinical spectrum and natural history." Pediatrics **79**(6): 953-9.

Andrews, N. W. (2000). "Regulated secretion of conventional lysosomes." Trends Cell Biol **10**(8): 316-21.

Arantes, R. M. and N. W. Andrews (2006). "A role for synaptotagmin VII-regulated exocytosis of lysosomes in neurite outgrowth from primary sympathetic neurons." J Neurosci **26**(17): 4630-7.

Bach, G. (2001). "Mucolipidosis type IV." Mol Genet Metab **73**(3): 197-203.

Ballabio, A. and V. Gieselmann (2009). "Lysosomal disorders: from storage to cellular damage." Biochim Biophys Acta **1793**(4): 684-96.

Bargal, R., N. Avidan, et al. (2000). "Identification of the gene causing mucolipidosis type IV." Nat Genet **26**(1): 118-23.

Bargal, R., N. Avidan, et al. (2001). "Mucolipidosis type IV: novel MCOLN1 mutations in Jewish and non-Jewish patients and the frequency of the disease in the Ashkenazi Jewish population." Hum Mutat **17**(5): 397-402.

Bargal, R., H. H. Goebel, et al. (2002). "Mucolipidosis IV: novel mutation and diverse ultrastructural spectrum in the skin." Neuropediatrics **33**(4): 199-202.

Bassi, M. T., M. Manzoni, et al. (2000). "Cloning of the gene encoding a novel integral membrane protein, mucolipidin-and identification of the two major founder mutations causing mucolipidosis type IV." Am J Hum Genet **67**(5): 1110-20.

Blott, E. J. and G. M. Griffiths (2002). "Secretory lysosomes." Nat Rev Mol Cell Biol **3**(2): 122-31.

Bonten, E., A. van der Spoel, et al. (1996). "Characterization of human lysosomal neuraminidase defines the molecular basis of the metabolic storage disorder sialidosis." Genes Dev **10**(24): 3156-69.

Botelho, R. J., C. C. Scott, et al. (2004). "Phosphoinositide involvement in phagocytosis and phagosome maturation." Curr Top Microbiol Immunol **282**: 1-30.

Boya, P. and G. Kroemer (2008). "Lysosomal membrane permeabilization in cell death." Oncogene **27**(50): 6434-51.
Bratosin, D., J. Mazurier, et al. (1998). "Cellular and molecular mechanisms of senescent erythrocyte phagocytosis by macrophages. A review." Biochimie **80**(2): 173-95.
Braulke, T. and J. S. Bonifacino (2009). "Sorting of lysosomal proteins." Biochim Biophys Acta **1793**(4): 605-14.
Braun, V., V. Fraisier, et al. (2004). "TI-VAMP/VAMP7 is required for optimal phagocytosis of opsonised particles in macrophages." EMBO J **23**(21): 4166-76.
Braun, V. and F. Niedergang (2006). "Linking exocytosis and endocytosis during phagocytosis." Biol Cell **98**(3): 195-201.
Burdakov, D., O. H. Petersen, et al. (2005). "Intraluminal calcium as a primary regulator of endoplasmic reticulum function." Cell Calcium **38**(3-4): 303-10.
Chapman, E. R. (2008). "How does synaptotagmin trigger neurotransmitter release?" Annu Rev Biochem **77**: 615-41.
Chavez, R. A., S. G. Miller, et al. (1996). "A biosynthetic regulated secretory pathway in constitutive secretory cells." J Cell Biol **133**(6): 1177-91.
Chawla, A. (2010). "Control of macrophage activation and function by PPARs." Circ Res **106**(10): 1559-69.
Chen, G., Z. Zhang, et al. (2012). "Lysosomal exocytosis in Schwann cells contributes to axon remyelination." Glia **60**(2): 295-305.
Cheng, X., J. Jin, et al. (2010). "TRP channel regulates EGFR signaling in hair morphogenesis and skin barrier formation." Cell **141**(2): 331-43.
Cheng, X., D. Shen, et al. (2010). "Mucolipins: Intracellular TRPML1-3 channels." FEBS Lett **584**(10): 2013-21.
Cheruku, S. R., Z. Xu, et al. (2006). "Mechanism of cholesterol transfer from the Niemann-Pick type C2 protein to model membranes supports a role in lysosomal cholesterol transport." J Biol Chem **281**(42): 31594-604.
Chow, C. W., G. P. Downey, et al. (2004). "Measurements of phagocytosis and phagosomal maturation." Curr Protoc Cell Biol **Chapter 15**: Unit 15 7.
Chow, C. Y., Y. Zhang, et al. (2007). "Mutation of FIG4 causes neurodegeneration in the pale tremor mouse and patients with CMT4J." Nature **448**(7149): 68-72.
Coorssen, J. R., H. Schmitt, et al. (1996). "Ca2+ triggers massive exocytosis in Chinese hamster ovary cells." EMBO J **15**(15): 3787-91.
Cosio, G. and S. Grinstein (2008). "Analysis of phosphoinositide dynamics during phagocytosis using genetically encoded fluorescent biosensors." Methods Mol Biol **445**: 287-300.
Cox, D., D. J. Lee, et al. (2000). "A Rab11-containing rapidly recycling compartment in macrophages that promotes phagocytosis." Proc Natl Acad Sci U S A **97**(2): 680-5.
Cox, D., C. C. Tseng, et al. (1999). "A requirement for phosphatidylinositol 3-kinase in pseudopod extension." J Biol Chem **274**(3): 1240-7.
Cox, T. M. and M. B. Cachon-Gonzalez (2012). "The cellular pathology of lysosomal diseases." J Pathol **226**(2): 241-54.
Cresswell, P. (1994). "Assembly, transport, and function of MHC class II molecules." Annu Rev Immunol **12**: 259-93.
Cuajungco, M. P. and M. A. Samie (2008). "The varitint-waddler mouse phenotypes and the TRPML3 ion channel mutation: cause and consequence." Pflugers Arch **457**(2): 463-73.

Cuellar-Mata, P., N. Jabado, et al. (2002). "Nramp1 modifies the fusion of Salmonella typhimurium-containing vacuoles with cellular endomembranes in macrophages." J Biol Chem **277**(3): 2258-65.
Curcio-Morelli, C., F. A. Charles, et al. (2010). "Macroautophagy is defective in mucolipin-1-deficient mouse neurons." Neurobiol Dis **40**(2): 370-7.
Czibener, C., N. M. Sherer, et al. (2006). "Ca2+ and synaptotagmin VII-dependent delivery of lysosomal membrane to nascent phagosomes." J Cell Biol **174**(7): 997-1007.
D'Souza-Schorey, C., G. Li, et al. (1995). "A regulatory role for ARF6 in receptor-mediated endocytosis." Science **267**(5201): 1175-8.
Di Palma, F., I. A. Belyantseva, et al. (2002). "Mutations in Mcoln3 associated with deafness and pigmentation defects in varitint-waddler (Va) mice." Proc Natl Acad Sci U S A **99**(23): 14994-9.
Di Paolo, G. and P. De Camilli (2006). "Phosphoinositides in cell regulation and membrane dynamics." Nature **443**(7112): 651-7.
Dong, X. P., X. Cheng, et al. (2008). "The type IV mucolipidosis-associated protein TRPML1 is an endolysosomal iron release channel." Nature **455**(7215): 992-6.
Dong, X. P., D. Shen, et al. (2010). "PI(3,5)P(2) Controls Membrane Traffic by Direct Activation of Mucolipin Ca Release Channels in the Endolysosome." Nat Commun **1**(4).
Dong, X. P., X. Wang, et al. (2009). "Activating mutations of the TRPML1 channel revealed by proline-scanning mutagenesis." J Biol Chem **284**(46): 32040-52.
Drecktrah, D., L. A. Knodler, et al. (2007). "Salmonella trafficking is defined by continuous dynamic interactions with the endolysosomal system." Traffic **8**(3): 212-25.
Duex, J. E., J. J. Nau, et al. (2006). "Phosphoinositide 5-phosphatase Fig 4p is required for both acute rise and subsequent fall in stress-induced phosphatidylinositol 3,5-bisphosphate levels." Eukaryot Cell **5**(4): 723-31.
Duex, J. E., F. Tang, et al. (2006). "The Vac14p-Fig4p complex acts independently of Vac7p and couples PI3,5P2 synthesis and turnover." J Cell Biol **172**(5): 693-704.
Eichelsdoerfer, J. L., J. A. Evans, et al. (2010). "Zinc dyshomeostasis is linked with the loss of mucolipidosis IV-associated TRPML1 ion channel." J Biol Chem **285**(45): 34304-8.
Eng, C. M., M. Banikazemi, et al. (2001). "A phase 1/2 clinical trial of enzyme replacement in fabry disease: pharmacokinetic, substrate clearance, and safety studies." Am J Hum Genet **68**(3): 711-22.
Falardeau, J. L., J. C. Kennedy, et al. (2002). "Cloning and characterization of the mouse Mcoln1 gene reveals an alternatively spliced transcript not seen in humans." BMC Genomics **3**(1): 3.
Falkenburger, B. H., J. B. Jensen, et al. (2010). "Phosphoinositides: lipid regulators of membrane proteins." J Physiol **588**(Pt 17): 3179-85.
Figueira, R. and D. W. Holden (2012). "Functions of the Salmonella pathogenicity island 2 (SPI-2) type III secretion system effectors." Microbiology **158**(Pt 5): 1147-61.
Flannagan, R. S., V. Jaumouille, et al. (2012). "The cell biology of phagocytosis." Annu Rev Pathol **7**: 61-98.
Gerasimenko, J. V., O. V. Gerasimenko, et al. (2001). "Membrane repair: Ca(2+)-elicited lysosomal exocytosis." Curr Biol **11**(23): R971-4.
Gillard, B. K., R. G. Clement, et al. (1998). "Variations among cell lines in the synthesis of sphingolipids in de novo and recycling pathways." Glycobiology **8**(9): 885-90.

Gillooly, D. J., A. Simonsen, et al. (2001). "Phosphoinositides and phagocytosis." J Cell Biol **155**(1): 15-7.
Gunshin, H., B. Mackenzie, et al. (1997). "Cloning and characterization of a mammalian proton-coupled metal-ion transporter." Nature **388**(6641): 482-8.
Hackam, D. J., O. D. Rotstein, et al. (1998). "v-SNARE-dependent secretion is required for phagocytosis." Proc Natl Acad Sci U S A **95**(20): 11691-6.
Haller, T., P. Dietl, et al. (1996). "The lysosomal compartment as intracellular calcium store in MDCK cells: a possible involvement in InsP3-mediated Ca2+ release." Cell Calcium **19**(2): 157-65.
Haller, T., H. Volkl, et al. (1996). "The lysosomal Ca2+ pool in MDCK cells can be released by ins(1,4,5)P3-dependent hormones or thapsigargin but does not activate store-operated Ca2+ entry." Biochem J **319 (Pt 3)**: 909-12.
Hamill, O. P. and B. Martinac (2001). "Molecular basis of mechanotransduction in living cells." Physiol Rev **81**(2): 685-740.
Haraga, A., M. B. Ohlson, et al. (2008). "Salmonellae interplay with host cells." Nat Rev Microbiol **6**(1): 53-66.
Henry, R. M., A. D. Hoppe, et al. (2004). "The uniformity of phagosome maturation in macrophages." J Cell Biol **164**(2): 185-94.
Hishikawa, T., J. Y. Cheung, et al. (1991). "Calcium transients during Fc receptor-mediated and nonspecific phagocytosis by murine peritoneal macrophages." J Cell Biol **115**(1): 59-66.
Holevinsky, K. O. and D. J. Nelson (1998). "Membrane capacitance changes associated with particle uptake during phagocytosis in macrophages." Biophys J **75**(5): 2577-86.
Hoppe, A. D. and J. A. Swanson (2004). "Cdc42, Rac1, and Rac2 display distinct patterns of activation during phagocytosis." Mol Biol Cell **15**(8): 3509-19.
Huotari, J. and A. Helenius (2011). "Endosome maturation." EMBO J **30**(17): 3481-500.
Huynh, K. K., J. G. Kay, et al. (2007). "Fusion, fission, and secretion during phagocytosis." Physiology (Bethesda) **22**: 366-72.
Infante, R. E., M. L. Wang, et al. (2008). "NPC2 facilitates bidirectional transfer of cholesterol between NPC1 and lipid bilayers, a step in cholesterol egress from lysosomes." Proc Natl Acad Sci U S A **105**(40): 15287-92.
Jabado, N., P. Cuellar-Mata, et al. (2003). "Iron chelators modulate the fusogenic properties of Salmonella-containing phagosomes." Proc Natl Acad Sci U S A **100**(10): 6127-32.
Jahn, R. and D. Fasshauer (2012). "Molecular machines governing exocytosis of synaptic vesicles." Nature **490**(7419): 201-7.
Jahn, R. and R. H. Scheller (2006). "SNAREs--engines for membrane fusion." Nat Rev Mol Cell Biol **7**(9): 631-43.
Jaiswal, J. K., N. W. Andrews, et al. (2002). "Membrane proximal lysosomes are the major vesicles responsible for calcium-dependent exocytosis in nonsecretory cells." J Cell Biol **159**(4): 625-35.
Jefferies, H. B., F. T. Cooke, et al. (2008). "A selective PIKfyve inhibitor blocks PtdIns(3,5)P(2) production and disrupts endomembrane transport and retroviral budding." EMBO Rep **9**(2): 164-70.
Jeyakumar, M., R. A. Dwek, et al. (2005). "Storage solutions: treating lysosomal disorders of the brain." Nat Rev Neurosci **6**(9): 713-25.
Karacsonyi, C., A. S. Miguel, et al. (2007). "Mucolipin-2 localizes to the Arf6-associated pathway and regulates recycling of GPI-APs." Traffic **8**(10): 1404-14.

Kerr, M. C., J. T. Wang, et al. (2010). "Inhibition of the PtdIns(5) kinase PIKfyve disrupts intracellular replication of Salmonella." EMBO J **29**(8): 1331-47.
Kim, H. J., Q. Li, et al. (2007). "Gain-of-function mutation in TRPML3 causes the mouse Varitint-Waddler phenotype." J Biol Chem **282**(50): 36138-42.
Kim, H. J., A. A. Soyombo, et al. (2009). "The Ca(2+) channel TRPML3 regulates membrane trafficking and autophagy." Traffic **10**(8): 1157-67.
Kirkegaard, T. and M. Jaattela (2009). "Lysosomal involvement in cell death and cancer." Biochim Biophys Acta **1793**(4): 746-54.
Kitano, M., M. Nakaya, et al. (2008). "Imaging of Rab5 activity identifies essential regulators for phagosome maturation." Nature **453**(7192): 241-5.
Kohyama, M., W. Ise, et al. (2009). "Role for Spi-C in the development of red pulp macrophages and splenic iron homeostasis." Nature **457**(7227): 318-21.
Kolter, T. and K. Sandhoff (2010). "Lysosomal degradation of membrane lipids." FEBS Lett **584**(9): 1700-12.
Kornfeld, S. and I. Mellman (1989). "The biogenesis of lysosomes." Annu Rev Cell Biol **5**: 483-525.
LaPlante, J. M., M. Sun, et al. (2006). "Lysosomal exocytosis is impaired in mucolipidosis type IV." Mol Genet Metab **89**(4): 339-48.
Lee, W. L., D. Mason, et al. (2007). "Quantitative analysis of membrane remodeling at the phagocytic cup." Mol Biol Cell **18**(8): 2883-92.
Lenk, G. M., C. J. Ferguson, et al. (2011). "Pathogenic mechanism of the FIG4 mutation responsible for Charcot-Marie-Tooth disease CMT4J." PLoS Genet **7**(6): e1002104.
Li, X., X. Wang, et al. (2013). "Genetically encoded fluorescent probe to visualize intracellular phosphatidylinositol 3,5-bisphosphate localization and dynamics." Proc Natl Acad Sci U S A **110**(52): 21165-70.
Lieberman, A. P., R. Puertollano, et al. (2012). "Autophagy in lysosomal storage disorders." Autophagy **8**(5): 719-30.
Link, T. M., U. Park, et al. (2010). "TRPV2 has a pivotal role in macrophage particle binding and phagocytosis." Nat Immunol **11**(3): 232-9.
Lloyd-Evans, E. and F. M. Platt (2011). "Lysosomal Ca(2+) homeostasis: role in pathogenesis of lysosomal storage diseases." Cell Calcium **50**(2): 200-5.
Lloyd-Evans, E., H. Waller-Evans, et al. (2010). "Endolysosomal calcium regulation and disease." Biochem Soc Trans **38**(6): 1458-64.
Luzio, J. P., N. A. Bright, et al. (2007). "The role of calcium and other ions in sorting and delivery in the late endocytic pathway." Biochem Soc Trans **35**(Pt 5): 1088-91.
Luzio, J. P., P. R. Pryor, et al. (2007). "Lysosomes: fusion and function." Nat Rev Mol Cell Biol **8**(8): 622-32.
Luzio, J. P., B. A. Rous, et al. (2000). "Lysosome-endosome fusion and lysosome biogenesis." J Cell Sci **113 (Pt 9)**: 1515-24.
Macia, E., M. Ehrlich, et al. (2006). "Dynasore, a cell-permeable inhibitor of dynamin." Dev Cell **10**(6): 839-50.
Martinez-Arca, S., R. Rudge, et al. (2003). "A dual mechanism controlling the localization and function of exocytic v-SNAREs." Proc Natl Acad Sci U S A **100**(15): 9011-6.
Matteoni, R. and T. E. Kreis (1987). "Translocation and clustering of endosomes and lysosomes depends on microtubules." J Cell Biol **105**(3): 1253-65.

McGeer, E. G. and P. L. McGeer (2003). "Inflammatory processes in Alzheimer's disease." Prog Neuropsychopharmacol Biol Psychiatry **27**(5): 741-9.
McGeer, P. L. and E. G. McGeer (2004). "Inflammation and neurodegeneration in Parkinson's disease." Parkinsonism Relat Disord **10 Suppl 1**: S3-7.
McMahon, H. T. and E. Boucrot (2011). "Molecular mechanism and physiological functions of clathrin-mediated endocytosis." Nat Rev Mol Cell Biol **12**(8): 517-33.
Medina, D. L., A. Fraldi, et al. (2011). "Transcriptional activation of lysosomal exocytosis promotes cellular clearance." Dev Cell **21**(3): 421-30.
Mellman, I. (1989). "Organelles observed: lysosomes." Science **244**(4906): 853-4.
Mellman, I., R. Fuchs, et al. (1986). "Acidification of the endocytic and exocytic pathways." Annu Rev Biochem **55**: 663-700.
Michell, R. H., V. L. Heath, et al. (2006). "Phosphatidylinositol 3,5-bisphosphate: metabolism and cellular functions." Trends Biochem Sci **31**(1): 52-63.
Micsenyi, M. C., K. Dobrenis, et al. (2009). "Neuropathology of the Mcoln1(-/-) knockout mouse model of mucolipidosis type IV." J Neuropathol Exp Neurol **68**(2): 125-35.
Miedel, M. T., Y. Rbaibi, et al. (2008). "Membrane traffic and turnover in TRP-ML1-deficient cells: a revised model for mucolipidosis type IV pathogenesis." J Exp Med **205**(6): 1477-90.
Miedel, M. T., K. M. Weixel, et al. (2006). "Posttranslational cleavage and adaptor protein complex-dependent trafficking of mucolipin-1." J Biol Chem **281**(18): 12751-9.
Mills, I. G., A. T. Jones, et al. (1999). "Regulation of endosome fusion." Mol Membr Biol **16**(1): 73-9.
Miyawaki, A., J. Llopis, et al. (1997). "Fluorescent indicators for Ca2+ based on green fluorescent proteins and calmodulin." Nature **388**(6645): 882-7.
Mizushima, N. (2011). "Autophagy in protein and organelle turnover." Cold Spring Harb Symp Quant Biol **76**: 397-402.
Mizushima, N., B. Levine, et al. (2008). "Autophagy fights disease through cellular self-digestion." Nature **451**(7182): 1069-75.
Montell, C. (2005). "The TRP superfamily of cation channels." Sci STKE **2005**(272): re3.
Mostov, K. and Z. Werb (1997). "Journey across the osteoclast." Science **276**(5310): 219-20.
Mrakovic, A., J. G. Kay, et al. (2012). "Rab7 and Arl8 GTPases are necessary for lysosome tubulation in macrophages." Traffic **13**(12): 1667-79.
Murray, P. J. and T. A. Wynn (2011). "Protective and pathogenic functions of macrophage subsets." Nat Rev Immunol **11**(11): 723-37.
Neiss, W. F. (1984). "A coat of glycoconjugates on the inner surface of the lysosomal membrane in the rat kidney." Histochemistry **80**(6): 603-8.
Neufeld, E. F. (1991). "Lysosomal storage diseases." Annu Rev Biochem **60**: 257-80.
Niedergang, F. and P. Chavrier (2004). "Signaling and membrane dynamics during phagocytosis: many roads lead to the phagos(R)ome." Curr Opin Cell Biol **16**(4): 422-8.
Ninomiya, Y., T. Kishimoto, et al. (1996). "Ca2+-dependent exocytotic pathways in Chinese hamster ovary fibroblasts revealed by a caged-Ca2+ compound." J Biol Chem **271**(30): 17751-4.
Nunes, P. and N. Demaurex (2010). "The role of calcium signaling in phagocytosis." J Leukoc Biol **88**(1): 57-68.
Pang, Z. P. and T. C. Sudhof (2010). "Cell biology of Ca2+-triggered exocytosis." Curr Opin Cell Biol **22**(4): 496-505.

Parkinson-Lawrence, E. J., T. Shandala, et al. (2010). "Lysosomal storage disease: revealing lysosomal function and physiology." Physiology (Bethesda) **25**(2): 102-15.
Piper, R. C. and J. P. Luzio (2004). "CUPpling calcium to lysosomal biogenesis." Trends Cell Biol **14**(9): 471-3.
Poccia, D. and B. Larijani (2009). "Phosphatidylinositol metabolism and membrane fusion." Biochem J **418**(2): 233-46.
Pryor, P. R., B. M. Mullock, et al. (2000). "The role of intraorganellar Ca(2+) in late endosome-lysosome heterotypic fusion and in the reformation of lysosomes from hybrid organelles." J Cell Biol **149**(5): 1053-62.
Pshezhetsky, A. V., C. Richard, et al. (1997). "Cloning, expression and chromosomal mapping of human lysosomal sialidase and characterization of mutations in sialidosis." Nat Genet **15**(3): 316-20.
Puertollano, R. and K. Kiselyov (2009). "TRPMLs: IN SICKNESS AND IN HEALTH." Am J Physiol Renal Physiol.
Puschmann, M. and A. M. Ganzoni (1977). "Increased resistance of iron-deficient mice to salmonella infection." Infect Immun **17**(3): 663-4.
Radtke, A. L. and M. X. O'Riordan (2006). "Intracellular innate resistance to bacterial pathogens." Cell Microbiol **8**(11): 1720-9.
Rao, S. K., C. Huynh, et al. (2004). "Identification of SNAREs involved in synaptotagmin VII-regulated lysosomal exocytosis." J Biol Chem **279**(19): 20471-9.
Reddy, A., E. V. Caler, et al. (2001). "Plasma membrane repair is mediated by Ca(2+)-regulated exocytosis of lysosomes." Cell **106**(2): 157-69.
Rodriguez, A., I. Martinez, et al. (1999). "cAMP regulates Ca2+-dependent exocytosis of lysosomes and lysosome-mediated cell invasion by trypanosomes." J Biol Chem **274**(24): 16754-9.
Rodriguez, A., P. Webster, et al. (1997). "Lysosomes behave as Ca2+-regulated exocytic vesicles in fibroblasts and epithelial cells." J Cell Biol **137**(1): 93-104.
Roy, D., D. R. Liston, et al. (2004). "A process for controlling intracellular bacterial infections induced by membrane injury." Science **304**(5676): 1515-8.
Ruivo, R., C. Anne, et al. (2009). "Molecular and cellular basis of lysosomal transmembrane protein dysfunction." Biochim Biophys Acta **1793**(4): 636-49.
Sagne, C. and B. Gasnier (2008). "Molecular physiology and pathophysiology of lysosomal membrane transporters." J Inherit Metab Dis **31**(2): 258-66.
Samie, M. A., C. Grimm, et al. (2009). "The tissue-specific expression of TRPML2 (MCOLN-2) gene is influenced by the presence of TRPML1." Pflugers Arch.
Sardiello, M. and A. Ballabio (2009). "Lysosomal enhancement: a CLEAR answer to cellular degradative needs." Cell Cycle **8**(24): 4021-2.
Sardiello, M., M. Palmieri, et al. (2009). "A gene network regulating lysosomal biogenesis and function." Science **325**(5939): 473-7.
Sawkar, A. R., S. L. Adamski-Werner, et al. (2005). "Gaucher disease-associated glucocerebrosidases show mutation-dependent chemical chaperoning profiles." Chem Biol **12**(11): 1235-44.
Schaible, U. E. and S. H. Kaufmann (2004). "Iron and microbial infection." Nat Rev Microbiol **2**(12): 946-53.
Schultz, M. L., L. Tecedor, et al. (2011). "Clarifying lysosomal storage diseases." Trends Neurosci **34**(8): 401-10.

Schulze, H., T. Kolter, et al. (2009). "Principles of lysosomal membrane degradation: Cellular topology and biochemistry of lysosomal lipid degradation." Biochim Biophys Acta **1793**(4): 674-83.

Schulze, H. and K. Sandhoff (2011). "Lysosomal lipid storage diseases." Cold Spring Harb Perspect Biol **3**(6).

Seby, F., M. Gagean, et al. (2003). "Development of analytical procedures for determination of total chromium by quadrupole ICP-MS and high-resolution ICP-MS, and hexavalent chromium by HPLC-ICP-MS, in different materials used in the automotive industry." Anal Bioanal Chem **377**(4): 685-94.

Settembre, C., C. Di Malta, et al. (2011). "TFEB links autophagy to lysosomal biogenesis." Science **332**(6036): 1429-33.

Settembre, C., A. Fraldi, et al. (2013). "Signals from the lysosome: a control centre for cellular clearance and energy metabolism." Nat Rev Mol Cell Biol **14**(5): 283-96.

Settembre, C., R. Zoncu, et al. (2012). "A lysosome-to-nucleus signalling mechanism senses and regulates the lysosome via mTOR and TFEB." EMBO J **31**(5): 1095-108.

Shen, D., X. Wang, et al. (2012). "Lipid storage disorders block lysosomal trafficking by inhibiting a TRP channel and lysosomal calcium release." Nat Commun **3**: 731.

Soyombo, A. A., S. Tjon-Kon-Sang, et al. (2006). "TRP-ML1 regulates lysosomal pH and acidic lysosomal lipid hydrolytic activity." J Biol Chem **281**(11): 7294-301.

Spampanato, C., E. Feeney, et al. (2013). "Transcription factor EB (TFEB) is a new therapeutic target for Pompe disease." EMBO Mol Med **5**(5): 691-706.

Stendahl, O., K. H. Krause, et al. (1994). "Redistribution of intracellular Ca2+ stores during phagocytosis in human neutrophils." Science **265**(5177): 1439-41.

Stinchcombe, J. C. and G. M. Griffiths (1999). "Regulated secretion from hemopoietic cells." J Cell Biol **147**(1): 1-6.

Sudhof, T. C. (2013). "Neurotransmitter release: the last millisecond in the life of a synaptic vesicle." Neuron **80**(3): 675-90.

Tapper, H., W. Furuya, et al. (2002). "Localized exocytosis of primary (lysosomal) granules during phagocytosis: role of Ca2+-dependent tyrosine phosphorylation and microtubules." J Immunol **168**(10): 5287-96.

Theler, J. M., D. P. Lew, et al. (1995). "Intracellular pattern of cytosolic Ca2+ changes during adhesion and multiple phagocytosis in human neutrophils. Dynamics of intracellular Ca2+ stores." Blood **85**(8): 2194-201.

Thompson, E. G., L. Schaheen, et al. (2007). "Lysosomal trafficking functions of mucolipin-1 in murine macrophages." BMC Cell Biol **8**: 54.

Venkatachalam, K., A. A. Long, et al. (2008). "Motor deficit in a Drosophila model of mucolipidosis type IV due to defective clearance of apoptotic cells." Cell **135**(5): 838-51.

Venugopal, B., M. F. Browning, et al. (2007). "Neurologic, gastric, and opthalmologic pathologies in a murine model of mucolipidosis type IV." Am J Hum Genet **81**(5): 1070-83.

Vergarajauregui, S., P. S. Connelly, et al. (2008). "Autophagic dysfunction in mucolipidosis type IV patients." Hum Mol Genet **17**(17): 2723-37.

Vergarajauregui, S., J. A. Martina, et al. (2009). "Identification of the penta-EF-hand protein ALG-2 as a Ca2+-dependent interactor of mucolipin-1." J Biol Chem **284**(52): 36357-66.

Vergarajauregui, S., R. Oberdick, et al. (2008). "Mucolipin 1 channel activity is regulated by protein kinase A-mediated phosphorylation." Biochem J **410**(2): 417-25.

Vergarajauregui, S. and R. Puertollano (2006). "Two di-leucine motifs regulate trafficking of mucolipin-1 to lysosomes." Traffic **7**(3): 337-53.
Vieira, O. V., R. J. Botelho, et al. (2002). "Phagosome maturation: aging gracefully." Biochem J **366**(Pt 3): 689-704.
Vinet, A. F., M. Fukuda, et al. (2008). "The exocytosis regulator synaptotagmin V controls phagocytosis in macrophages." J Immunol **181**(8): 5289-95.
Walkley, S. U. (2009). "Pathogenic cascades in lysosomal disease-Why so complex?" J Inherit Metab Dis **32**(2): 181-9.
Walkley, S. U. and M. T. Vanier (2009). "Secondary lipid accumulation in lysosomal disease." Biochim Biophys Acta **1793**(4): 726-36.
Wanachiwanawin, W. (2000). "Infections in E-beta thalassemia." J Pediatr Hematol Oncol **22**(6): 581-7.
Weber, S. S., C. Ragaz, et al. (2009). "Pathogen trafficking pathways and host phosphoinositide metabolism." Mol Microbiol **71**(6): 1341-52.
Wynn, T. A., A. Chawla, et al. (2013). "Macrophage biology in development, homeostasis and disease." Nature **496**(7446): 445-55.
Xu, J., T. Mashimo, et al. (2007). "Synaptotagmin-1, -2, and -9: Ca(2+) sensors for fast release that specify distinct presynaptic properties in subsets of neurons." Neuron **54**(4): 567-81.
Yeung, T., B. Ozdamar, et al. (2006). "Lipid metabolism and dynamics during phagocytosis." Curr Opin Cell Biol **18**(4): 429-37.
Yogalingam, G., E. J. Bonten, et al. (2008). "Neuraminidase 1 is a negative regulator of lysosomal exocytosis." Dev Cell **15**(1): 74-86.
Young, J. D., S. S. Ko, et al. (1984). "The increase in intracellular free calcium associated with IgG gamma 2b/gamma 1 Fc receptor-ligand interactions: role in phagocytosis." Proc Natl Acad Sci U S A **81**(17): 5430-4.
Yu, L., C. K. McPhee, et al. (2010). "Termination of autophagy and reformation of lysosomes regulated by mTOR." Nature **465**(7300): 942-6.
Zhang, X., X. Li, et al. (2012). "Phosphoinositide isoforms determine compartment-specific ion channel activity." Proc Natl Acad Sci U S A **109**(28): 11384-9.
Zhang, Y., S. N. Zolov, et al. (2007). "Loss of Vac14, a regulator of the signaling lipid phosphatidylinositol 3,5-bisphosphate, results in neurodegeneration in mice." Proc Natl Acad Sci U S A **104**(44): 17518-23.
Zolov, S. N., D. Bridges, et al. (2012). "In vivo, Pikfyve generates PI(3,5)P2, which serves as both a signaling lipid and the major precursor for PI5P." Proc Natl Acad Sci U S A **109**(43): 17472-7.